AN ABSTRACT OF THE THESIS OF

Jack C. Eslick for the Master of Science degree in Physical Sciences presented on 22 April 2002.

Title: Use of Remote Sensing Data to Evaluate Change in the Endla Nature Reserve and Emajõe Suursoo Mire Complex in Estonia

Abstract approved: 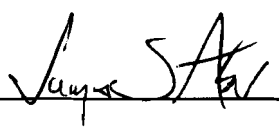

This study used multispectral data acquired by Landsat satellites and a geographic information systems (GIS) program to evaluate change between 1988 and 1999 at two wetlands areas in Estonia–Endla Nature Reserve and Emajõe Suursoo Mire Complex. Recent political changes in Estonia make this country a good location for this type of study. Estonia was a Soviet republic from 1944 until it because an independent nation in 1991. After Estonia became at independent nation, many environmental changes were made which should be reflected in improving conditions at the study areas.

GIS analytical techniques such as image differencing, image ratioing, normalized difference vegetation index analysis, tasseled-cap transformation analysis, and correlation analysis, as well as visual comparison of the images, were used to evaluate change that occurred between the image dates. Detailed image classification was not attempted due to the lack of georeferenced ancillary data and because no means was available by which error assessment could be performed.

The analyses show that change occurred in both study areas between 1988 and 1999. The most significant change occurred around the periphery of the reserves. The data suggest that Lake Endla had a greater biomass concentration in 1988 than in 1999. The water level of Lake Peipsi appears to have declined prior to the acquisition of the 1999 data. Vegetation appears more vigorous at both study areas in 1999 than in 1988. In general, the bogs themselves appeared to have been stable over the time period covered by the study.

The use of a GIS program and remote sensing data proved useful in identifying change in Estonian wetlands. The remote sensing data would need to be augmented with larger scale data in order to perform more detailed analyses.

USE OF REMOTE SENSING DATA TO EVALUATE CHANGE IN THE ENDLA NATURE RESERVE AND EMAJÕE SUURSOO MIRE COMPLEX IN ESTONIA

A Thesis Presented to

The Physical Sciences Department

EMPORIA STATE UNIVERSITY

In Partial Fulfillment of the Requirements for the

Master of Science Degree in Physical Sciences

Jack C. Eslick

April 2002

Approved by Major Advisor

Approved by Committee Member

Approved by Committee Member

Approved by Departmental Chair

Approved by Dean of Graduate Studies and Research

Acknowledgements

I wish to state my appreciation and indebtedness to Dr. James Aber for his assistance and guidance throughout my graduate studies at Emporia State University. Dr. Aber was most helpful in the learning experience and research associated with the preparation of this thesis. In all of Dr. Aber's endeavors with which I have had the good fortune to be associated, I have always noted his passion for science and enthusiasm for sharing his knowledge with others.

TABLE OF CONTENTS

TABLE OF CONTENTS (continued)

TABLE OF CONTENTS (continued)

TABLE OF CONTENTS (continued)

LIST OF TABLES

LIST OF TABLES (continued)

LIST OF FIGURES

LIST OF FIGURES (continued)

LIST OF FIGURES (continued)

LIST OF FIGURES (continued)

LIST OF FIGURES (continued)

LIST OF FIGURES (continued)

Chapter One
Introduction

1.1 Study Scope and Goals

Estonia is a country with many wetlands areas, ten of which have been designated by the Ramsar Convention on Wetlands as being wetlands of international importance (Ramsar Information Bureau, 2000). This study focused on two of these areas–Endla Nature Reserve and Emajõe Suursoo Mire Complex. The goal of this study was to determine if a Geographic Information System (GIS) program could be employed with multispectral satellite images, acquired about eleven years apart, to identify change in the wetlands areas.

Recent political changes in Estonia makes this country a good location for this type of study. Estonia came under Soviet rule in 1944 and remained a Soviet republic until 1991. The Soviets showed little concern for environmental issues and natural resource conservation. After Estonia became an independent nation, many environmental changes were made; marginal agricultural land was taken out of production, policies were established to limit peat and timber harvesting to sustainable levels, and more natural areas were given a protected status. The first set of satellite images used in this study was acquired in 1988 when Estonia was a Soviet republic and the second set was acquired in 1999, about eight years after Estonia became an independent nation.

Wetlands are important elements in our biosphere. They provide food and shelter to migratory birds, support endemic flora and fauna, sequester atmospheric carbon, filter pollutants from water, and provide resources of economic value. In addition to the tangible benefits provided by wetlands, one must also recognize them for their intrinsic aesthetic value.

This study was limited to the analysis of change detection. The potential causes for the change such as precipitation patterns were not within the scope of this study.

1.2 Physical Setting

1.2.1 Location

Estonia is located in northern Europe. The country is bordered by the Gulf of Finland to the north, the Baltic Sea to the west, Latvia to the south, and Russia to the east. Lake Peipsi (Peipus) and the Narva River generally demarcate the border between Estonia and Russia. Estonia is situated between latitudes 59° 40′ N and 57° 30′ N and longitudes 28° 40′ E and 22° 40′ E. A map of Estonia is shown on Figure 1.1: Map of Estonia.

Estonia has an area of 45,227 square kilometers of which ten percent is contained on the approximately 1,500 islands along the coastline (Taylor, 1999). The four largest islands are: Saaremaa (2,668 km^2), Hiiumaa (1,023 km^2), Muhu (204 km^2), and Vormsi (93 km^2) (Raud, 1953; Taylor, 1999).

Map Source: Central Intelligence Agency, 2001
Map Date: 1999

Figure 1.1: Map of Estonia

1.2.2 Climate

The Estonian climate is described on the Estonian County Guide web page (http://www.ciesin.ee/ESTCG/NATURE, 1993). The climate information in this section was obtained from the referenced web page.

The climate of Estonia is influenced by the country's maritime location. The mean temperature for the mainland is 4.2 to 4.5° C. The average annual precipitation is 500 millimeters (mm) along the coastal regions and approaches 700 mm inland. Late summer is generally the period with the greatest precipitation. In most winters, snow cover begins in early December or January and lasts until about the end of March. The snow depth may reach one half meter.

1.2.3 Geology

Estonia is part of the northern European plain and is generally flat with an average elevation of 50 meters above mean sea level (Raud, 1953). Much of the current topography is the result of the last period of glaciation, which ended about 10,000 years ago. In the north, glacial sediments are thin, but thicken to the south and east. The center of the country as well as the south and west have soils comprised of sands and clays, which are favorable to agriculture.

The bedrock underlying Estonia consists mainly of Ordovician and Silurian limestones and dolomites in the northern part of the country and Devonian sandstones in the south (Raud, 1953). The limestone forms cliffs up to 56 meters high along the Baltic Sea (http://www.ciesin.ee/ESTCG/NATURE, 1993).

Surface water is abundant. There are more than 1,400 lakes and 420 rivers with lengths greater than 10 kilometers (http://www.ciesin.ee/ESTCG/NATURE, 1993). Some of the lakes are finger lakes, formed by glacial forces. There are about 12,000 fens and bogs, the cumulative areas of which cover 9,000 km^2 (http://www.ciesen/ee./ESTCG/-NATURE/).

1.3 History

1.3.1 Introduction

The land-use patterns and attitudes toward the land and conservation in Estonia have been controlled by political events for the past millennium. Estonia has been primarily an agrarian country. A government that does not have appropriate respect for the land and the many fragile ecosystems present in Estonia can cause or foster attitudes that allow major ecological damage. This section presents a brief overview of Estonian history and discusses how land use and environmental attitudes have been impacted by history.

A brief chronology of Estonian history adapted from Taagepera (1993) is given in Table 1.1: Chronology of Estonia Rule. For the purpose of this study, the history of Estonia is divided into three time units; the pre-Soviet Era, the Soviet Era, and the post-Soviet Era.

Table 1.1:
Chronology of Estonia Rule

Dates	Type of Rule
Prior to 1227	Independent Rule
1227 – 1561	German Rule
1561 – 1710	Swedish Rule
1710 – 1917	Russian Rule
1917 – 1939	Independent Rule
1939 – 1941	Soviet Occupation
1941 – 1944	German Occupation
1944 – 1991	Soviet Rule
1991 to present	Independent Rule

1.3.2 Pre-Soviet Era

The pre-Soviet Era covers the period from 1227 to 1944. During this period, Estonia was subjected to outside rule for all but 22 years. This outside rule affected land use and attitudes toward the land.

Beginning in about 1202, crusades were undertaken by German bishops to Christianize Estonia (Raud, 1953). By 1227, the crusades led by the Knights of the Sword and the Order of the Teutonic Knights with the assistance of Denmark had conquered the country (Raud, 1953). Under German rule, a feudal system based on the German system was implemented (Taagepera, 1993). Serfdom began in the second half of the fourteenth century (Taagepera, 1993). Under this system, crusading knights and other Germans owned most of the property.

The Order of the Teutonic Knights was defeated by Ivan the Terrible early in the Livonian Wars, which resulted in Estonia becoming loyal to Sweden in 1591 (Raun, 1991). Under Swedish rule, the conditions of the Estonian people began to improve; however, the German landlords still exerted much control over the peasants and the land (Konstantin Päts Fund., 1974). During the time of Swedish rule, the amount of control the government allowed the German landlords varied depending on the amount of military help the Swedes needed with conflicts in other regions. While conditions under Swedish rule were far from ideal, in relative comparison to previous and future conditions, this time would later be known as the "*good Swedish times*" (Vesterinen, 1921).

The generally ice-free ports along Estonia's northern coast were desired by Russia which, led by Peter the Great, gained control of Estonia in 1710 (Taylor, 1999). Under Russian rule, the peasants were recognized as property of the landowners (Raud, 1953). Vesterinen (1921) gives the following conditions that were imposed on the Estonian people by the Russian government:

1. *The peasants belong body and soul to the landowner and are his property;*
2. *They may not own anything themselves, but may only gather property for their lord, who disposes everything according to his desire;*
3. *Taxes and the degree of the peasant's slavery are decided by the landowner according to his wishes, there being no limit to the landowner's power in this respect; and*

4. *The landowners have unlimited power to punish their peasants, against which no appeal can be made by the latter.*

A peasant revolt in 1805 resulted in peasants being freed in northern Estonia in 1816 and in southern Estonia in 1819; however, peasant lands remained under the control of predominately German nobility (Raud, 1953) Russian rule continued until the collapse of tsarist Russia and the defeat of Imperial Germany in World War I.

On 28 November 1917, the Maapäev assembly declared Estonia's sovereignty (Taagepera, 1993). At this point, however, the struggle for independence was far from over. Prior to the end of World War I, Estonia was invaded by Germany. Germany was forced to withdraw from Estonia with the signing of the armistice of 11 November 1918 (Taagepera, 1993). Russia again tried to fill the power void left after the German withdrawal. Following a period of military and political conflict, the Tartu Peace Treaty between Russia and Estonia was signed on 2 February 1920 (Taagepera, 1993), and Estonia became a free country.

With independence came land reforms. Baronial estates were claimed by the Estonian government (Vesterinen, 1921). These estates, numbering about 750, were divided into about 55,000 smaller parcels (Konstantin Päts Fund., 1974). The average size parcel was 24 hectares (Kõll, 1994). The ownership and management of nonarable lands remained with the government.

1.3.3 Soviet Era

The Estonian government was forced to sign a mutual assistance pact with the Soviet Union on 28 September 1939 (Konstantin Päts Fund., 1974). The pact gave the Soviet Union the right to establish military bases in Estonia. On 6 August 1940, Estonia was annexed into the Soviet Union and the country fell under the total control of the Soviet Union (Konstantin Päts Fund., 1974). Land was taken from the farmers and collective farms were established.

Germany attacked the Soviet Union on 22 June 1941 and within three months, the Germans occupied all of Estonia (Taagepera, 1993). Estonians were forced to provide agricultural products and labor for Germany's war effort (Taagepera, 1993). German firms were given possession of the land that had been confiscated from the Russians.

The Soviet army recaptured Estonia in October 1944 (Taagepera, 1993). This time, Soviet rule was to last for 47 years. The Soviets undertook to exploit the Estonian people and their natural resources to the maximum extent possible in order to advance the communist ideology.

The Soviets focused on building fuel and chemical industries, the manufacture of machine tools, metal refining, and the lumber, paper, and pulp industries (Raun, 1991). The Soviet News (1950) reported that metalworking industries experienced a 63% production increase in a single year and that in the same year textile production increased

by 109%. While production figures from the Soviet News Agency may be suspect, it does show the Soviet's focus on maximizing the industrial output in Estonia.

Agriculture was greatly affected by Soviet policy. The Soviets began to collectivize farms and by 1952, 97% of farms were collectivized (Raun, 1991). With collective farms and centralized controls, agricultural production steadily declined (Raun, 1991). One response to the decreased output was to put additional land into agricultural production (Soviet News, 1950).

The heavy industrial activities, chemical and fuel industries, and military production all had detrimental effects on the soil, air, and water quality. The exploitation of the land and natural resources such as oil shale and peat further served to degrade environmental conditions.

1.3.4 Post Soviet Era

Soviet control over Estonia began to loosen in the early 1980s (Taagepera, 1993). In 1987, Estonians gathered to protest against Soviet plans for the expansion of phosphate mining which threatened to pollute Lake Peipsi. Following these protests, Estonians began to push for autonomy. Freedom came in small increments until the Soviet Union recognized Estonia's sovereignty in 1991.

An Estonian constitution was adopted on 28 June 1992 (Central Intelligence Agency, 2001). Free elections were held on 5 October 1992. The country has three branches of government – executive, legislative, and judicial. The executive branch consists of a

president, prime minister and a cabinet (council of ministers). The president is elected. The prime minister is nominated by the president and approved by parliament. The legislature consists of single chamber (unicameral) with 101 members who are elected to four-year terms. The judicial branch consists of a National Court, the chairman of which receives a lifetime appointment from the parliament.

The 2000 gross domestic product (GNP) was 14.7 billion dollars (Central Intelligence Agency, 2001). In 1999, agricultural products provided the smallest contribution to the GNP (3.6%), followed by industrial products (30.7%). The largest portion of the GNP was derived from services, which accounted for 65.7% of the GNP. Agriculture provides employment for 11% of the population. Agricultural products include potatoes, fruits, vegetables, livestock, dairy products, and fish.

In 2000, Estonia had a negative trade balance, with exports of 3.1 billion dollars and imports of 4.0 billion dollars (Central Intelligence Agency, 2001). Major exports include machinery, wood products, textiles, food products, metals, and chemicals. Finland, Sweden, and Russia are the major trading partners of Estonia; combined these countries accounted for 47.8% of exports and 45.6% of imports in 1999.

1.3.5 History's Effects on the Environment

Estonia is a small country, which means that a large emphasis must be placed on the environment if the land is to be productive and support life. The lack of sovereignty prevented Estonians from exercising control over the environment or environmental

policy throughout most of their history. The following quote from Taagepera (1993) summarizes the Estonian perception of the Soviet's attitude toward the environment; "*The attitude of the Russian planners, managers, and even individual miners reveals this tendency: Our country* [the Soviet Union] *is vast; if we mess it up here* [Estonia], *we can always go somewhere else.*"

Chapter Two
Wetlands in Estonia

2.1 Defining Wetlands

Many natural phenomena with cultural, social, economic, and environmental facets suffer from the lack of definition that is acceptable across the disciplines, and wetlands are certainly no exception. Tiner (1999) devotes the first chapter of his book to reviewing and developing a working definition for the term "wetlands." This section discusses elements present in the identified definitions and develops a definition that is applicable to the use of remote sensing for wetlands identification and delineation. A summary of the primary definitions reviewed by Tiner (1999) is given in Table 2.1 Wetlands Definitions.

Three of the definitions in Table 2.1: Wetlands Definitions (Cowardin et al., 1979; National Research Council, 1995; National Wetlands Working Group, 1987) have three common elements – hydric soils, hydrophytic vegetation, and saturation or inundation with water at least part of the year. For the purpose of this study, the definition used to identify, delineate, and measure temporal change in wetlands will be based on the type of floral community present. The rationale for defining wetlands based on the floral community includes:

1. Unique floral communities are associated with wetlands;
2. Changes in wetlands extent and conditions are readily and quickly expressed through the status of the floral community; and

Table 2.1: Wetlands Definitions

After Tiner (1999)

Definition, Source, and Original Reference	Definition
U.S. Geological Survey (Shaler, 1890)	*All areas...in which the natural declivity is insufficient, when forest cover is removed to reduce the soil to a measure of dryness necessary for agriculture.*
U.S. Fish and Wildlife Service (Cowardin et al., 1979)	*Wetlands are lands transitional between terrestrial and aquatic systems where the water table is usually at or near the surface and the land is covered by shallow water. For the purpose of this classification wetlands must have one or more of the three following attributes: (1) at least periodically, the land supports predominantly hydrophytes; (2) the substrate is predominantly undrained hydric soil; and (3) the substrate is nonsoil and is saturated with water or covered by shallow water at some time during the growing season each year.*

Table 2.1: Wetland Definitions (cont.)

After Tiner (1999)

Definition, Source, and Original Reference	Definition
National Research Council (National Research Council, 1995)	*A wetland is an ecosystem that depends on constant or recurrent, shallow inundation, or saturation at or near the surface of the substrate. The minimum essential characteristics of a wetland are recurrent, sustained inundation, or saturation at or near the surface and the presence of physical, chemical, and biological features reflective of recurrent sustained inundation or saturation. Common diagnostic features of wetlands are hydric soils and hydrophytic vegetation.*
National Wetlands Working Group (National Wetlands Working Group, 1987)	*[L]and that is saturated with water long enough to promote wetland or aquatic processes as indicated by poorly drained soils, hydrophytic vegetation, and various kinds of biological activity which are adapted to a wet environment.*
Ramsar Convention (Ramsar Information Bureau, 1998)	*[A]reas of marsh, fen, peat land, or water, whether natural or artificial, permanent or temporary, with water that is static or flowing, fresh, brackish, or salty, including areas of marine water the depth of which the low tide does not exceed 6 m. Wetlands may incorporate riparian and coastal zone adjacent to the wetlands ...*

3. Changes to wetlands flora can be identified and quantified using remotely sensed data.

For this study, wetlands will be defined as an area with a unique flora community that is dependent on the presence of a substrate that is permanently or temporarily saturated or inundated sufficiently long each year to promote and sustain the floral community.

Tiner (1999) describes four types of vegetation that may be associated with wetlands. These vegetation types are summarized in Table 2.2: Types of Wetlands Flora.

Table 2.2: Types of Wetlands Flora

Type of Flora	Probability of Presence in Wetland	Probability of Presence in Non-wetlands
Obligate wetland[1]	> 99%	< 1%
Facultative wetland[2]	67 to 99%	1 to 33%
Facultative[3]	34 to 66%	34 to 66%
Upland[4]	1 to 33%	67 to 99%

Notes: 1) Obligate wetlands plants require a wetland-type environment to survive.
2) Facultative wetland plants can survive in wetlands and uplands; however, they are most suited for a wetlands environment.
3) Facultative plants can survive equally well in either type of environment.
4) Upland plants are generally habitants of upland areas; however, some can survive in a wetlands environment.

Niering (1998) identifies five kinds of wetlands: (1) marshes, (2) swamps and floodplain forests, (3) bogs, (4) rivers and streams, and (5) lakes and ponds. With this system of classification, the wetlands of interest in this study would be considered bogs. Bogs are unique ecological communities found in most climatic zones of the world from the high latitudes to the equatorial region.

2.2 Significance of Wetlands

2.2.1 Introduction

Wetlands are important elements in our biosphere. Wetlands provide food and shelter for migrating birds, support endemic flora and fauna, sequester atmospheric carbon, filter pollutants from water, and provide resources of economic value. In addition to the tangible benefits provided by wetlands, one must also recognize wetlands for their intrinsic aesthetic values.

2.2.2 Flora and Fauna

Wetlands are an important habitat for birds. Niering (1998) estimates that 150 species of birds are dependant on wetlands. Wetlands are a rich source of food and nesting sites. Migrating birds often stop at wetlands to rest and replenish their energy reserves. While birds are represented by more species than other vertebrates in wetlands, there are also diverse populations of mammals, reptiles, fishes, and amphibians.

Many species of plants can survive only in a wetlands environment. Flora which are dependent on a wetlands environment for survival are known as wetland obligates. These

plants include mosses (e.g., *Sphagnum spp.*), cattails (*Typha spp.*), many sedges (*Carex spp.*), and rushes (*Juncus spp.*). Some plants, known as facultative wetlands plants, can survive under some non-wetlands conditions; however, they have a strong affinity to wetlands environments (Tiner, 1999). Example facultative wetland plants include; several varieties of red maple (*Acer rubrum drummondii*, *A. rubrum triobum*) and an oak (*Quercus stellata paludosa*),

2.2.3 Carbon Sequestration

The Earth receives solar energy in the form of shortwave radiation centered around 0.5 micrometers and emits energy in the form of longer wave radiation centered around 10 micrometers (Mackenzie, 1998). The transmittance of longwave (outgoing) radiation is inhibited by the presence of greenhouse gasses in the atmosphere; whereas, shortwave (incoming) radiation is not appreciably attenuated by these gasses. Greenhouse gasses affect the energy flux and allow more energy to be retained on the Earth, which causes the mean surface temperature to increase. The most common greenhouse gas is carbon dioxide. Whenever carbonaceous materials are oxidized, a stoichiometric quantity of carbon dioxide is generated.

$$C + O_2 \rightarrow CO_2$$

Equation 2.1

This means that for every mole of carbon oxidized, one mole of carbon dioxide is produced. Oxidation can occur rapidly, as in a forest fire, or less rapidly as in biological metabolism. Gravimetrically, for every gram of carbon oxidized, approximately 3.75 grams of carbon dioxide are produced. It is now recognized that achieving an appropriate

level of atmospheric carbon dioxide is requisite to preventing anthropogenically induced climate change.

Bogs are an important carbon sink. Davis (1946) gives the following equation of the conversion of cellulose to peat.

$$C_{72} + H_{120} + O_{60} \rightarrow C_{62}H_{72}O_{24} + H_2O + CO_2 + CH_4$$

Equation 2.2

When stoichiometrically balanced, this equation becomes:

$$C_{72} + H_{120} + O_{60} \rightarrow C_{62}H_{72}O_{24} + 20H_2O + 8CO_2 + 2CH_4$$

Equation 2.3

For every mole of cellulose (1 mole of cellulose equals 1, 944 grams of cellulose) converted to peat 8 moles of carbon dioxide (352 grams), 2 moles of methane (32 grams), and 20 moles of water (360 grams) are generated, leaving 744 grams of carbon sequestered in the peat. Based on this simplified analysis, at maturity, dried peat would have a maximum organic carbon content of about 38 percent.

2.2.4 Filtration of Pollutants

Wetlands systems have the ability to trap and use nutrients and to sequester or degrade organic pollutants (Niering, 1998). Agricultural runoff from areas where excessive fertilizer has been applied often contains nitrogen and phosphorous. Some of the nutrient load is buried in the wetlands, while some is utilized by the native flora.

Bacteria and chemical conditions within a wetlands system may promote degradation of complex hydrocarbons into carbon dioxide and water. Organic compounds, which are common pollutants in many industrial wastewater streams, may become immobilized as a result of binding to the organic carbon in the peat.

Wetlands serve an important role in removing pollutants from water so that groundwater and surface water quality is improved. Excessive nutrients and pollutants can degrade or poison wetlands to the point that the viability of the system is jeopardized.

2.2.5 Economic Significance

Wetlands are a source of materials, which are of appreciable economic significance. Peat is the most significant resource. Peat can be used for livestock bedding, amendment of agricultural soils, raw material for manufactured products, and as an energy source.

Estonia has peat reserves of about 3×10^9 metric tons, of which about 2.4×10^9 metric tons are economically accessible (Baltic Environmental Forum, 2000). In 1999, approximately 1.26×10^6 metric tons of peat were harvested, which is below the annual harvesting limit of 2.78×10^6 metric tons allowed by current regulation (Baltic Environmental Forum, 2000). The current regulatory limit is thought to exceed the current peat accumulation rate; however, the actual harvest rate is less than the accumulation rate (Baltic Environmental Forum, 2000).

2.3 Study Areas

2.3.1 Introduction

This study examined two non-contiguous wetlands areas in eastern Estonia. These areas are identified as Endla Nature Reserve and Emajõe Suursoo Mire Complex. The study areas are shown on Figure 2.1: Study Areas. Endla Nature Reserve is located about 20 km north-northwest of the town of Jõgeva and lies west and south of Highway 39. Emajõe Suursoo Mire Complex is located on the western shore of Lake Peipsi in the delta of the Emajõe River about 35 km east of Tartu.

Both study areas are included on the Ramsar List of Wetlands of International Importance (Ramsar Information Bureau, 2001a). The Ramsar Convention on Wetlands was initiated in 1971 to identify and protect wetlands with *"international significance in terms of biology, botany, zoology, limnology, or hydrology"* (Frazier, 1999). Estonia became a signatory to the convention on 29 July 1994 (Peck, 2000). At the end of 1998, there were 957 Ramsar sites, ten of which are in Estonia (Frazier, 1999).

2.3.2 Endla Nature Reserve

Endla Nature Reserve has an area of 8,050 hectares and is located in Jõgeva, Järva, and Lääne-Viru counties. The Endla Nature Reserve was known as Endla-Oostriku Mire Reserve prior to 1985, when the reserve was expanded and renamed (Aaviksoo et al., 1997). The reserve was added to the Ramsar list in June 1997.

Base Map Source: Central Intelligence Agency, 2001
Map Date: 1999

Ⓐ Endla Nature Reserve

Ⓑ Emajõe Suursoo Mire Complex

Figure 2.1: Study Areas

The Endla mire system formed after the end of the last ice age when sedimentation and isostatic rebound caused Great Lake Endla to decline in area leaving only several remnant lakes (Aaviksoo et al., 1997). The largest of these remnant lakes is Endla Lake, which has an area of about 2,871 hectares. The mire system is underlain by lake sediments and moraine sands and gravels which overlie the Ordovician limestone and dolomite bedrock (Ramsar Information Bureau, 2001a). Peat deposits may be up to 7.3 meters thick.

There are seven bogs within the mire complex. The size and maturity of the bogs vary. In addition to peat bogs, the mire complex also includes freshwater lakes, rivers, swamp forests, and mixed forests (Ramsar Information Bureau, 2001a).

The bogs are shown of Figure 2.2: Topographic Map – Endla Nature Reserve. A composite image prepared from Landsat TM bands 3, 4, and 5 for the Endla Nature Reserve and surrounding area is given on Figure 2.3: Composite Image of the Endla Nature Reserve – 1999.

Endla Nature Reserve is home to many important and endangered species. The reserve supports populations of *Canis lupis* (gray wolf) and *Lutra lutra* (otter). The reserve is a breeding ground for many birds including the species listed in Table 2.3: Important Bird Species of the Endla Nature Reserve.

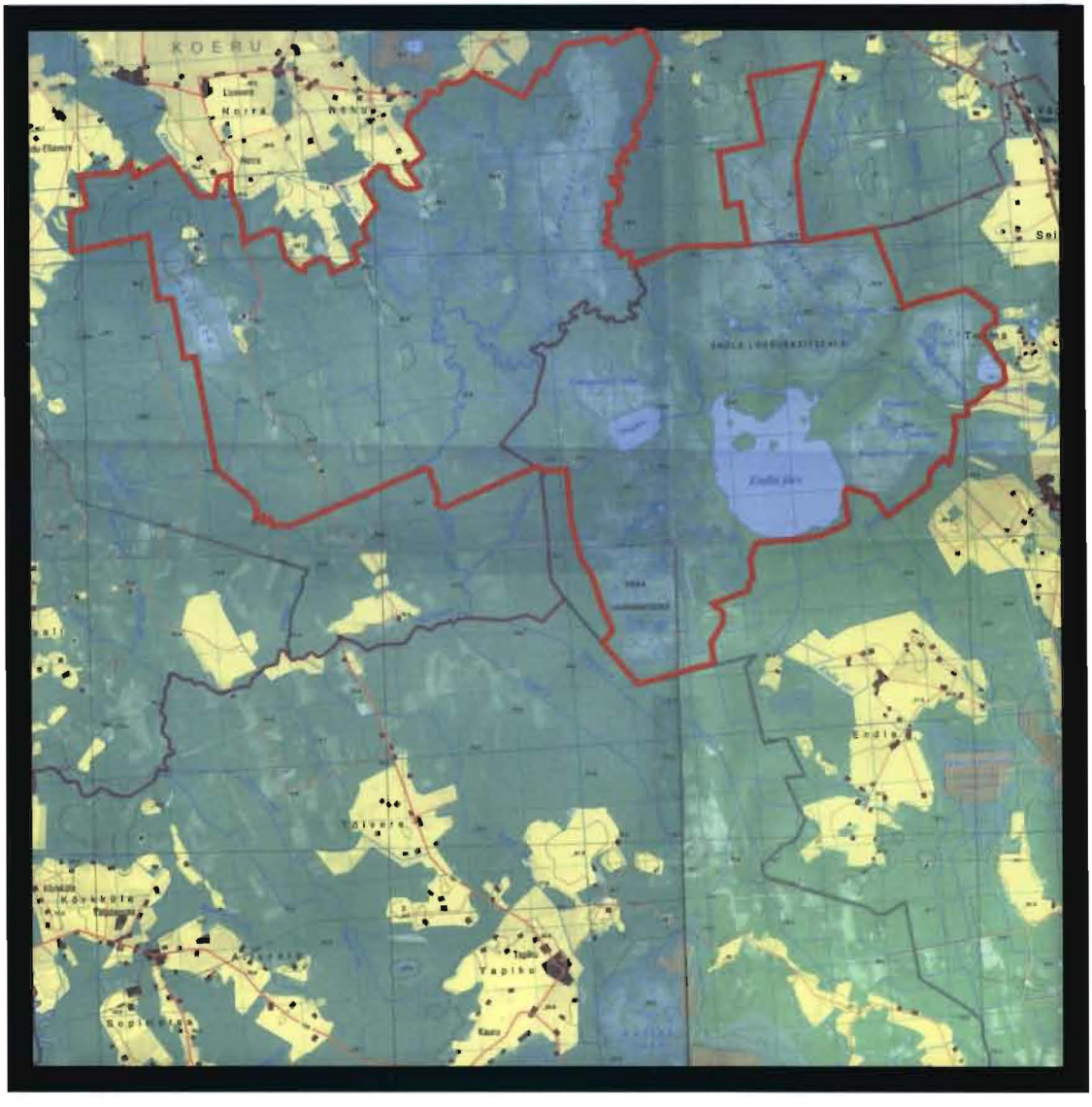

Base Map Source: Eesti Kaardikeskus, 1996a, b, c, d
Map Scale 1:125,000
Boundary of Endla Nature Reserve

0 1 2 3 4 5
Scale (km)

Figure 2.2: Topographic Map -- Endla Nature Reserve

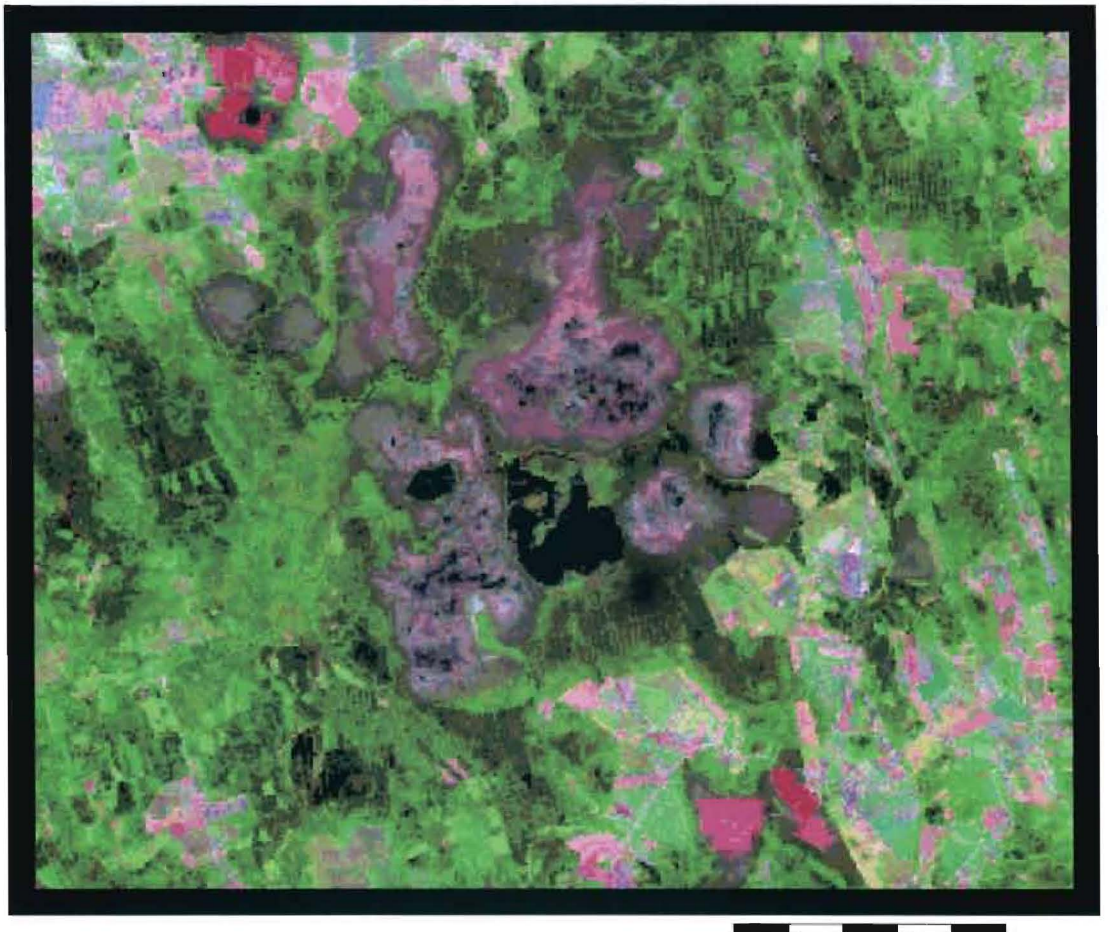

Map Scale 1:140,000

0 1 2 3 4 5
Scale (km)

Composite image prepared from Landsat TM bands 3, 4, and 5 of the Endla Nature Reserve - 1999

Generalized classification (forest classification after Aber (2001)

Dark green - Spruce forest
Olive green - Pine forest
Light green - Deciduous forest
Open water - Black
Active peat harvesting areas - Bright pink (also note geometric patterns)
Undisturbed peat - Purple to pinkish gray

Figure 2.3: Cornposite Image of the Endla Nature Reserve - 1999

2.3: Important Bird Species of the Endla Nature Reserve

Source: Ramar Information Bureau (2001a)

Alcedo atthis (kingfisher)	*C. pygargus* (montagus harrier)
Aquila chrysaetos (golden eagle)	*Grus grus* (common crane)
A. pomarina (lesser spotted eagle)	*Haliaeetus albicilla* (white-tailed hawk)
Bonsasia bonasia (hazel grouse)	*Pandion haliaetus* (osprey)
Botaurus stellaris (bittern)	*Pluvials apricaria* (Eurasian plover)
Bubo bubo (Eurasian eagle owl)	*Prozana prozana* (spotted crake)
Caprimulgus europaeus (nightjar)	*Tetrax tetrax* (little bustard)
Ciconia nigra (black stork)	*Tetro urogallus* (capercaillie)
Circus aeruginosus (marsh harrier)	*Tringa glareola* (wood sandpiper)

The reserve is also home to several species of endangered plants such as *Cypripedium calceolus* (yellow lady's slipper), *Malaxis monophyllos* (adder's mouth), *Rubus arcticus* (nagoonberry), *Hyperzia selago* (mountain club moss), and *Najas intermedia* (bladderwort) (Ramsar Information Bureau, 2001a).

2.3.3 Emajõe Suursoo Mire Complex

Emajõe Suursoo Mire complex together with Piirissaare Island forms a nature reserve of 32,600 hectares. The Emajõe Suursoo Mire complex has an area of approximately 18,500 hectares. Piirissaare Island is not included in this study. The Emajõe Suursoo Mire complex is located in the delta of the Emajõe River at its discharge to Lake Peipsi. The mire complex covers about three-fourths of the river delta (Aaviksoo et al., 1997).

The mire complex is shown on Figure 2.4: Topographic Map – Emajõe Suursoo Mire Complex. A composite image prepared from Landsat TM bands 3, 4, and 5 for the Emajõe Suursoo Mire Complex and surrounding area is given on Figure 2.5: Composite Image of the Emajõe Suursoo Mire Complex – 1999.

The Emajõe Suursoo mire complex serves an important role in the removal of contaminants and nutrients from the waters of the Emajõe River prior to discharge to Lake Peipsi (Ramsar Information Bureau, 2001b). The water level of Lake Peipsi rises in the spring causing flooding of much of the mire complex (Ramsar Information Bureau, 2001b).

Like Endla Nature Reserve, Emajõe Suursoo Mire is a breeding ground for many birds. Emajõe Suursoo Mire is also an important spawning area for many fishes, some of which are listed in Table 2.4: Important Fish Species Spawning in the Emajõe Suursoo Mire Complex.

Table 2.4:
Important Fish Species Spawning in the Emajõe Suursoo Mire Complex
(Source: Ramsar Information Bureau, 2001b)

Abramis brama (carp bream)	*Lucioperca lucioperca* (zander)
Alburnus alburnus (ukelei)	*Perca fluviatilis* (European perch)
Coregonus albula (verdace)	*Rutilus rutilus* (roach)
C. lavaretus maraenoides (Peipsi whitefish)	*Scardinius erythrophtalmus* (rudd)
Esox lucius (northern pike)	*Siluris glanis* (welo)
Leuciscus idus (ide)	

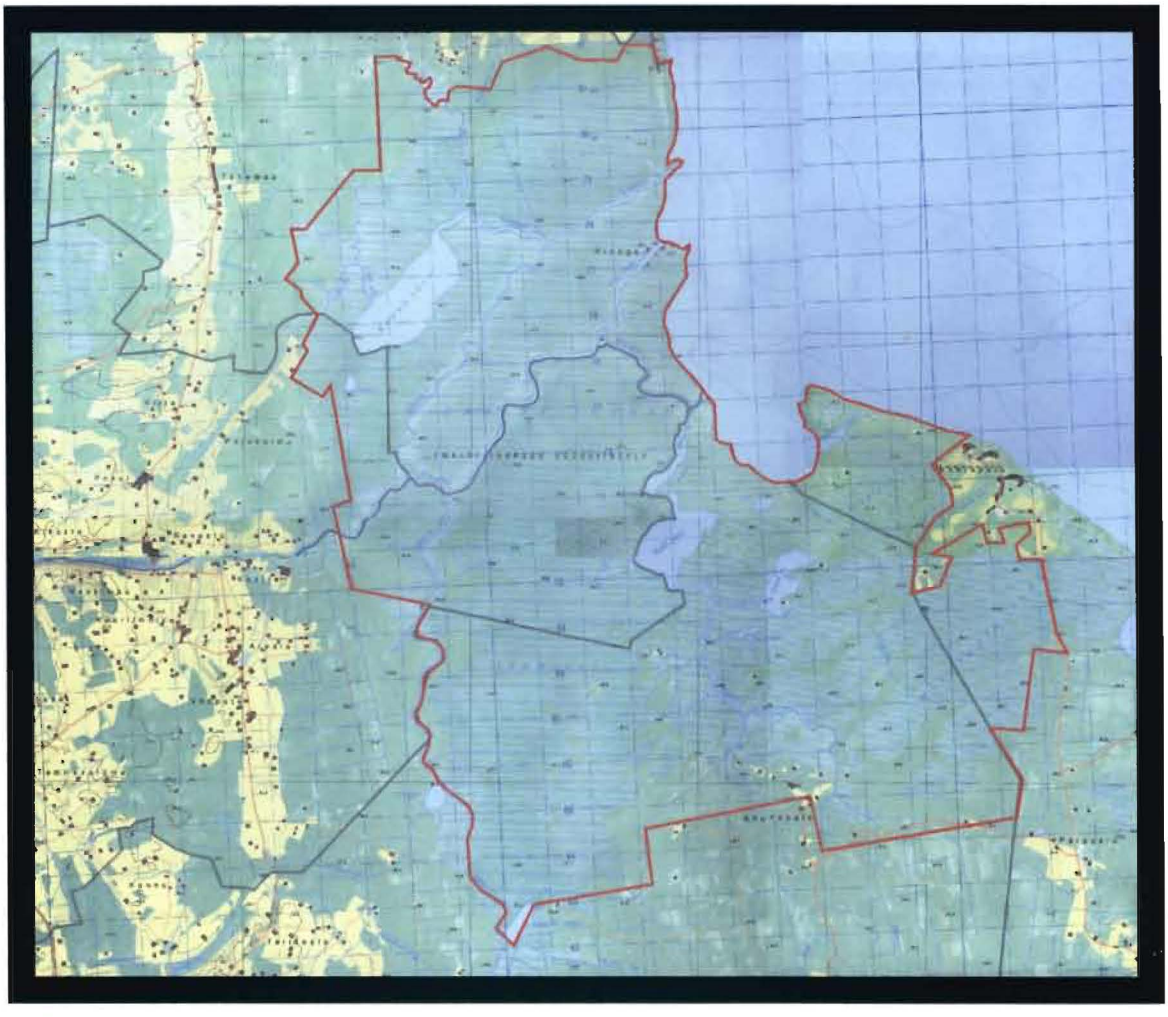

Base Map Source: Eesti Kaardikeskus, 1996e, f, 1998a, b

Map Scale 1:167,000

Boundary of the Emajõe Suursoo Mire Complex

0 2 4 6 8 10

Scale (km)

Figure 2.4: Topographic Map -- Emajõe Suursoo Mire Complex

Map Scale 1:220,000

0 2 4 6 8 10
Scale (km)

Composite image prepared from Landsat TM bands 3, 4, and 5 of the Emajõe Suursoo Mire Complex - 1999

Generalized classification (forest classification after Aber (2001)
Dark green - Spruce forest
Olive green - Pine forest
Light green - Deciduous forest
Open water - Black
Undisturbed peat - Purple to pinkish gray

Figure 2.5: Composite Image of the Emajõe Suursoo Mire Complex - 1999

S. glanis is an endangered species and *C. lavaretus maraenoides* is endemic to the Lake Peipsi region (Ramsar Information Bureau, 2001b). The mire complex is also home to the gray wolf, otter, beaver, and moose (Ramsar Information Bureau, 2001b).

The Emajõe Suursoo Mire Reserve was established in 1981. Peat mining, logging, and fertilizer use in the reserve are prohibited (Ramsar Information Bureau, 2001b).

2.3.4 Summary

Endla Nature Reserve and Emajõe Suursoo Mire Complex are important resources because they provide critical habitat for many rare and endangered flora and fauna. The reserves also provide a resting place for many migratory birds and breeding grounds for many others. The reserves are important from aesthetic and educational perspective. As people become more aware of the importance of ecosystem preservation through direct observation and participation, the greater the collective emphasis placed on conservation. This conservation interest can have effects reaching for beyond the boundaries of the reserves.

Chapter Three
Description of Study

3.1 Introduction

Estonia has experienced significant political change in the last twelve years. This change has had a large effect on public policy related to the restoration and protection of natural areas such as wetlands. Wetlands play an important role in the biosphere and their health may serve as an indicator of environmental conditions on a larger scale.

It would be expected that the political and policy changes in the post-Soviet era have caused environmental conditions to improve. Marginally productive agricultural lands have been removed from production, emissions of pollutants have decreased, and better environmental management practices have been implemented to limit natural resource exploitation. With these factors in mind, Estonia should be an excellent region to test the use of remote sensing techniques in detecting and quantifying changes in wetlands.

3.2 Previous Studies

A literature search was conducted using traditional library search methods and Scirus, which is a scientific document Internet search engine provided by Elsevier Science (http://www.scirus.com). Literature was identified related to the use of remote sensing in wetlands delineation and change detection. Numerous authors have cited remote sensing as a useful tool in wetland delineation (e.g., Avery and Berlin, 1992; Daiz Barrios et al.,

1998; Dappen and Tooze, 2001; Environmental Laboratory, 1987; Forse et al., ; Neuenschwander et al., 1998; Perry et al., 1997; Ullah, ; Vanderbilt et al., 1997; Von Hansen and Sties, 1999). Many studies have been published which used remote sensing as a tool in wetlands delineation and change analysis.

The areal extent of wetlands can vary from less than one hectare to thousands of hectares; therefore, scale and resolution are important considerations in determining appropriate remote sensing technologies of a study. The prevalence of the identified studies used scales obtainable with fixed-wing aircraft either solely or in concert with lower resolution satellite data.

Daiz Barrios et al. (1998), Perry et al., (1997), and Vanderbilt et al. (1997) reported successful delineation of wetlands vegetation using Polarization and Directionality of Earth Reflectance (POLDER) data. POLDER is a French multispectral radiometer that collects spectral data from eight bands, three of which can detect polarization states (Rees, 1999). Data acquisition for these studies was accomplished with a C-130 fixed-wing cargo aircraft. Unsupervised classification with color infrared aerial photography was used by Daiz Barrios et al. (1998) for data analysis. Perry et al. (1997) also used POLDER data with color infrared photography for classification analysis. The authors reported POLDER to a be a "*potentially powerful new approach for classifying and estimating the areal extent of northern , high latitude wetlands.*" Vanderbilt et al. (1997) used classification and Normalized Difference Vegetation Index (NDVI) for analysis. The authors do not reference the use of field-collected or smaller scale photography in the

data analysis. The authors conclude that POLDER is useful in classification and delineation of high-latitude wetlands.

Von Hansen and Sties (1999) conducted wetlands delineation studies using multispectral data collected with an airborne DAEDALUS sensor that provides a ground resolution of 2.5 meters. Data analysis was conducted using supervised classification with training areas developed by field mapping teams. At the time the paper was published, data analysis was not complete; however, the authors stated that promising results were expected.

Neuenschwander et al. (1998) used hyperspectral data acquired using Airborne Visible Infrared Imaging Spectrometer (AVIRIS) with a spatial resolution of 18 meters for a coastal wetlands study at the Kennedy Space Center in Florida. Data were analyzed using neutral network and maximum likelihood analyses. When the neutral network analysis was combined with a Maximum Noise Fraction Transformation algorithm to decrease the noise to signal ratio, the authors reported an overall classification accuracy of 93.5 percent.

Dappen and Tooze (2001), Forse et al. (accessed 2002), and Ullah (accessed 2002) used Landsat Thematic Mapper (TM) multispectral data in their wetlands studies. Dappen and Tooze, (2001) augmented the TM data with Farm Service Agency data, Digital Orthophoto Quarter Quadrangle (DOQQ) photographs, National Wetlands Inventory data, and field-collected spectral signatures. Ullah (accessed 2002) augmented the TM

data with color infrared and black-and-white photography from the National Aerial Photography Program, black-and-white aerial photography, and the National Wetlands Inventory database. Forse et al. (accessed 2002) do not reference the use of ancillary data for their study.

Dappen and Tooze, (2001) used Landsat TM data along with the afore referenced ancillary data to delineate land-use patterns in the Central Platte River Basin in Nebraska. The authors used supervised and unsupervised classification to map land use. They reported that the success with supervised classification was directly dependent on the accuracy of the training sites. With unsupervised classification, the ancillary data were critical to the assignment of classes. The authors reported an overall classification accuracy of 78.53 percent. The number of wetlands were too few for meaningful statistically analysis to determine an individual accuracy for this class.

Ullah (accessed 2002) used Landsat TM data along with the afore referenced ancillary data in a study to detect change in wetland conditions in Brown County, Nebraska. The author concluded that Landsat TM data, when used with larger scale ancillary data and analytical techniques like tasseled-cap transformation (TCT), could be used to delineate and monitor changes in wetlands.

Forse et al. (accessed 2002) used Landsat TM data to analyze changes in coastal wetlands in Thailand. The authors did not augment the Landsat TM data with larger scale data. The data were analyzed by determining changes in NDVI between image dates and by

classification with the National Oceanic and Atmospheric Administration (NOAA) Coastal Change Analysis Program (C-CAP). The authors reported problems associated with differentiating between land cover classes and with respect to C-CAP concluded, "*that a determination could not be made as to whether variations in the marsh were due to differences in vegetation or due to water stress without field work.*" In this study, NDVI analysis did not prove useful in detecting changes in land cover.

3.3 Study Objectives

The objectives of this study were to:

1) Evaluate the applicability of the use of satellite-acquired remote sensing data to change detection at two wetlands reserves in Estonia;
2) Evaluate and apply Geographic Information System (GIS) analytical techniques to detect and quantify change at the wetlands reserves; and
3) Determine the extent to which Landsat TM and ETM+ data could be used without larger scale ancillary data in the detection of change in wetlands.

3.4 Study Limitations

This study used remote sensing data with a spatial resolution of thirty meters. Detailed image classification was not attempted due to the lack of supporting georeferenced ancillary data and because no means were available through which error assessment analyses could be performed. Spectral curves were not available that would be applicable to the specific vegetation regimes at the study areas.

Several elements exist that could cause conditions to vary within the year or between years that are not related to change in wetlands management or restoration practices. Differences in the phenological cycle between the two images exist. The 1988 dataset was collected on 9 June 1988, which is the 161st day of the year. The 1999 dataset collected on 10 July 1999, which is the 191st day of the year. No attempt was made to correlate wetland conditions to precipitation patterns.

Chapter Four
The Application of Remote Sensing

4.1 Introduction to Remote Sensing

Remote sensing is defined by Sabins (1996) as; "*methods that employ electromagnetic energy, such as light, heat, and radio waves, as a means of detecting and measuring target characteristics.*" The data used for this study compare remotely sensed light intensity as a function of wavelength. These data were collected by multispectral imaging instruments mounted in satellites with a sun synchronous orbit at an altitude of 705 kilometers (Farr, 1999). Conventional photographs collected by means of kite-aerial photography (KAP) were used to better visualize portions of the study area and to provide a means for identification of typical floral regimes on a non-georeferenced basis (Aber and Aber, 2001).

Satellite images can provide an immense amount of data about the Earth's surface with many advantages over land-based data acquisition techniques. These advantages include:

1) Low data acquisition cost per unit area;
2) Standard digital data formats that allow for ease in sharing and analyzing data;
3) High temporal resolution is possible;
4) Data acquisition is not affected by inhospitable subaerial conditions;
5) No limitation imposed by geopolitical boundaries; and

6) Ability to sense and separate bands of the electromagnetic spectrum, including regions not detectable by human vision.

4.2 Satellite Acquisition of Data

Two digital datasets were used for this study. The first dataset was acquired by the Thematic Mapper (TM) multispectral scanner aboard Landsat 5 satellite on 9 June 1988 (day 161 of 1988). The second dataset was acquired by the Enhanced Thematic Mapper Plus (ETM+) multispectral scanner aboard Landsat 7 satellite on 10 July 1999 (day 191 of 1999).

The Landsat program began data acquisition 23 July 1972 with the launch of Landsat 1. The latest addition to the Landsat program is Landsat 7, which was launched 15 April 1999. Currently, Landsats 5 and 7 are the only satellites in the Landsat program that remain with operational TM or ETM+ instruments aboard. Both satellites have near-polar, sun-synchronous orbits with altitudes of 705 kilometers and temporal resolutions of 16 days.

4.3 Data Collection Instrumentation

The TM was used for collection of the 9 June 1988 dataset and the ETM+ was used for the collection of the 10 July 1999 dataset. The datasets collected by these instruments are compatible with one another so that change may be detected by comparative analyses of the datasets. Both instruments collect data from seven spectral bands. ETM+ also has a panchromatic band, which has a higher spatial resolution.

The specifications for the spectral bands for each of the instruments are summarized in Table 4.1: Landsat Instrument Specifications. The visible portion of the electromagnetic spectrum range begins at 0.4 micrometers (blue) and ends at 0.7 μm (red) (Jensen, 1996). Bands 1, 2, and 3 are within the visible portion of the spectrum. Bands 4, 5, and 7 lie within the infrared portion of the spectrum and are outside the range that is detectable by human vision. Band 6 is in the thermal infrared portion of the spectrum. Some applications for each band are given in Table 4.2: Applications for Spectral Bands.

Table 4.1: Landsat Instrument Specifications
Adapted from Farr (1999)

Band	Thematic Mapper		Enhanced Thematic Mapper	
	Spectral Range (μm)	Ground Resolution (m)	Spectral Range (μm)	Ground Resolution (m)
1	0.45 – 0.53	30	0.45 – 0.52	30
2	0.52 – 0.60	30	0.53 – 0.61	30
3	0.63 – 0.69	30	0.63 – 0.69	30
4	0.76 – 0.90	30	0.75 – 0.9	30
5	1.55 – 1.75	30	1.55 – 1.75	30
6	10.40 – 12.50	120	10.40 – 12.5	60
7	2.08 – 2.35	30	2.09 – 2.35	30
Pan	---	---	0.52 – 0.90	15

Table 4.2: Applications for Spectral Bands
Based on Jensen (1996) and Lo (1986)

Band	Example Applications
1	Penetration of water bodies Discriminating between soil and vegetation Discriminating between coniferous and deciduous vegetation
2	Measuring vegetative vigor
3	Soil and geological boundary delineation Discrimination of types of vegetative cover
4	Determination of biomass content Determination of soil-crop and land-water interfaces
5	Determination of moisture content of vegetation Determination of moisture content of soil Discrimination between clouds, ice, and snow
6	Soil moisture content discrimination Vegetative stress analyses Thermal Mapping
7	Discriminating rock types thermal mapping
Pan	Visual identification surface features

4.4 Use of GIS in the Analysis of Remotely Sensed Data

4.4.1 Introduction

After remotely sensed data have been acquired, they must be analyzed with a geographic information system (GIS) program to extract meaningful information. The preparation of composite images and the use of spectral signatures relevant to the land cover types present can allow land cover maps to be prepared and further analyzed. Many methods exist for using mathematical procedures on the remotely sensed data to determine information about the land cover and factors related to conditions of the land cover. This section provides a brief overview of GIS analytical methods applicable to delineating wetlands and detecting and measuring factors related to wetlands conditions and change.

4.4.2 Preparation of Composite Images

A composite image is prepared by combining images from multiple spectral bands to form a single image to better contrast or identify features of interest. A composite image allows data from three spectral bands to be portrayed simultaneously in a single image. The composite image is prepared by assigning spectral bands to the blue, green, and red image bands, Idrisi32 then produces the composite image by stretching the three input images such that each cell has an integer digital number (DN) value between 0 and 5 and then calculating a new DN from which to construct the composite image (Eastman, 2000). Idrisi32 calculates the DN values for the composite image in accordance with equation 4.1.

$$composite\,DN = blue\,DN + green\,DN * 6 + red\,DN * 36$$

Equation 4.1

The TM and ETM+ datasets have six compatible bands (bands 1, 2, 3, 4, 5, and 7) from which composite images can be prepared. Band 6, the thermal infrared band, does not have the same resolution as the other bands and cannot be directly used in the preparation of composite images. If the composite images are formed such that the data used for the composite image are entered in ascending order (i.e., blue has the lowest band number, red has the highest band number, and the band used for green lies between those of red and blue), then twenty unique composite images can be formed from the six spectral bands.

Some composite images are potentially more useful than others because of greater contrast between the bands. The degree of contrast between the bands is determined by calculating the optimal index factor (OIF) for the image combination (Jensen, 1996). The OIF is calculated by equation 4.2.

$$OIF = \frac{\sum_{k=1}^{k=3} S_k}{\sum_{j=1}^{j=3} Abs(r_j)}$$

Equation 4.2

Where: S_k = Standard Deviation for Band K

r_j = Correlation Coefficient Between Bands

Idrisi32 does not directly calculate the OIFs; however, Idrisi32 modules can be used to extract the required variables for equation 4.2. The standard deviation for the DN values

for a band is printed as part of the image histogram available in the HISTO module. The interband correlation coefficient is printed as part of the output for the REGRESS module. The data necessary to calculate the OIFs for the 1988 Endla image are given in Table 4.3: Data for OIFs Calculations for 1988 Endla Scene.

The data in Table 4.3 were used to calculate the OIFs for the composite images that could be prepared from the 1988 Endla data set. The calculation for the composite image prepared with bands 1, 2, and 3 is given below.

$$OIF = \frac{\sum_{k=1}^{k=3} S_k}{\sum_{j=1}^{j=3} Abs(r_j)} = \frac{9.1525 + 5.9097 + 10.1724}{0.961747 + 0.959319 + 0.942536} = 8.812$$

The OIFs for all the possible band combinations for the 1988 Endla scene were calculated and data are given in Table 4.4: Possible Band Combination and OIFs for 1988 Endla Scene. The greater the OIF, the greater the contrast of the composite image produced from the band combination. Two example images that illustrate differing contrast are given in Figure 4.1: Composite Images.

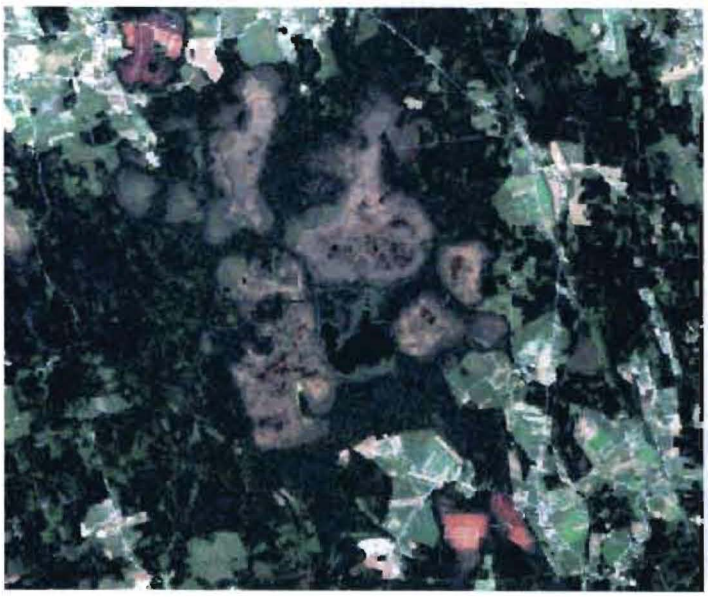

Endla Nature Reserve
Composite of Landsat TM Bands 1, 2, and 3 (1988). OIF = 8.8

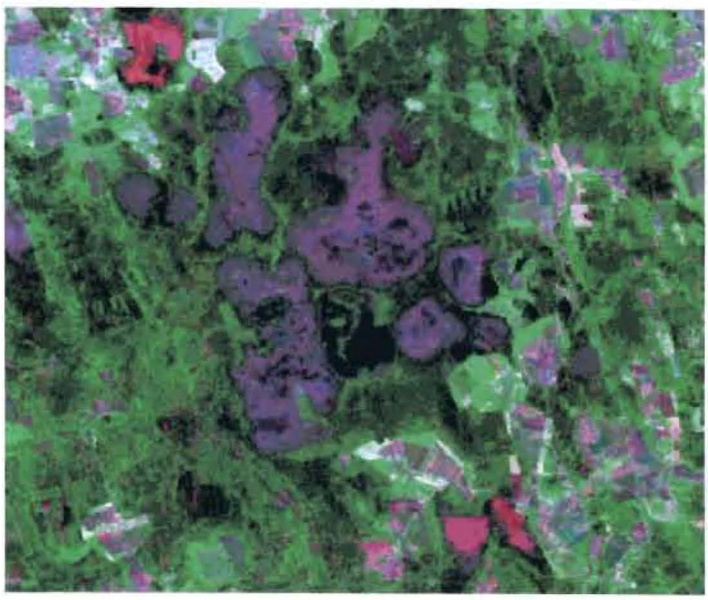

Endla Nature Reserve
Composite of Landsat TM Bands 3, 4, and 7 (1988). OIF = 50.8

Figure 4.1: Composite Images

Table 4.3: Data for OIFs Calculations for 1988 Endla Scene

Standard Deviation for DNs		Correlation Coefficients	
Band	Standard Deviation	Band Pair	Correlation Coefficient
1	9.1525	1 – 2	0.961747
2	5.9097	1 – 3	0.959319
3	10.1724	1 – 4	0.155518
4	26.1177	1 – 5	0.861088
5	26.6954	1 – 7	0.915858
7	17.6231	2 – 3	0.942536
		2 – 4	0.272122
		2 – 5	0.894271
		2 – 7	0.904028
		3 – 4	0.018520
		3 – 5	0.856712
		3 – 7	0.947501
		4 – 5	0.400885
		4 – 7	0.095285
		5 – 7	0.928683

Table 4.4:

Possible Band Combination and OIFs for 1988 Endla Scene

Band Combination	OIF
123	8.8
124	29.6
125	15.4
127	11.8
134	40.1
135	17.2
137	13.1
145	43.7
147	45.3
157	19.8
234	34.2
235	15.9
237	12.1
245	37.5
247	39.1
257	18.6
345	49.4
347	50.8
357	28.7
457	49.4

Some bands are particularly useful in identifying certain features and these combinations should not be eliminated from analyses due to a low OIF. A composite prepared from bands 1, 2, and 3 produces a natural-color image that shows a scene in a manner that approximates the way the it would appear when viewed directly with human vision. A composite image from bands 1, 2, and 3 is useful in that in allows visual recognition of features; however, this composite combination has the lowest possible OIF (OIF = 8.8) of all the possible image combinations from the Endla 1988 data set. A composite prepared from bands 2, 3, and 4 is useful in identifying healthy vegetation, urban areas, and wetlands (Jensen, 1996). This composite has an OIF of 34.2 for the Endla 1988 data set. The composite image prepared from bands 3, 4, and 5 is useful in delineating soil and water interfaces, vegetation types, and soil moisture (Jensen, 1996). Another useful composite for wetlands delineation and vegetation vigor assessment can be prepared from bands 2, 4, and 7. The composite image prepared from these bands with the Endla 1988 data set has an OIF of 39.1 and is useful for determining relative moisture content of soils and vegetation, wetlands, urban areas, and forests (Jensen, 1996).

Composite images–particularly those with bands 1, 2, and 3; bands 2, 3, and 4; and bands 2, 4, and 7–are effective to help delineate wetlands. These composite images can also aid in measuring relative vegetation vigor and in determining the types of vegetation present in the study area.

4.4.3 Direct Mathematical Manipulation of Image Bands

Mathematical operations (map algebra) can be performed on an intra- or inter-band basis to produce a resultant image. These operations may be scalar, transformed, or combinational (Eastman, 2000).

A common use for the scalar operation is haze correction, which is performed by adjusting the image histogram so that the left tail of the histogram is equal to zero (Richards and Jia, 1999). This operation was used to perform haze correction on the datasets used in this study and is further discussed in Section 5.2: Image Haze Correction.

Image transformations can be performed using nonlinear operations such as logarithmic or trigonometric operations. An example use of a nonlinear function is the calculation of the transformed vegetation index (Richards and Jia, 1999). The transformed vegetation index (TVI) is calculated by equation 4.3 (Jensen, 1996; Richards and Jia, 1999).

$$TVI = \sqrt{Vegetation\ Index + 0.5}$$

Equation 4.3

Combinational operations are useful in determining vegetation vigor. A frequently used combinational operation for quantifying vegetation vigor is the normalized difference vegetation index (NDVI). The NDVI is calculated by equation 4.4 (Jensen, 1996).

$$NDVI = \frac{band\,4 - band\,3}{band\,4 + band\,3}$$

Equation 4.4

4.4.4 Analysis of Spectral Signatures to Identify Surface Features

Many features and vegetation types can be distinguished by their reflectance and emittance properties. A spectral curve or signature for an object is generated by plotting the object's reflectance intensity as a function of wavelength (Avery and Berlin, 1992). Spectral curves can be generated using a portable radiometer (Avery and Berlin, 1992). Spectral signatures can be used with satellite-acquired multispectral data to identify surface features and vegetation types.

Spectral data for several floral species are available from the United States Geological Society (USGS) Spectroscopy Laboratory (Clark et al., 1993). The spectral data for selected floral species are given in Table 4.5: Spectral Data for Selected Floral Species. Spectral curves for these species are given in Appendix A: Spectral Curves for Selected Floral Species.

The data in Table 4.5 show that it may be possible to determine the type of vegetation present using the USGS spectral curves; although, not necessarily to the species level using spectral data from the TM and ETM+ spectral bands. In general, it should be possible to categorize woody vegetative as being deciduous or evergreen. Composite images prepared from the bands showing the greater difference in reflectance between the vegetation types of interest would be useful in the discrimination of vegetation types.

Table 4.5: Spectral Data for Selected Floral Species

(Data Source: Clark et al., 1993)

Band	Maximum Reflectance					
	Blue Spruce	Fir	Pinion Pine	Walnut	Maple	Dry Long Grass
1	0.11	0.08	0.15	0.08	0.10	0.32
2	0.11	0.48	0.52	0.52	0.10	0.34
3	0.30	0.54	0.55	0.54	0.55	0.36
4	0.40	0.53	0.52	0.53	0.65	0.38
5	0.11	0.20	0.18	0.34	0.38	0.30

Chapter Five

Preparation of Datasets

5.1 Introduction

Before the images can be used for analysis for change, certain standardizations and adjustments must be made to each image. The operations described in this chapter are applicable to each band within the image set.

The first operation (haze correction) removes atmospheric distortion and ensures a common origin for the brightness values (digital numbers). Following haze correction the images are geometrically adjusted such that images collected on different dates can be overlain for comparison. This operation is called resampling.

5.2 Haze Correction

Haze correction is a process by which the image histograms are shifted to the left such that the left tail of curve has an x-value of zero or one. Haze correction is performed to subtract atmospheric effects on the digital numbers that represent brightness level (Richards and Jia, 1999). Haze correction is a scalar operation whereby a constant is subtracted from each digital number in the image. For this study, the histograms were shifted such that the minimum digital number was equal to one. One was selected as the minimum digital number for haze correction so that zero could be reserved for indicating an area not covered by the image during the resampling process.

In Idrisi32 (Eastman, 2000), haze correction is performed by determining the minimum digital number in the image and then subtracting the appropriate constant. The minimum digital number is determined by using the FILE EXPLORER module to view the metadata for the image. The SCALAR module is then used to subtract the appropriate constant from each digital number. This operation is performed for each band. The original and haze corrected histograms for band 2 of the 1988 image are given on Figure 5.1: Histograms for Haze Correction.

5.3 Resampling

Prior to use of the datasets for analyses to determine changes in land use and cover, corrections to one or both of the images must be made to account for geometric distortion (Richards and Jia, 1999). This correction must be made to data from each band that is to be used; however, since all bands are correctly registered to one another, the correction technique used for any band may be applied to the remaining bands. Resampling was conducted using the general linear model (GLM) to perform multiple regression to derive two predictor equations; one for the y value and one for the x value needed to adjusted the geometric grid of the image being resampled to match that of the image to be used for comparison in the data analyses. Resampling was performed on the whole scene prior to selecting the scene windows for the study areas.

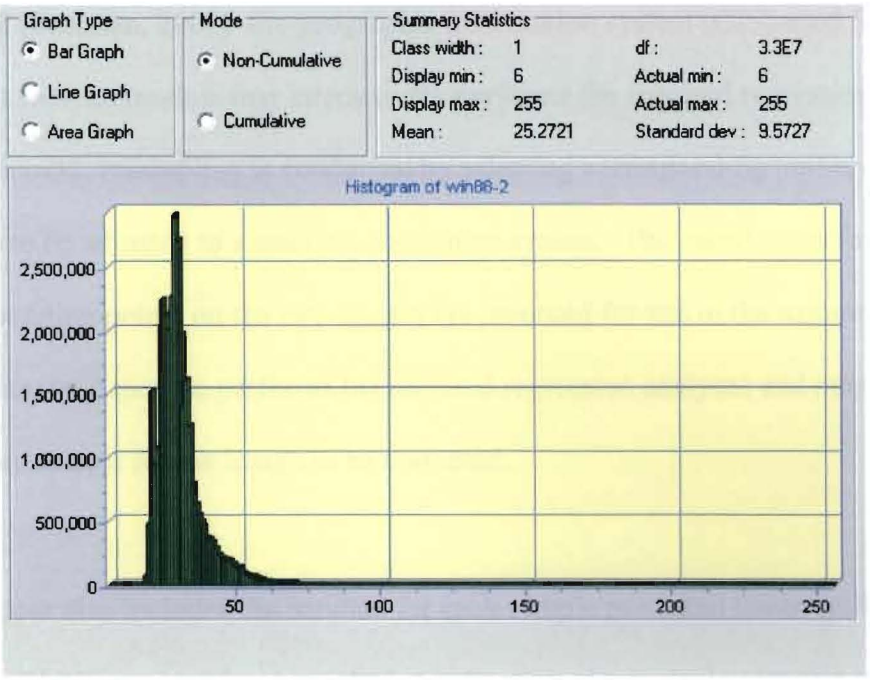

Histogram for Band 2 of Original 1988 Image

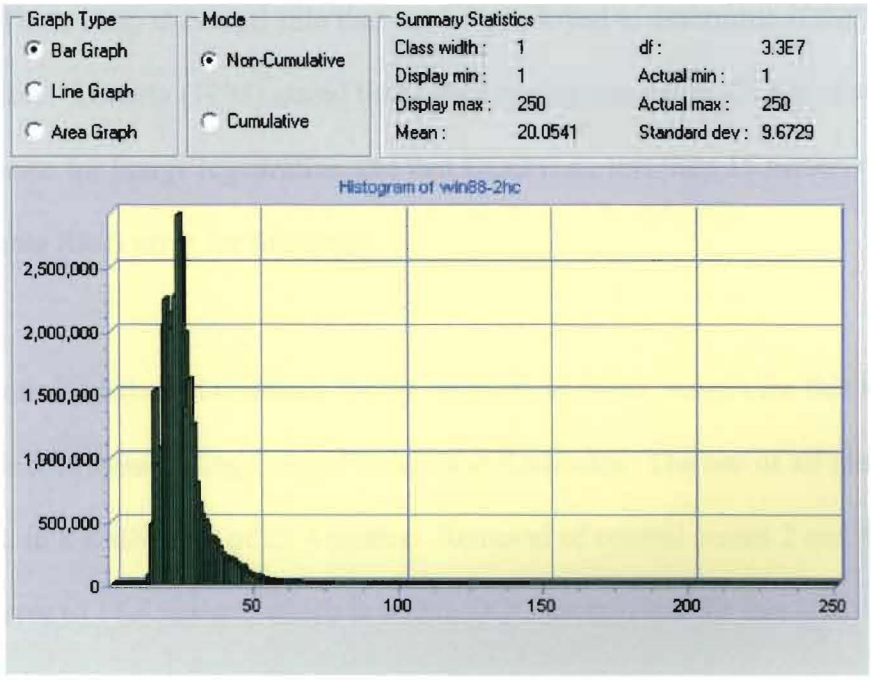

Histogram of Band 2 for Haze Corrected 1988 Image
Note that the histogram has shifted to the left by five units

Figure 5.1: Histogram for Haze Correction

Idrisi32 (Eastman, 2000)–the geographic information system (GIS) used for this study–has a RESAMPLE module that interactively performs the required regression analyses. With Idrisi32, resampling is conducted by selecting corresponding points on the two images to be adjusted to a uniform coordinate system. The coordinates for the corresponding points on the two images are recorded for use in the RESAMPLE module. The RESAMPLE module performs the required regression analyses and outputs the old and new coordinates for the image to be corrected.

The output also includes the residual for each sample point and the overall root mean square (RMS) error. A large residual is indicative of a control point that was not well matched. Removal of control points with large residuals will improve the overall RMS error. There is no universal rule that can be employed to determine if the RMS error is acceptable. Lunetta (1998) stated that a data quality objective (DQO) of ±0.5 pixel width is adequate for image registration and that DQO (i.e., less than 15 meters) was used as an acceptable RMS error for this study.

The control points and residuals for the resampling of the images for this study are given in Table 5.1: Resampling Control Points and Residuals. The use of all nine control points resulted in a RMS error of 25.4 meters. Removal of control points 2 and 4 reduced the RMS error to 11.5 meters, which is within DQO established for this study.

Table 5.1: Resampling Control Points and Residuals

Point	Old $X^{(1)}$	Old $Y^{(1)}$	New $X^{(2)}$	New $Y^{(2)}$	Residual
1	86.654239	37.210182	73.592907	34.880849	0.009547
2	26.119046	23.351162	11.516019	37.920695	0.039696
3	97.238226	115.99090	105.03730	107.96762	0.006118
4	21.788635	72.736363	20.703937	86.684937	0.042521
5	63.527200	74.708746	61.465950	77.307729	0.017765
6	21.014207	79.726001	21.857826	93.695564	0.017696
7	10.058951	76.680834	10.511541	93.717980	0.0099338
8	26.051061	23.288796	11.496545	37.884555	0.008392
9	21.207948	72.056284	19.984653	86.234524	0.004362

Notes: (1) Old refers to the original coordinate value prior to resampling
(2) New refers to the modified coordinate value after resampling

The regression equations generated by the Idrisi32 RESAMPLE module are given as equations 5.1 and 5.2.

$$Old\ x = \beta_{0x} + \beta_{1x}(new\ x) + \beta_{2x}(new\ y)$$

Equation 5.1

$$Old\ y = \beta_{0y} + \beta_{1y}(new\ x) + \beta_{2y}(new\ y)$$

Equation 5.2

Where: $\beta_{0x} = 25.1886334$

$\beta_{1x} = 0.962759$

$\beta_{2x} = -0.269323$

$\beta_{0y} = -16.248158$

$$\beta_{1y} = 0.270904$$

$$\beta_{2y} = 0.961199$$

The calculations for the control point one are given below.

$$Old\ x = 25.1886334 + 0.9627594(73.592907) - 0.269323(34.880849) = 86.646671$$

$$Old\ y = -16.24815841 + 0.2709037(73.592907) + 0.9611986(34.880849) = 37.215854$$

The residual for the control point is calculated by equation 5.3.

$$residual = \sqrt{(measured\ old\ x - calculated\ old\ x)^2 + (measured\ old\ y - calculated\ old\ y)^2}$$

Equation 5.3

The calculation for the residual at control point one is given below.

$$residual = \sqrt{(86.654239 - 86.646671)^2 + (37.210182 - 37.215854)^2} = 0.0094575$$

5.4 Windowing

The original images covered a much larger area than was applicable to this study; therefore, it was necessary to extract two sub-images that covered the study areas from the original images. The original 1988 image covered an area of 29,000 km^2 and the 1999 image covered an area of 17,784 km^2. Idrisi32 has a WINDOW module for extracting sub-images.

For both study areas, a sub-image was selected that included the reserve plus a peripheral area. This peripheral area is important because change within the reserve can be influenced by change in the less regulated reserve periphery.

The sub-image for the Endla Nature Reserve was extracted to provide an area of approximately 320 km^2. This includes the Endla Nature Reserve area of 80.5 km^2 plus a peripheral area around the perimeter of the reserve. The sub-image extracted for the Emajõe Suursoo Reserve has an area of 665 km^2 of which about 185 km^2 are located with the boundary of the reserve.

Chapter Six
Analysis of Change

6.1 Introduction

Change can be detected in either a qualitative or a quantitative manner. Qualitatively, multiple images can be compared to see if visual distinctions can be made between the images. Visual comparison is a good starting point for the identification of salient areas and inter-image change; however, it is not adequate for documenting change or for numerically describing the amount of change. This study focused on the application of numerical methods to analyze multispectral images to identify and quantify changes in land cover that occurred between 1988 and 1999. Analysis of change was conducted by image differencing, image ratioing, normalized difference vegetation index analysis, tasseled-cap transformation, and correlation analysis.

Image classification using either supervised or unsupervised classification was used in many of the studies in the literature review. In most successful cases, the investigators augmented the multispectral data with other data such as field surveys or georeferenced photography. In this study, classification was not used due to the lack of georeferenced ancillary data and the absence of a means by which to prepare an error matrix. Without a means to access the accuracy of the land cover classifications, it would not be possible to determine if differences were attributable to change or the result of classification error.

6.2 Image Differencing

Detection of change in two temporally spaced images can be determined by subtracting digital numbers (DNs) of one image from those of the image being compared. Image differencing is simple, can be conducted at low-cost, and allows tremendous amount of data to be processed in a short amount of time. A difficulty encountered in using image differencing for detecting change is determining what amount of difference constitutes a statistically significant change.

A schematic example of this operation is given in Figure 6.1: Image Differencing. Theoretically, a difference of zero in a cell should indicate that no change has occurred between the two dates; however, due to noise within the data acquisition system it should be expected that some numerical difference exists that is not due to actual change in land cover. For the purpose of this study, no change offset was taken to be the mean difference between the two data sets being compared. A difference of one standard deviation from the mean difference between the two data sets was used as the statistical threshold value for determining if change had occurred.

Image A

2	8	6	4
2	6	0	6
8	5	2	3
7	4	6	3

–

Image B

3	7	2	3
8	5	2	6
3	2	1	0
1	2	0	4

=

Image C

-1	1	4	1
-6	1	-2	0
5	3	1	3
6	2	6	-1

Figure 6.1: Image Differencing

After the image differencing operations were performed, a new image was prepared for each band using the Idrisi32 RECLASS module to identify areas of change (i.e., those area that are more than one standard deviation from the mean difference of the two datasets). The summary statistics for the image differencing are given in Table 6.1: Summary Statistics for Image Differencing – Endla and Table 6.2: Summary Statistics for Image Differencing – Emajõe. The original images, the difference images, and reclassed images are given in Appendix B: Image Differencing – Endla and Appendix C: Image Differencing – Emajõe.

Table 6.1: Summary Statistics for Image Differencing – Endla

Band	Mean Difference	Standard Deviation	Minimum DN	Maximum DN	Percent of Area < Mean Minus 1 s.d.	Percent of Area > Mean Plus 1 s.d.
1	-14.34	7.08	72	-113	5.4	10.6
2	-6.53	5.06	41	-124	13.0	7.7
3	-5.12	9.19	73	-182	10.1	7.2
4	-23.84	20.82	100	-134	11.2	12.1
5	2.68	19.03	113	-114	10.0	11.8
7	-7.18	14.69	82	-129	9.3	8.5

Table 6.2: Summary Statistics for Image Differencing – Emajõe

Band	Mean Difference	Standard Deviation	Minimum DN	Maximum DN	Percent of Area < Mean Minus 1 s.d.	Percent of Area > Mean Plus 1 s.d.
1	-12.28	12.97	-64	144	2.8	12.3
2	-3.78	7.11	-76	63	12.8	10.2
3	-2.05	9.33	-104	79	8.5	10.1
4	-16.06	24.62	-152	132	16.2	11.8
5	1.36	17.59	-113	137	9.3	10.5
7	-5.77	12.14	-133	94	9.2	6.5

6.3 Image Ratios

Image ratioing to identify change is conducted by dividing the DNs of one data set by those of a temporally separated data set of the same spectral band. This method is a simple and fast method for identifying change (Yuan et al., 1988). A schematic example of this operation is shown in Figure 6.2: Image Ratioing.

Image ratioing is not a linear transform (Richards and Jia, 1999). Two methods have been proposed to aid in the interpretation of nonlinear data resulting from the ratioing operation. Yuan et al. (1988) suggested that the original datasets may be transformed in order that the resultant data may have a more normal distribution. Eastman et al. (2000), suggests transforming the resultant data from the ratioing operation by using a log transformation. The method of Eastman et al. (2000) was used in this study.

The summary statistics for the image ratios are given in Table 6.3: Summary Statistics for Image Ratios – Endla and Table 6.4: Summary Statistics for Image Ratios – Emajõe. The original images, ratioed images, and reclassified images are given in Appendix D: Image Ratios – Endla and Appendix E: Image Ratios – Emajõe.

Image A

2	8	6	4
2	6	4	6
8	5	2	3
7	4	6	3

÷

Image B

3	7	2	3
8	5	2	6
3	2	1	1
1	2	6	4

=

Image C

0.67	1.14	3	1.33
0.25	1.2	2	1
2.67	2.5	2	3
7	2	1	0.75

Figure 6.2: Image Ratioing

Table 6.3:

Summary Statistics for Log Transformed Image Ratioing – Endla

Band	Mean Transformed DN	Standard Deviation	Minimum DN	Maximum DN	Percent of Area < Mean Minus 1 s.d.	Percent of Area > Mean Plus 1 s.d.
1	-0.4116	0.1933	-1.4641	0.9458	9.4	2.3
2	-0.2231	0.1414	-1.7214	0.9237	12.6	11.1
3	-0.1584	0.2123	-1.9273	1.2379	20.2	10.0
4	-0.2669	0.2228	-2.3026	2.5729	9.6	12.7
5	0.0224	0.2363	-2.5494	1.8083	11.0	12.3
7	-0.2784	0.3407	-2.5903	1.3754	10.3	11.8

Table 6.4:

Summary Statistics for Log Transformed Image Ratioing – Emajõe

Band	Mean Difference	Standard Deviation	Minimum DN	Maximum DN	Percent of Area < Mean Minus 1 s.d.	Percent of Area > Mean Plus 1 s.d.
1	-0.4199	0.3496	-1.8458	1.5876	10.5	15.2
2	-0.1397	0.2380	-1.2470	1.5041	10.0	11.7
3	-0.0812	0.2529	-1.5702	1.5241	9.6	12.6
4	0.0968	0.7083	-3.091	3.2958	4.7	21.9
5	-0.0331	0.3717	-2.7408	2.0919	15.5	10.5
7	-0.3215	0.4141	-3.434	1.8718	12.7	11.5

6.4 Normalized Difference Vegetation Index

The normalized difference vegetation index (NDVI) was developed in 1974 by J. Rouse et al. (in Jensen, 2000). The NDVI is calculated by equation 6.1.

$$NDVI = \frac{DN_{Band\,4} - DN_{Band\,3}}{DN_{Band\,4} + DN_{Band\,3}}$$

Equation 6.1

NDVI values can range from –1 to 1. Healthy green vegetation is represented by NDVI values in the upper end of the range while water and soil are represented by values in the lower end of the range (Sabins, 1996).

The NDVI images for the 1988 and 1999 datasets along with an image prepared by subtracting the 1999 dataset from the 1988 dataset are included in Appendix F: NDVI Images – Endla. The NVDI images for Emajõe are included in Appendix G: NDVI Images – Emajõe.

6.5 Tasseled-Cap Transformation

The tasseled-cap transformation (TCT) is a pixel-wise transformation that is useful in determining vegetation and soil properties (Rees, 1999). For TM and ETM+ data, three transforms are generated. These transforms are; brightness, greenness, and wetness. The TCT is calculated by equation 6.2 (Eastman, 2000; Rees, 1999).

$$x_i' = \sum_{j=1}^{N} a_{ij} * x_j + b_i$$

Equation 6.2

Where: x_1' = brightness transform
x_2' = greenness transform
x_3' = wetness transform

$$a_{ij} = \begin{bmatrix} 0.304 & 0.279 & 0.434 & 0.559 & 0.508 & 0.186 \\ -0.285 & -0.244 & -0.544 & 0.724 & 0.084 & -0.180 \\ 0.151 & 0.179 & 0.330 & 0.341 & -0.711 & -0.457 \end{bmatrix}$$

x_j = DN band j

b_i = optional offset, if x_i' is to be positive. Idrisi32 uses $\begin{bmatrix} 0 \\ 0 \\ 0 \end{bmatrix}$

Idrisi32 can calculate the TCT using the TCA module or it can be calculated using the image calculator function with equation 6.2. Rees (1999) cautions that since the TCT coefficients were derived for agricultural areas in the United States, their use for other applications should be evaluated critically.

Image differencing was used to identify areas of change based on the TCT images. The percent of the areas more than one standard deviation from the mean for the Endla dataset are given in Table 6.5: TCT Areas More Than One Standard Deviation from the Mean – Endla. The Emajõe data are given in Table 6.6: TCT Areas More Than One Standard Deviation from the Mean – Emajõe. The TCT images, difference images, and reclassification images Endla are given in Appendix H: TCT Images – Endla and Appendix I: TCT Images – Emajõe.

Table 6.5: TCT Areas More Than One Standard Deviation from the Mean – Endla

TCT Transformation	% of Image < mean minus one standard deviation	% of Image > mean plus one standard deviation
Brightness	10.6	11.3
Greenness	10.8	10.3
Moisture	10.4	9.1

Table 6.6: TCT Areas More Than One Standard Deviation from the Mean – Emajõe

TCT Transformation	% of Image < mean minus one standard deviation	% of Image > mean plus one standard deviation
Brightness	12.1	10.5
Greenness	12.8	10.7
Moisture	10.8	5.8

6.6 Correlation Analysis

Regression analyses can be used to measure the correlation between two images collected on separate dates to assess change. The regression analyses can be performed using the general linear model to fit the data to a regression line using the method of least squares. The regression analyses produce a line equation of the form given by equation 6.3.

$$\hat{y} = \hat{\beta}_0 + \hat{\beta}_1 x$$

Equation 6.3

Where: $\hat{y}$ = estimated value of y

$\hat{\beta}_0$ = estimated intercept of line

$\hat{\beta}_1$ = estimated slope of line

Equation 6.4 is used to determine $\hat{\beta}_1$ and $\hat{\beta}_1$ is determined by equation 6.5.

$$\hat{\beta}_1 = \frac{\sum_{i=1}^{N}\left(DN_{ix} - \overline{DN}_x\right)\left(DN_{iy} - \overline{DN}_y\right)}{\sum_{i=1}^{N}\left(DN_{ix} - \overline{DN}_x\right)^2}$$

Equation 6.4

$$\hat{\beta}_0 = \overline{DN}_y - \hat{\beta}_1 \overline{DN}_x$$

Equation 6.5

Where: $\hat{\beta}_1$ = estimated value for slope of regression line

$\overline{DN}_x$ = mean digital number for image x

DN_{ix} = digital number for datum i from image x

$\overline{DN}_y$ = mean digital number for image y

$\overline{DN}_{iy}$ = digital number for data i from image y

$\hat{\beta}_0$ = estimated value of the intercept of the regression line

The correlation between the two images is calculated by equation 6.6. The range of correlation coefficients (r) is from –1 to 1. An r value of zero indicates there is no correlation between the two data sets. Values near –1 indicated a high degree of correlation between the two data sets and a regression line with a negative slope. Values near 1 indicate a high degree of correlation between the two data sets and a regression line with a positive slope.

$$r = \hat{\beta}_1 \sqrt{\frac{\sum_{i=1}^{N} \left(DN_{ix} - \overline{DN}_x\right)^2}{\sum_{i=1}^{N} \left(DN_{iy} - \overline{DN}_y\right)^2}}$$

Equation 6.6

Regression analyses can be performed in Idrisis32 with the REGRESS module. The image can also be saved in the byte/ascii format which will allow the data to be imported into a statistical analysis program, if information is required beyond that provided the Idrisi32 REGRESS module. For this study, the Idrisi32 REGRESS module was used for the analyses; however, one set of data (band 1 for Endla 1988 and Endla 1999) was exported to STATVIEW for regression analyses to verify the algorithm used by Idrisi32. Both techniques produced the same result.

The summary data for the regression analyses are given in Table 6.7: Summary Data for Regression Analyses – Endla and Table 6.8: Summary Data for Regression Analyses – Emajõe. The regression plots produced by IDRISI32 are given in Appendix J: Regression Plots – Endla and Appendix K: Regression Plots – Emajõe.

Table 6.7: Summary Data for Regression Analyses – Endla

Band	$\hat{\beta}_0$	$\hat{\beta}_1$	r	r^2	RMS Error
1	34.142	0.356	0.639	0.408	3.922
2	8.478	0.925	0.7352	0.537	5.040
3	14.211	0.699	0.634	0.402	8.664
4	49.776	0.686	0.683	0.466	19.144
5	26.632	0.602	0.602	0.362	15.794
7	20.873	0.531	0.610	0.372	12.148

Table 6.8: Summary Data for Regression Analyses – Emajõe

Band	$\hat{\beta}_0$	$\hat{\beta}_1$	r	r^2	RMS Error
1	39.000	0.098	0.305	0.093	4.149
2	11.82	0.669	0.584	0.341	6.698
3	16.748	0.490	0.548	0.300	7.708
4	3.002	1.204	0.886	0.785	23.29
5	11.762	0.764	0.855	0.731	15.689
7	14.025	0.630	0.686	0.471	10.619

Chapter Seven
Data Interpretation

7.1 Interpretation of Data for Endla Nature Reserve

7.1.1 Image Differencing

Image differencing was performed on bands 1, 2, 3, 4, 5, and 7 by subtracting the digital numbers of the 1999 images from those of the 1988 images on a pixel-wise basis. The summary statistics for the operation are given in Table 6.1: Summary Statistics for Image Differencing – Endla. The image differencing images, including reclassified images showing areas deviating from the mean by more than one standard deviation, are included in Appendix B: Image Differencing – Endla.

A difference of more than one standard deviation from the mean between the two datasets was used as the statistical threshold value for defining change. With this criterion, the percentage of the image affected by change between the dates ranged from 11.0 percent (band 1) to 23.3 percent (band 4), with the mean change being 18.7 percent.

A visual examination of the reclassified images shows that change has been most dramatic around the periphery of the nature reserve. Little change is noted in the portion of the image in which the nature reserve is located. The image produced from band 4 shows a change in Endla Lake. The reclassified image for band 4 is given on Figure 7.1: Image Difference Landsat Band 4 – Endla Nature Reserve. This change is probably due to a greater biomass concentration in the lake in 1988 than was present in 1999.

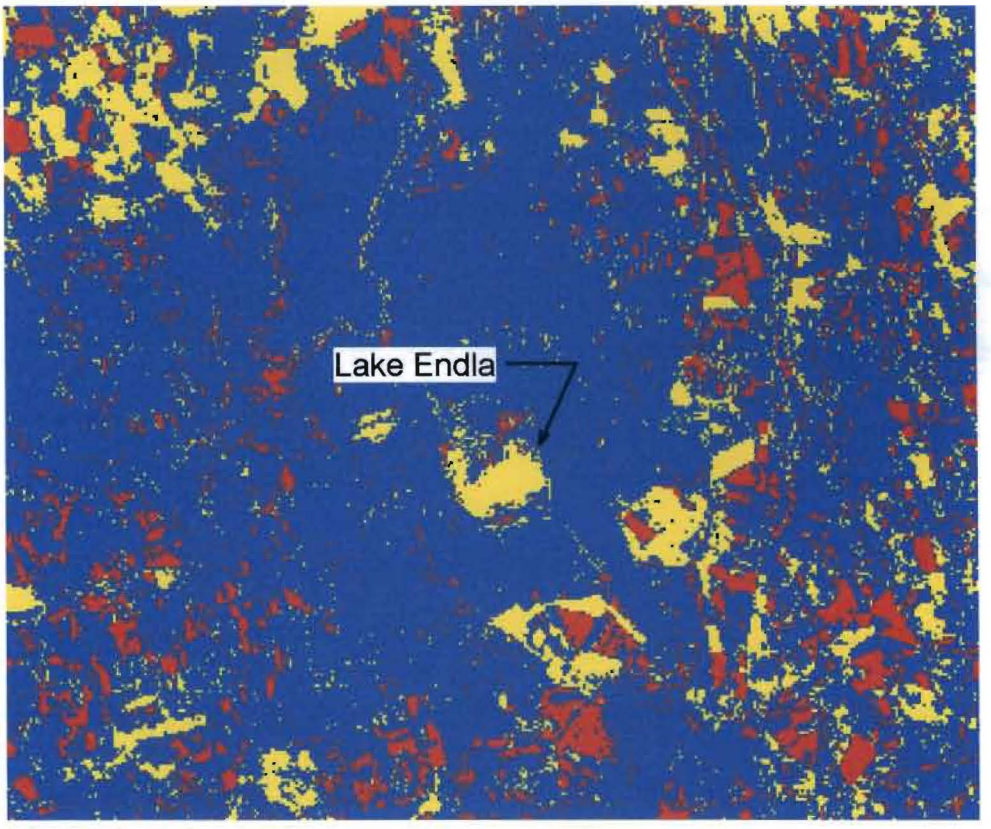

Map Scale 1:137,500

0 1 2 3 4 5
Scale (km)

1988 Band 4 minus 1999 Band 4 - Reclassified
Blue is within one standard deviation (s.d.) of mean
Yellow is more than 1 s.d. greater than mean
Red is more than 1 s.d. less than mean

Figure 7.1: Image Difference Landsat Band 4 -- Endla Nature Reserve

7.1.2 Image Ratioing

Image ratioing was conducted by dividing the digital numbers from the 1988 image by those from the 1999 image on a pixel-wise basis. The resultant data were transformed by taking their natural logarithms as suggested by Eastman (2000). This resulted in a dataset more closely conforming to a normal distribution. The summary statistics for the operation are given in Table 6.3 Summary Statistics for Log Transformed Image Ratios – Endla. The image ratio images, including reclassified images showing areas that deviate from the mean by more than one standard deviation, are included in Appendix D: Image Ratios – Endla.

As with image differencing, a deviation of more than one standard deviation from the mean was classified as change. The percentage of the image areas affected by change was between 11.6 percent (band 1) and 30.2 percent (band 3), with the mean amount of change being 22.2 percent.

The reclassification images show most of the change to have occurred around the periphery of the nature reserve. The reclassified images for bands 4 and 5 show change in Endla Lake. The reclassified image for band 4 shows Endla Lake to be more than one standard deviation greater than the mean; whereas, the band 5 image shows Endla Lake to be more than one standard deviation less than the mean. The image prepared from band 4 is given on Figure 7.2: Image Ratio Landsat Band 4 – Endla Nature Reserve. This could be the result of greater biomass in Endla Lake in 1988 than was present in 1999.

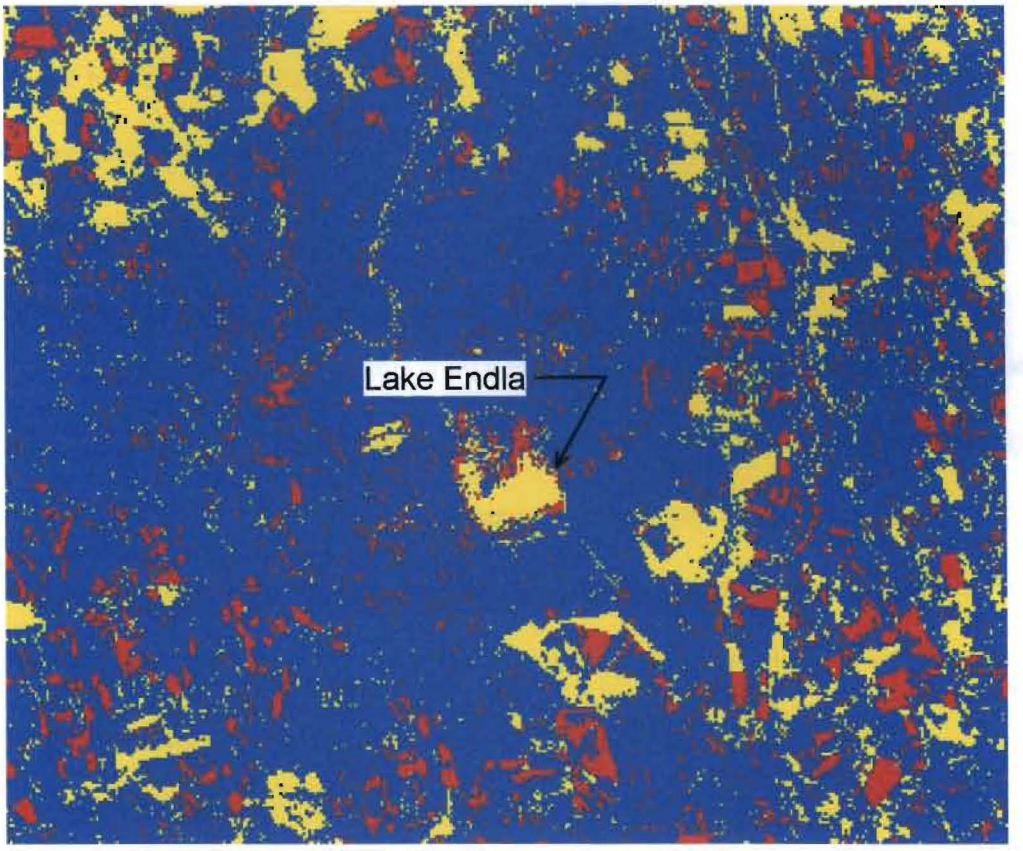

Map Scale 1:137,500

0 1 2 3 4 5
Scale (km)

1988 Band 4 divided by 1999 Band 4 - Reclassified
Blue is within one standard deviation (s.d.) of mean
Yellow is more than 1 s.d. greater than mean
Red is more than 1 s.d. less than mean

Figure 7.2: Image Ratio Landsat Band 4 -- Endla Nature Reserve

7.1.3 Normalized Difference Vegetation Index

Normalized difference vegetation index (NDVI) calculations were performed to determine if a change in vegetation vigor could be noted. The NDVI images are given in Appendix F: NDVI Images – Endla. NDVI values can range from –1 to 1. Healthy green vegetation is represented by NDVI values in the upper end of the range; whereas, water and soil are represented by values in the lower end of the range (Sabins, 1996).

The NDVI image from 1999 shows significantly more vigorous vegetation than does 1988 image. The NDVI images that illustrate this change in vegetation vigor are given on Figure 7.3: NDVI – Endla Nature Reserve. This change is present throughout the entire scene; however, the change is most significant around the periphery of the nature reserve. Vegetation in Estonia is generally more vigorous in July than in June, so some of this change may be attributable to differences in the phenologic cycle.

7.1.4 Tasseled-Cap Transformation

Tasseled-cap transformations were performed as described in Section 6.5: Tasseled-Cap Transformations. The summary statistics for this operation are given in Table 6.5: TCT Areas More than One Standard Deviation from the Mean. The tasseled-cap transformation images are given in Appendix H: TCT Images – Endla.

The change distribution for the transforms appears to be symmetrically distributed, with the percentage of reclassified scene exceeding the mean by more than one standard

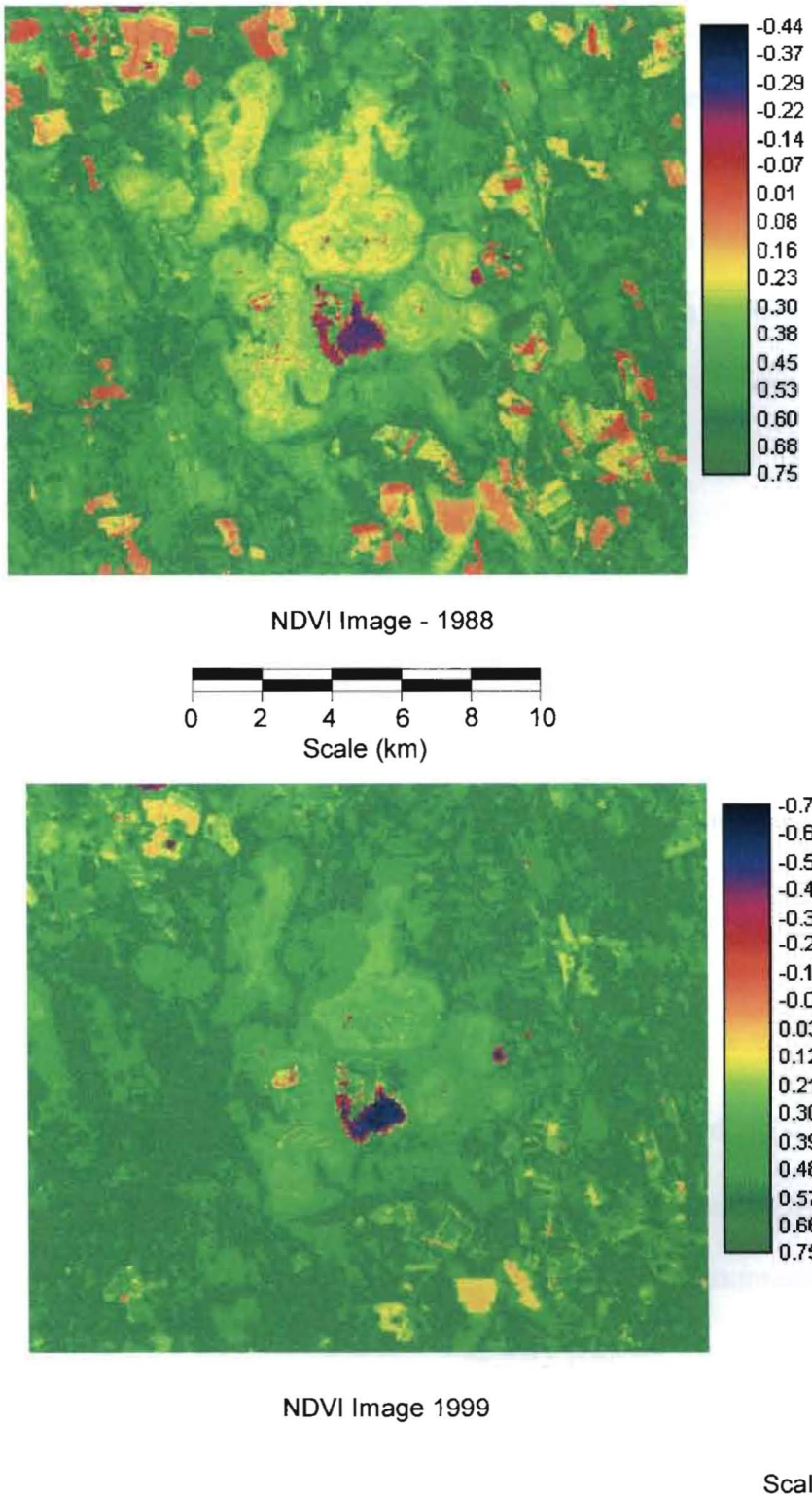

Figure 7.3: NDVI -- Endla Nature Reserve

deviation being approximately equal to the amount of the scene being more than one standard deviation less than the mean. The most interesting tasseled-cap transformation image is the greenness transformation, which shows vegetation to be more vigorous in 1999 than in 1988. The tasseled-cap images that illustrate this change are given on Figure 7.4: Tasseled-Cap Greenness Transformation – Endla Nature Reserve. The change shown in this image is generally concordant with that shown by the NVDI image and shows an increase in vegetation vigor and distribution in the 1999 scene.

7.1.5 Correlation Analysis

Regression analyses were conducted to measure the correlation between the 1988 and the 1999 image bands. The analyses were conducted using the general linear model to fit a regression line using the method of least squares as described in Section 6.6: Correlation Analysis.

In a case where no change has occurred, the regression line would have an intercept ($\hat{B}_o$) equal to zero and a slope ($\hat{B}_1$) equal to one. In a no change condition, the correlation coefficient (r^2) is equal to one, which is also the case where change has occurred but all change in y-values can be explained by the change in x-values. The summary data for the regression analyses are given in Table 6.7: Summary Data for Regression Analyses – Endla. The data are presented graphically in Appendix J: Regression Plots – Endla. The data show change occurred between 1988 and 1999. The intercept values ranged from

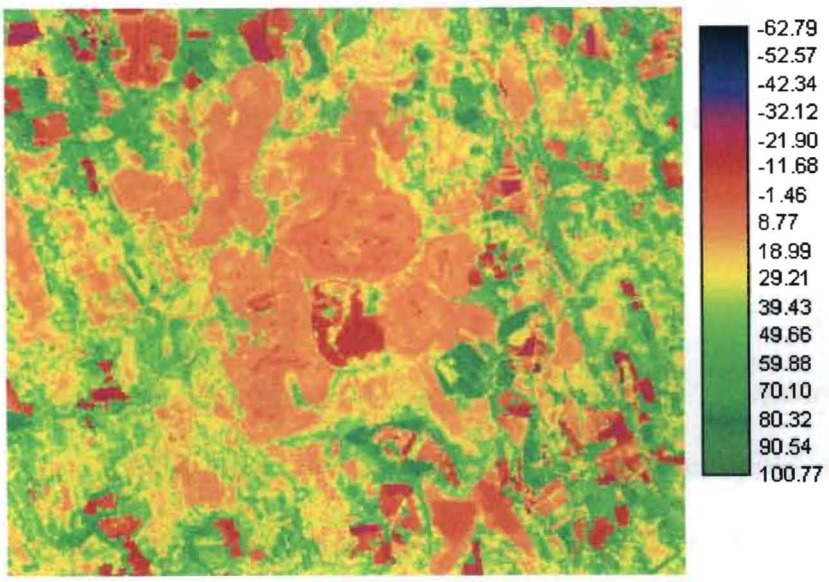

Tasseled-cap Greenness Transformation -- 1988

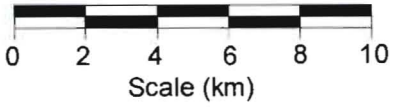

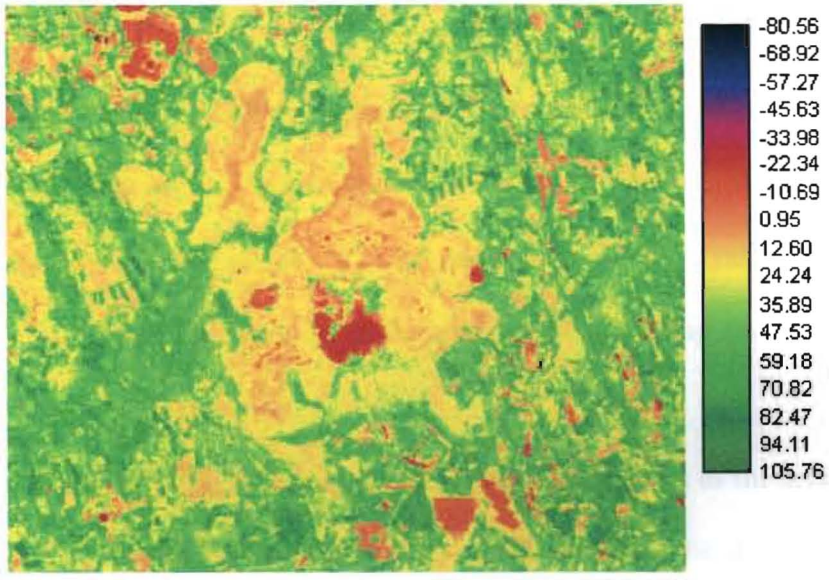

Tasseled-cap Greenness Transformation -- 1999

Scale 1:212,000

Figure 7.4: Tasseled-Cap Greenness Transformations -- Endla Nature Reserve

8.5 (band 2) to 49.8 (band 4) and the line slopes ranged from 0.356 (band 1) to 0.925 (band 2). The correlation coefficients ranged from 0.362 (band 5) to 0.537 (band 2).

7.2 Interpretation of Data for Emajõe Suursoo Mire Complex

7.2.1 Image Differencing

Image differencing was performed on bands 1, 2, 3, 4, 5, and 7 by subtracting the digital numbers of the 1999 images from those of the 1988 images on a pixel-wise basis. The summary statistics for the operation are given in Table 6.2: Summary Statistics for Image Differencing – Emajõe. The image differencing images, including reclassified images showing areas deviating from the mean by more than one standard deviation, are included in Appendix C: Image Differencing – Emajõe.

A difference of more than one standard deviation from the mean between the two datasets was used as the statistical threshold value for defining change. With this criterion, the percentage of the image affected by change between the dates ranged from 15.1 percent (band 1) to 29.0 percent (band 2), with the mean change being 21.0 percent.

A visual examination of the reclassified images shows much of the area where change was identified is attributable to an area of cloud cover near the shore of Lake Peipsi that was present in the 1988 image. Sun glitter from the lake surface may also contribute to the area statistically identified as change. Little change is noted in the portion of the

image in which mire complex is located. The area to the west of the mire complex boundary shows more change than does the mire complex.

7.2.2 Image Ratioing

Image ratioing was conducted by dividing the digital numbers from the 1988 image by those from the 1999 image on a pixel-wise basis. The resultant data were transformed by taking their natural logarithms as suggested by Eastman (2000). This resulted in a dataset more closely conforming to a normal distribution. The summary statistics for the operation are given in Table 6.4 Summary Statistics for Log Transformed Image Ratios – Emajõe. The image ratio images, including reclassified images showing areas that deviate from the mean by more than one standard deviation, are included in Appendix E: Image Ratios – Emajõe.

As with image differencing, a deviation of more than one standard deviation from the mean was classified as change. The percentage of the image areas affected by change was between 21.7 percent (band 2) and 26.6 percent (band 4), with the mean amount of change being 24.4 percent. Image ratioing can cause data noise to be magnified. An example of this noise is the line banding than is present in Lake Peipsi.

The image reclassification images show most of the change to be attributable to cloud cover that was present in the 1988 image. Some change is present west of the boundary of the mire complex. Little change is noted within the mire complex.

7.2.3 Normalized Difference Vegetation Index

Normalized difference vegetation index (NDVI) calculations were performed to determine if a change in vegetation vigor could be noted. The NDVI images are given in Appendix G: NDVI Images – Emajõe. NDVI values can range from –1 to 1. Healthy green vegetation is represented by NDVI values in the upper end of the range; whereas, water and soil are represented by values in the lower end of the range (Sabins, 1996).

The NDVI image from 1999 shows the vegetation to be more vigorous than does 1988 image. In the 1999 image, vegetation appears sparser along the coastline than it does in the 1988 image. The NDVI images that illustrate this change are given in Figure 7.5: NDVI – Emajõe Suursoo Mire Complex.

7.2.4 Tasseled-Cap Transformation

Tasseled-cap transformations were performed as described in Section 6.5: Tasseled-Cap Transformations. The summary statistics for this operation are given in Table 6.6: TCT Areas More than One Standard Deviation from the Mean – Emajõe. The tasseled-cap transformation images are given in Appendix I: TCT Images – Emajõe.

The moisture transformation shows moisture level being lower in the 1999 image than in the 1988 image. The tasseled-cap moisture transformations that illustrate this change are given on Figure 7.6: Tasseled-Cap Moisture Transformation – Emajõe Suursoo Mire Complex. This coupled with low vegetation vigor along the coastline may be indicative the water level elevation in Lake Peipsi being lower in 1999 than in 1988.

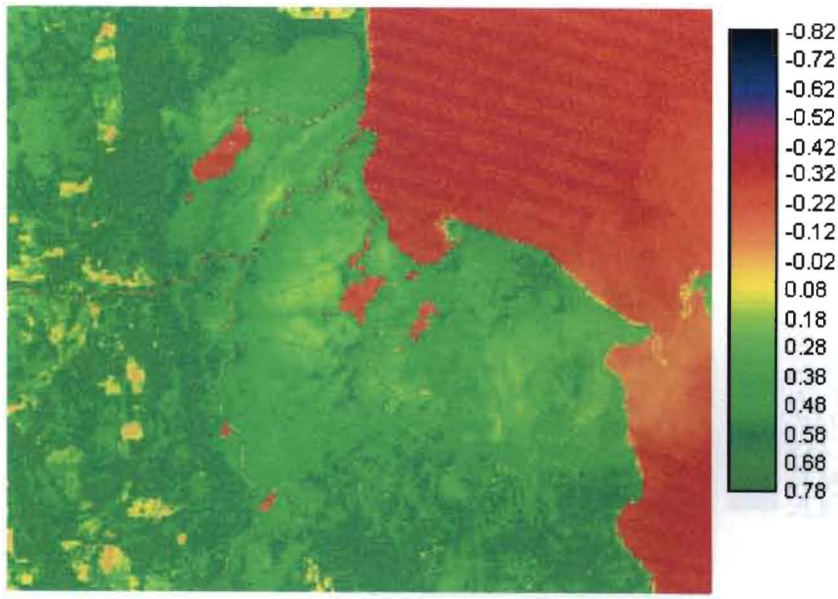

NDVI Image - 1988

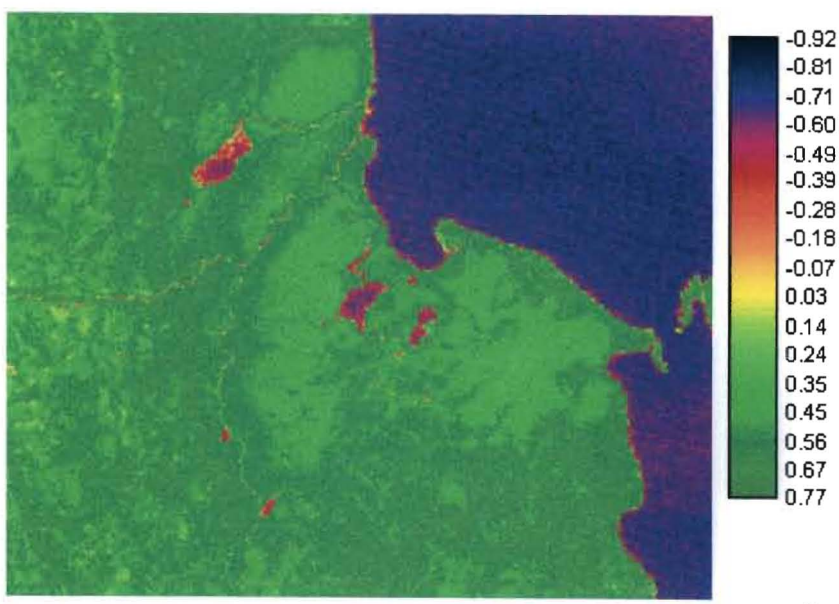

NDVI Image 1999

Figure 7.5: NDVI -- Emajõe Suursoo Mire Complex

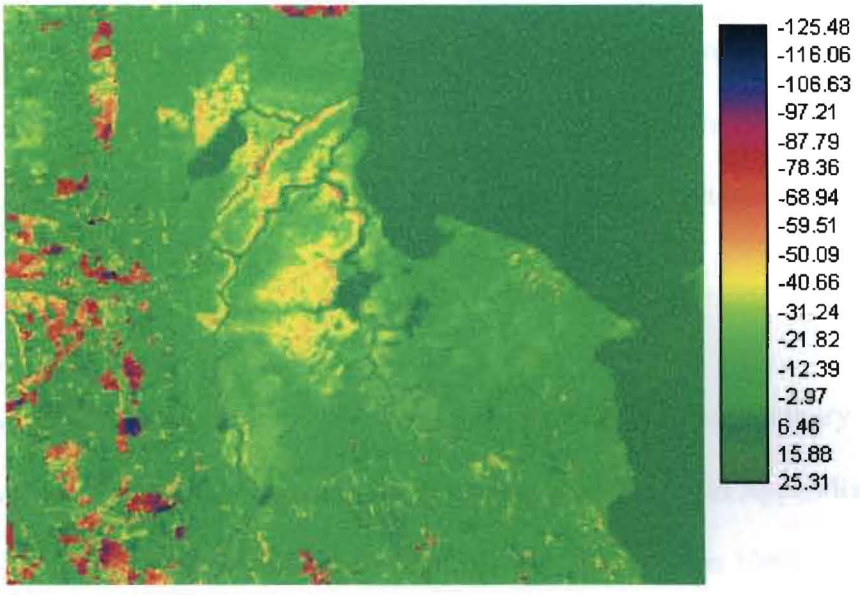

Tasseled-cap Moisture Transformation - 1988

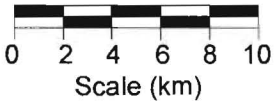

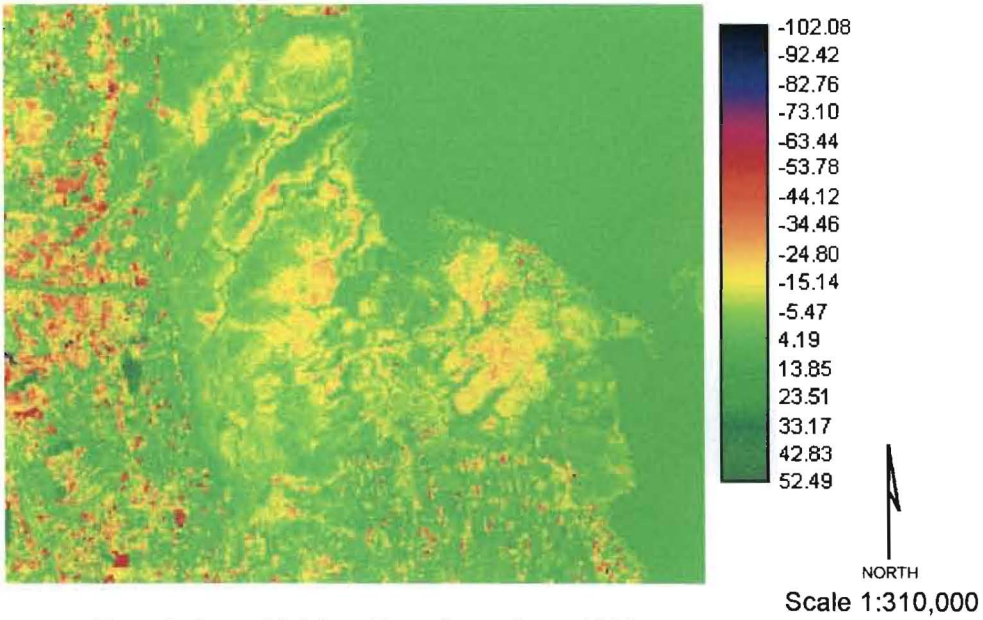

Tasseled-cap Moisture Transformation - 1999

Figure 7.6: Tasseled-Cap Moisture Transformation -- Emajõe Suursoo Mire Complex

7.2.5 Correlation Analysis

Regression analyses were conducted to measure the correlation between the 1988 and the 1999 image bands. The analyses were conducted using the general linear model to fit a regression line using the method of least squares as described in Section 6.6: Correlation Analysis.

The summary data for the regression analyses are given in Table 6.8: Summary Data for Regression Analyses – Emajõe. The data are presented graphically in Appendix K: Regression Plots – Emajõe. The data show change occurred between 1988 and 1999. The intercept values ranged from 3.0 (band 4) to 39.0 (band 1) and the line slopes ranged from 0.098 (band 1) to 1.2 (band 4). The correlation coefficients ranged from 0.093 (band1) to 0.785 (band 4).

Chapter Eight
Conclusions

8.1 Endla Nature Reserve

The analyses for the Endla Nature Reserve show that change occurred in the reserve area between the date of the first image (1988) and that of the second image (1999). Image differencing and image ratioing show that the most significant changes occurred around the periphery of the reserve. Normalized difference vegetation index and tasseled-cap transformation analyses show vegetation both in the nature reserve and around the periphery of the reserve to have been more widely distributed and more vigorous in 1999 than in 1988.

Some change was noted in Lake Endla. The data suggest that the lake may have had a greater biomass concentration in 1988 than in 1999. Analysis of the cause for this change is beyond the scope of this study; however, it should be noted that a potential cause for the decreased biomass concentration (e.g. algae and duckweed) might be less fertilizer runoff entering the lake from agricultural areas adjacent to the nature reserve.

The bog areas appear to have been generally stable in areal extent between 1988 and 1999. The data also suggest that environmental conditions were better in 1999 than in 1988. This improvement is shown by the increased vegetation vigor and the decreased biomass concentrations in Lake Endla, which were noted in the 1999 images.

8.2 Emajõe Suursoo Mire Complex

Localized cloud cover was present near the shoreline of Lake Peipsi in the 1988 image that caused the numerical degree of change to be overestimated. It does appear that changes did occur in the mire complex area between 1988 and 1999. As with Endla Nature Reserve, the majority of the changes are around the periphery of the mire complex.

The vegetation both in and around the mire complex appears more vigorous in 1999 than in 1988. There is a notable absence of vegetation along the Lake Peipsi shoreline in the 1999 image. The tasseled-cap moisture transformation shows a decrease in moisture in 1999. These facts suggest that the water level elevation of Lake Peipsi was lower in 1999 than in 1988, but that it had not been lower long enough for vegetation to become established along the new shoreline or to cause excessive stress to vegetation away from the shoreline.

8.3 Suitability of GIS Techniques with Landsat Multispectral Data for Change Detection in Wetlands

This study used multispectral data acquired by Landsat satellites to detect change in wetlands. The multispectral scanner data has a spatial resolution of thirty meters. Larger scale ancillary data was not used in this study.

The lack of larger scale data and ground truthing precluded the use of image classification as a tool to detect change in vegetation regimes. Without ground truthing

data, an error matrix could not be prepared to evaluate classification accuracy. Where the potential degree of change is small, the classification uncertainty may mask or exaggerate the amount of change to the extent that reliable conclusions cannot be made.

This study used five quantitative techniques for change analysis – image differencing, image ratioing, normalized difference vegetation index analysis, tasseled-cap transformations, and correlation analysis. Image differencing and image ratioing proved useful in identifying areas of change. With image ratioing, signal noise within the dataset was increased. Both of these techniques would be useful in identifying areas of potential change that might warrant confirmatory field investigation. Normalized difference vegetation index analysis and tasseled-cap transformations were useful in assessing vegetation vigor and moisture levels. The matrix coefficients used in the tasseled-cap transformation were derived for use with agricultural crops. The suitability of this technique for wetlands studies could be greatly enhanced by the development of coefficients derived explicitly for wetlands. Correlation analysis was of limited use in this study. This technique compares change on a scene-basis and does not identify areas of potential change. The analysis is also adversely affected by signal noise within the datasets. Correlation analysis might prove useful for evaluation of small areas within a scene.

Overall, the GIS techniques used in this study proved suitable in the identification of change in Estonia wetlands. The reliability and usefulness of a study of this nature could be greatly enhanced by the inclusion of larger scale data and the collection of field data.

References Cited

Aaviksoo, K., Kadarik, H., and Masing, V., 1997, Aerial views and close-up pictures of 30 Estonian mires: the first book on telmatography: Tallinn.

Aber, J.S., 2001, Vegetation Analysis Vormsi, Estonia: Lecture notes for ES771 Remote Sensing: http://academic.emporia.edu.aberjame/remote/lab08/lab08.htm, accessed: 1 March 2002.

Aber, J.S., and Aber, S.W., 2001, Potential of kite aerial photography for peatland investigations with examples from Estonia: Suoseura - Finnish Peatland Society, v. 52(2), p. 45 - 56.

Avery, T.E., and Berlin, G.L., 1992, Fundamentals of remote sensing and airphoto interpretation: Upper Saddle River, NJ, Prentice-Hall, Inc., 472 p.

Baltic Environmental Forum, 2000, Baltic State of the Environment Report: http://www.bef.lv/baltic/baltic2/contents/htm, accessed: 2 February 2002.

Central Intelligence Agency, 2001, The world factbook - Estonia: http://www.cia.gov/publications/factbook/docs/concopy.html, accessed: 3 March 2002.

Clark, R.N., Swayze, G.A., Gallagher, T.V.V., and Calvin, W.M., 1993, The U.S. Geological Survey, Digital Spectral Library: Version 1: 0.2 to 3.0 microns, U.S. Geological Survey Open File Report 93-592: http://speclab.cr.usgs.gov, accessed: 23 December 2001.

Cowardin, L.M., Carter, V., Golet, F.C., and LaRoe, E.T., 1979, Classification of wetlands and deepwater habitats in the United States: Washington, D.C., U.S. Fish and Wildlife Service.

Daiz Barrios, M.C., Ustin, S.L., Pinzón, J.E., Perry, G.L., Vanderbilt, V.C., Livingston, G.P., Morriessey, L.A., Breon, F.M., and Leroy, M., 1998, Discrimination of inundated and non-inundated community types with multi-spectral multi-angle POLDER data: http://www.cstars/ucdavis.edu/papers/html/diazbarriosetal1998b/paperfr.html, accessed: 3 March 2002.

Dappen, P., and Tooze, M., 2001, Delineation of land use patterns for the cooperative hydrology study in the Central Platte River Basin: University of Nebraska, Center of Advanced Land Management Information Technologies, Lincoln, NE, 73 p.

Davis, J.H., 1946, The peat deposits of Florida: their occurrence, development, and uses, Geological Bulletin No. 30: Tallahassee, FL, Florida Geological Survey, 240 p.

Eastman, R.J., 2000, Idrisi32: Worcester, Massachusett, Clarks Labs.

Eastman, R.J., McKendry, J., E., and Fulk, M.A., 2000, Change and time series analysis: Worcester, MA, Clark Labs for Cartographic Technology and Geographic Analysis.

Eesti Kaardikeskus,1996a, Estonia Base Map: Järva-Jaani 6413, Estonia Map Center State Enterprise.

Eesti Kaardikeskus,1996b, Estonia Base Map: Jõgeva 6412, Estonia Map Center State Enterprise.

Eesti Kaardikeskus,1996c, Estonia Base Map: Põltsammaa 6411, Estonia Map Center State Enterprise.

Eesti Kaardikeskus,1996d, Estonia Base Map: Rakke 6414, Estonia Map Center State Enterprise.

Eesti Kaardikeskus,1996e, Estonia Base Map: Tabivere 5443, Estonia Map Center State Enterprise.

Eesti Kaardikeskus,1996f, Estonia Base Map: Tartu 5441, Estonia Map Center State Enterprise.

Eesti Kaardikeskus,1998a, Estonia Base Map: Kolkja 5444, Estonia Map Center State Enterprise.

Eesti Kaardikeskus,1998b, Estonia Base Map: Võnna 5442, Estonia Map Center State Enterprise.

Environmental Laboratory, 1987, Corp of Engineers Wetlands delineation manual: available online at: http://wwwwes.army.mil/el/wetlands/pdfs/wlman87.pdf, accessed: 5 March 2002.

Farr, R., 1999, Comparison of landsat missions: http://landsat.gsfc.nasa.gov/project/Comparison.html, accessed: Oct. 13, 2001.

Forse, J.E., Leach, J.H., Choowaew, S., and Bishop, I.D., Change detection analysis of coastal land cover in Thailand using Landsat thematic mapper: http://www.sli.unimelb.edu.au/cgism/TIL.paper1.html, accessed: 5 March 2002.

Frazier, S., 1999, Ramsar sites overview: a symopsis of the world's wetlands of international importance: Ottawa, Ontario, Wetlands International, 42 p.

http://www.ciesin.ee/ESTCG/NATURE, 1993, Estonia country guide - nature: http://www.ciesin.ee/ESTCG/NATURE/, accessed: 11 September 2001.

Jensen, J.R., 1996, Introductory digital image processing: a remote sensing perspective: Upper Saddle River, NJ, Prentice-Hall, Inc., 318 p.

Jensen, J.R., 2000, Remote sensing of the environment: an earth science perspective: Upper Saddle River, NJ, Prentice-Hall, Inc., 544 p.

Kõll, A.M., 1994, Peasants on the world market: agricultural experience of independent Estonia 1919-1939: Stockholm, Sweden, Centre for Baltic Studies, 150 p.

Konstantin Päts Fund., 1974, Estonia: story of a nation: New York, NY, Estonia House, 98 p.

Lo, C.P., 1986, Applied remote sensing: New York, NY, Longman, Inc., 393 p.

Lunetta, R.S., 1998, Applications, project formulation, and analytical approach, *in* Elvidge, C.D., ed., Remote sensing change detection: environmental monitoring methods and applications: Chelsea, MI, Ann Arbor Press, p. 318.

Mackenzie, F.T., 1998, Our changing planet: an introduction to earth system science and environmental change: Upper Saddle River, NJ, Prentice-Hall, Inc., 486 p.

National Research Council, 1995, Wetlands charateristics and boundaries: Washington, D.C., National Academic Press.

National Wetlands Working Group, 1987, The Canadian wetlands classification system, Ecological Land Classification Series No. 21: Ottawa, Ontario, Canadian Wildlife Service.

Neuenschwander, A.L., Crawford, M.M., and Provancha, M.J., 1998, Mapping of coastal wetlands via hyperspectral AVIRIS data: http://www.ftp.csr.utexas.edu/projects/rs/rs9802.html, accessed: 4 March 2002.

Niering, W.A., 1998, National Audubon Society nature guides: Wetlands: New York, NY, Alfred A. Knopf, Inc., 638 p.

Peck, D., 2000, The annotated Ramsar list: Estonia: http://ramsar.org/profiles_estonia.htm, accessed: 6 August 2001.

Perry, G.L., Stearn, J.A., Vanderbilt, V.C., Ustin, S.L., Daiz Barrios, M.C., Morriessey, L.A., Livingston, G.P., Breon, F.M., Bouffies, S., Leroy, M., Herman, M., and Balois, J.Y., 1997, Remote sensing of high-latitude wetlands using polarized wide angle imagery: http://www.cstars.ucdavis.edu/papers/html/perryetal1997a/paperfr.html, accessed: 4 March 2002.

Ramsar Information Bureau, 1998, What are wetlands?, Ramsar Information Paper No. 1: Gland, Switzerland.

Ramsar Information Bureau, 2000, Annotated Ramsar List: Estonia: http://ramsar.org/profiles_estonia.htm, accessed: 6 August 2001.

Ramsar Information Bureau, 2001a, A directory of wetlands of international importance: Estonia 3EE004: http://www.wetlands.agro.nl/Ramsar_Database/HTML_DIR/Estonia/EE004D99.htm, accessed: 6 August 2001.

Ramsar Information Bureau, 2001b, A directory of wetlands of international imporatance: Estonia 3EE003:

http://www.wetlands.agro.nl/Ramsar_Database/HTML_DIR/Estonia/EE003D99.htm, accessed: 6 August 2001.

Raud, V., 1953, Estonia: a reference book: London, UK, The Nordic Press, Inc., 158 p.

Raun, T.U., 1991, Estonia and Estonians: Stanford, CA, Hoover Institution Press, 336 p.

Rees, G., 1999, The remote sensing data book: Cambridge, UK, Cambridge University Press, 262 p.

Richards, J.A., and Jia, X., 1999, Remote sensing digital image analysis: an introduction: New York, NY, Springer-Verlag, 363 p.

Sabins, F.F., 1996, Remote sensing: principles and interpretation: New York, NY, W. H. Freeman and Company, 494 p.

Shaler, N., 1890, General account of the freshwater morasses of the United States, with a description of the Dismal Swamp District of Viginia and North Carolina 10th Annual Report 1888 - 1889, U.S. Geological Survey, 261 - 339 p.

Soviet News, 1950, The sixteen republics of the Soviet Union: London, UK, Soviet News, 96 p.

Taagepera, R., 1993, Estonia: return to independence: Bolder, CO, Westview Press, Inc., 268 p.

Taylor, N., 1999, Estonia - the Brandt travel guide: Old Saybrook, CT, The Globe Pequot Press, Inc., 202 p.

Tiner, R.W., 1999, Wetland indicators: a guide to wetland identification, delineation, classification, and mapping: Boca Raton, FL, Lewis Publishers, 392 p.

Ullah, A., 2002, Potentials of geographic information systems and remote sensing for an examination of environmental variability through analysis of historical spectral

and spatical data: http://www.ucgis.org.oregon/papers/ullah.htm, accessed: 5 March 2002.

Vanderbilt, V.C., Perry, G.L., Steam, J.A., Ustin, S.L., Diaz Barrios, M.C., Zedler, S., Syder, J., Morriessey, L.A., Livingston, G.P., Breon, F.M., Bouffies, S., Leroy, M., Herman, A., and Balois, J.Y., 1997, Discrimination of wetland and non-wetland community types with multispectral multi-angle, polarized data: http://www.cstars.ucdavis.edu/papers/html/vanderbiltetal1997a/paperfr.html, accessed: 3 March 2002.

Vesterinen, E., 1921, Agricultural conditions in Esthonia: Helsinki, Tietosanakirja-Osakeyhtiö, 64 p.

Von Hansen, W., and Sties, M., 1999, Can digital remote sensing techniques contributes to the management of protected wetlands?: http://www-ipf.bau-verm.uni-karlsruhe.de/Personen/hansen/halle/hansen1.htm, accessed: 5 March 2002.

Yuan, D., Elvidge, C., and Lunetta, R., 1988, Survey of multispectral methods for land cover change analysis, *in* Elvidge, C.D., ed., Remote sensing change detection: environmental monitoring methods and applications: Chelsea, MI, Ann Arbor Press, p. 21-39.

Appendix A:
Spectral Curves for Selected Floral Species

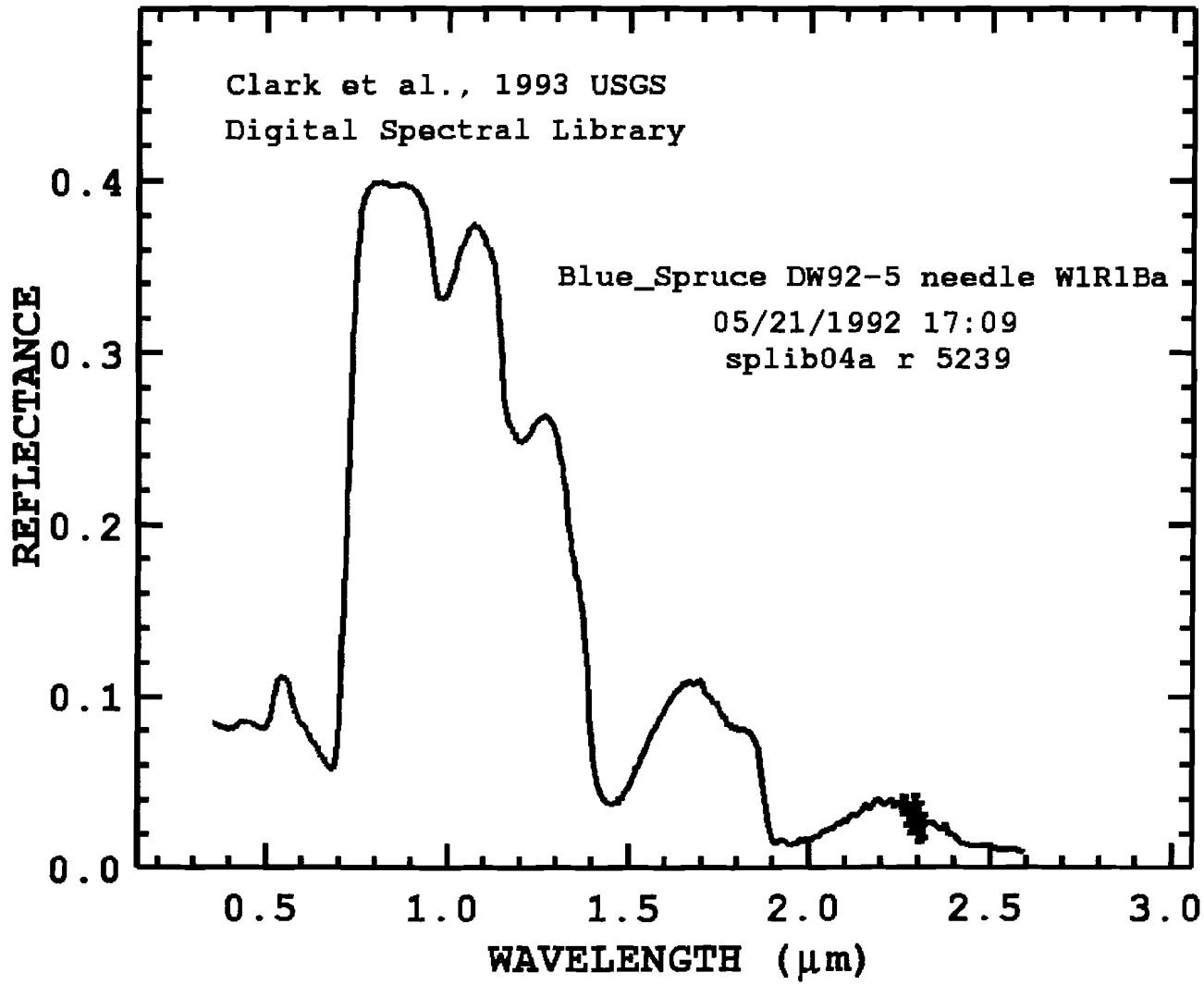

Figure A.1: Spectral Curve -- Blue Spruce

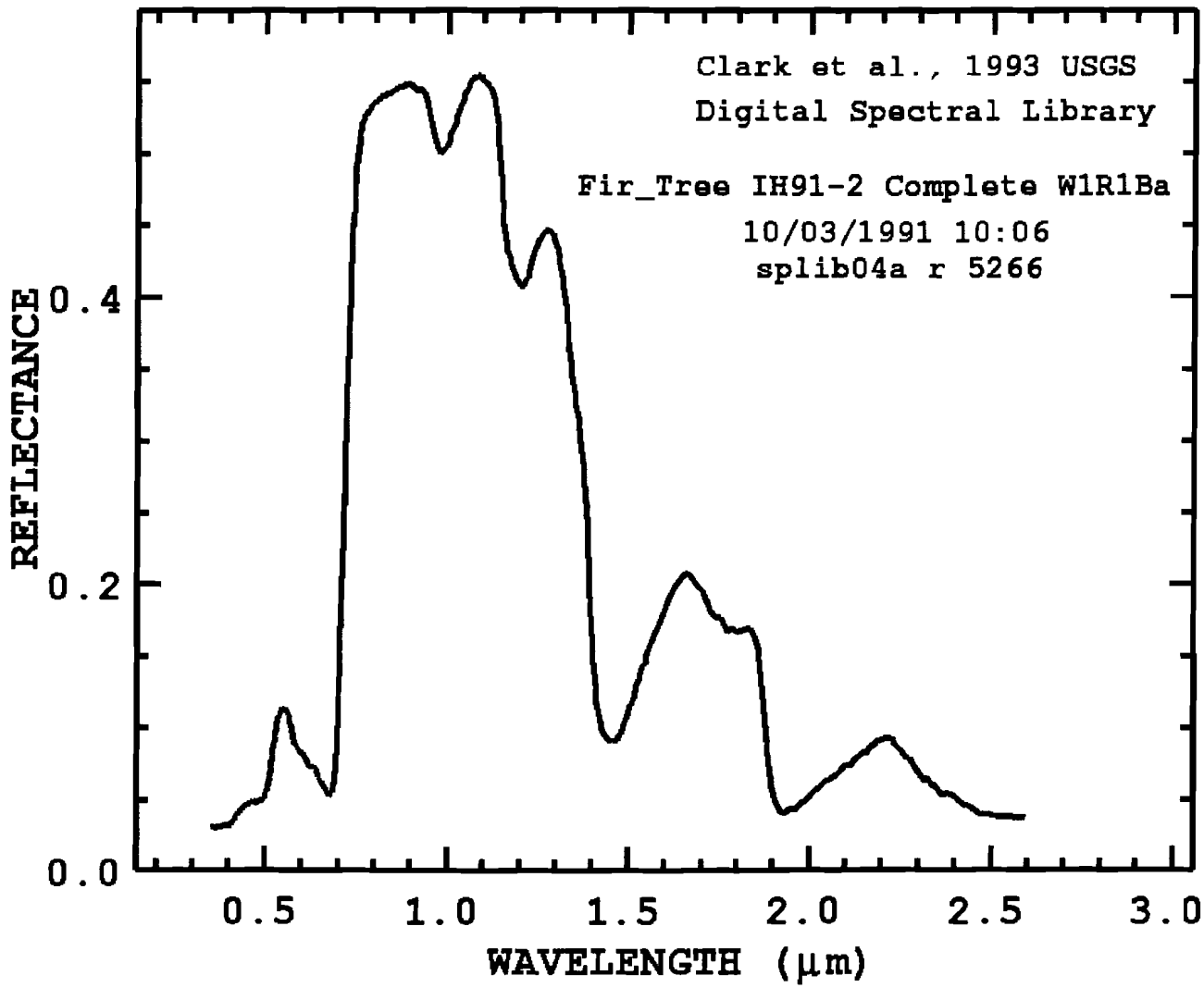

Figure A.2: Spectral Curve -- Fir

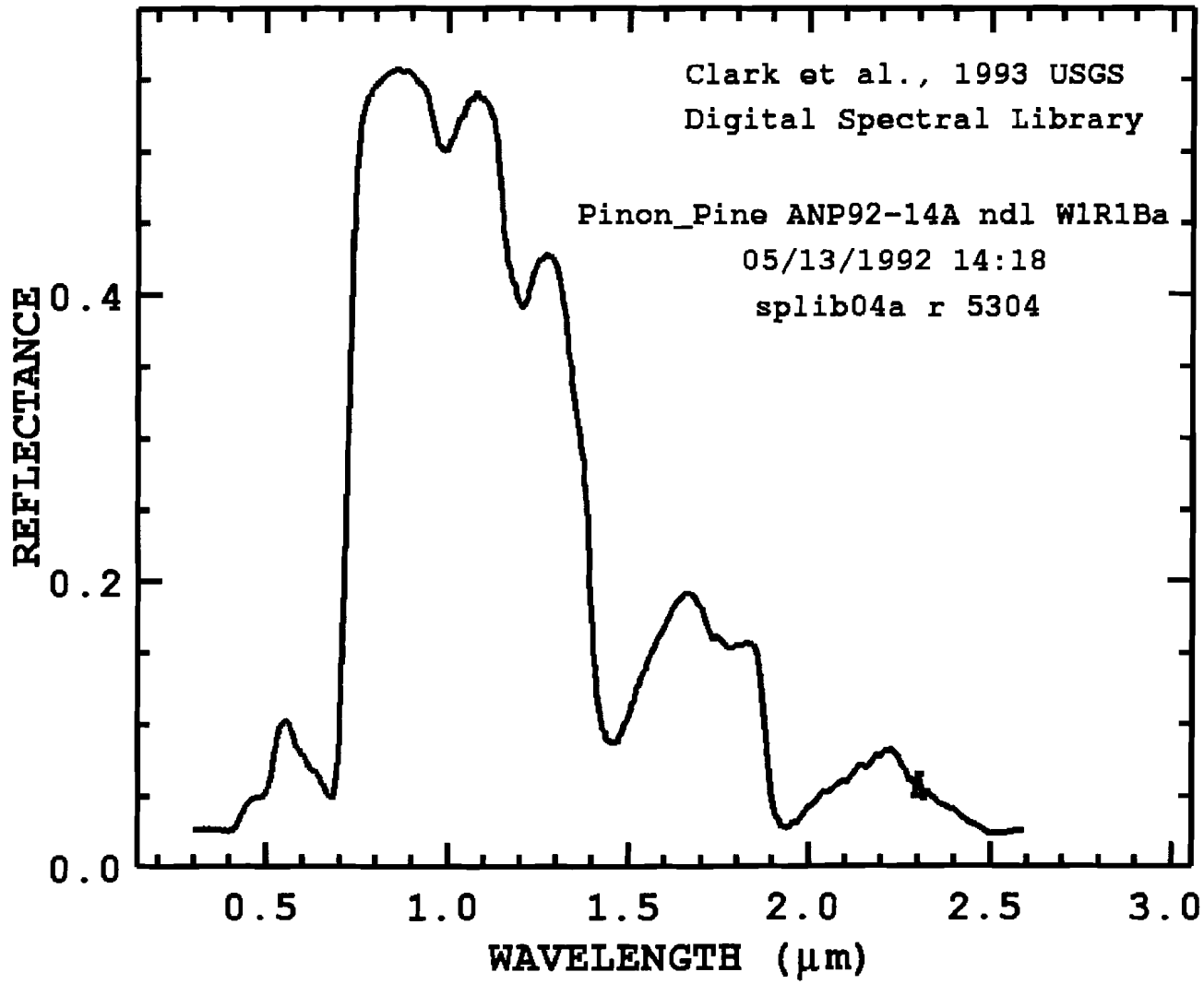

Figure A.3: Spectral Curve -- Pinon Pine

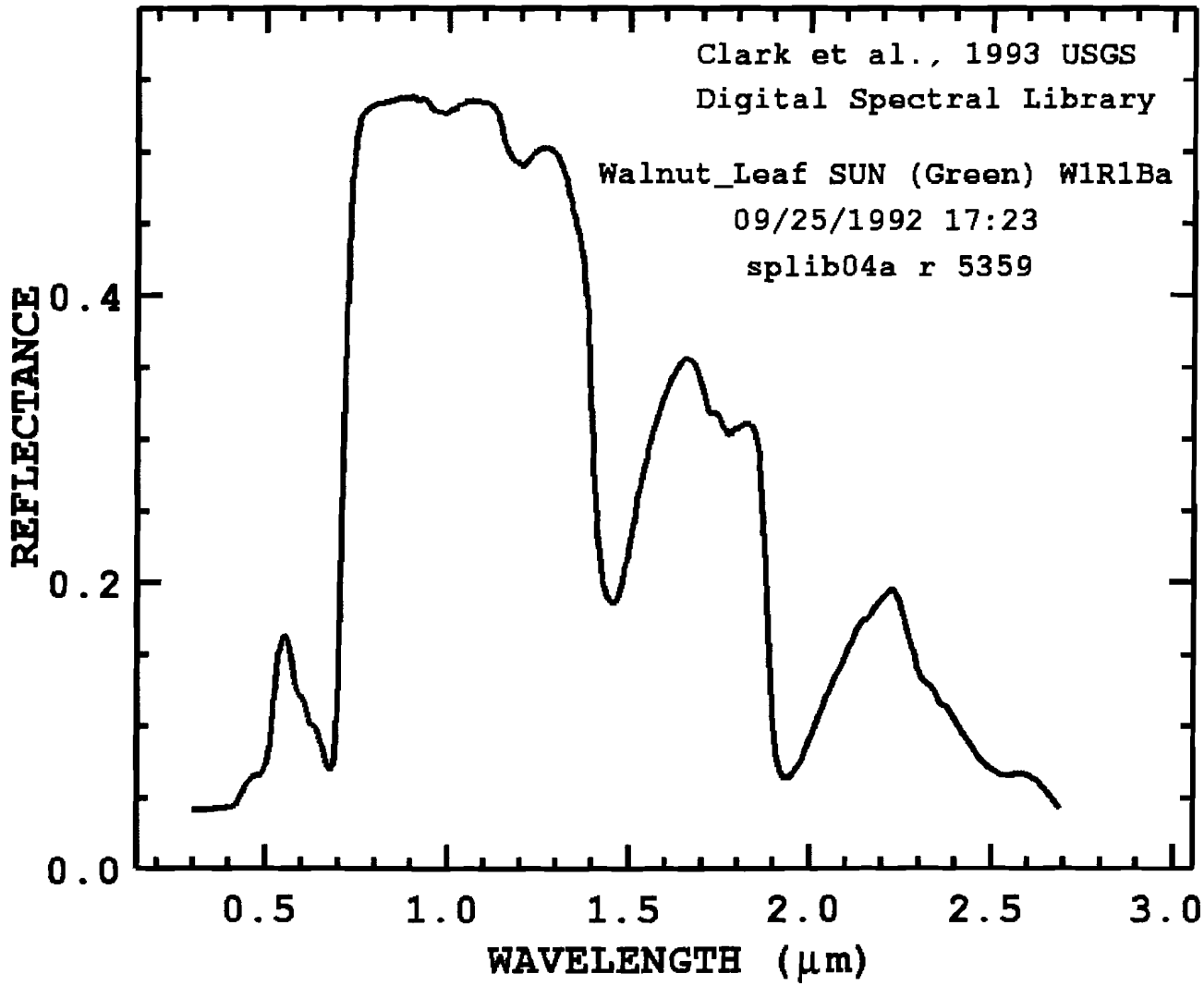

Figure A.4: Spectral Curve -- Walnut

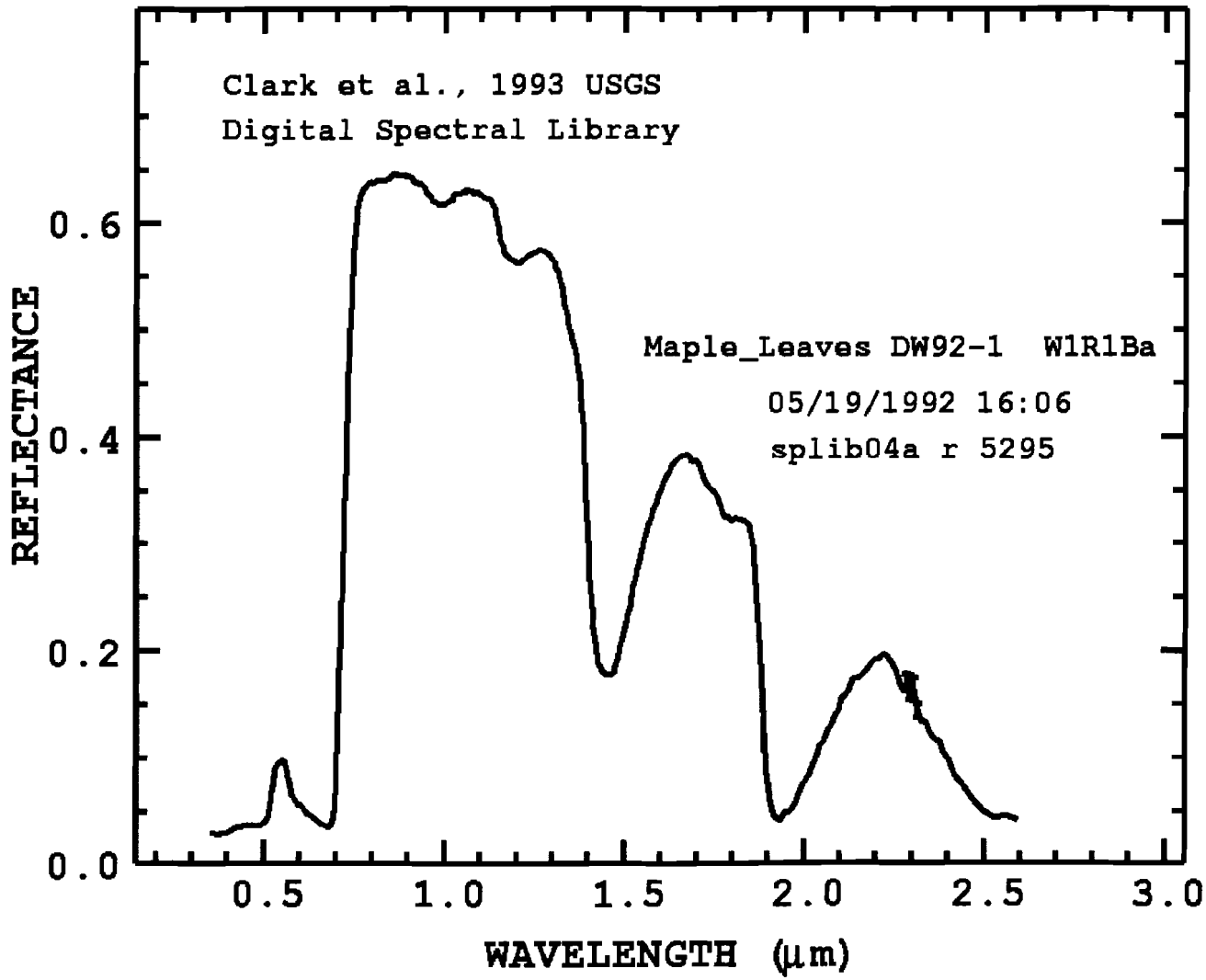

Figure A.5: Spectral Curve -- Maple

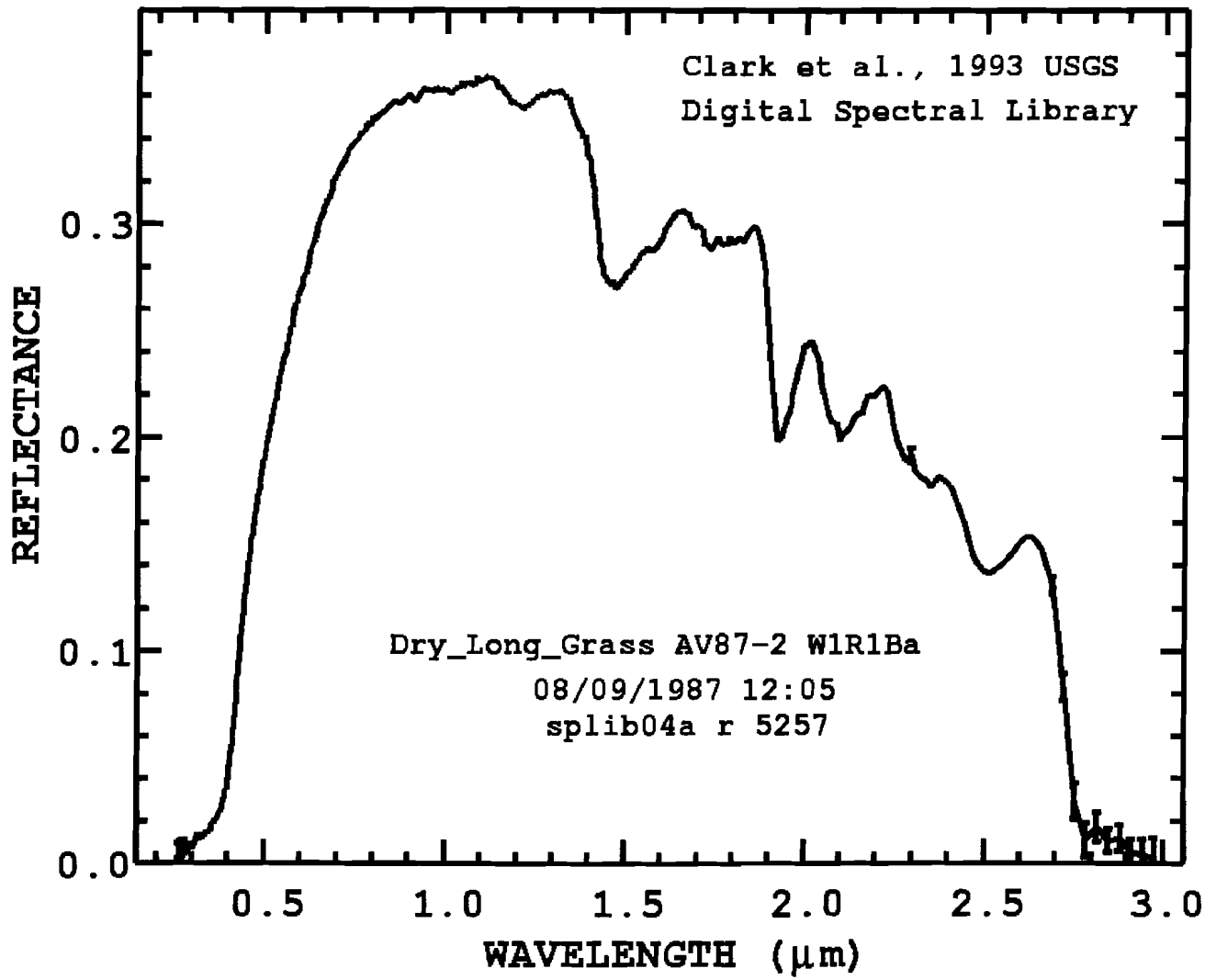

Figure A.6: Spectral Curve -- Dry Long Grass

Appendix B:
Image Differencing – Endla

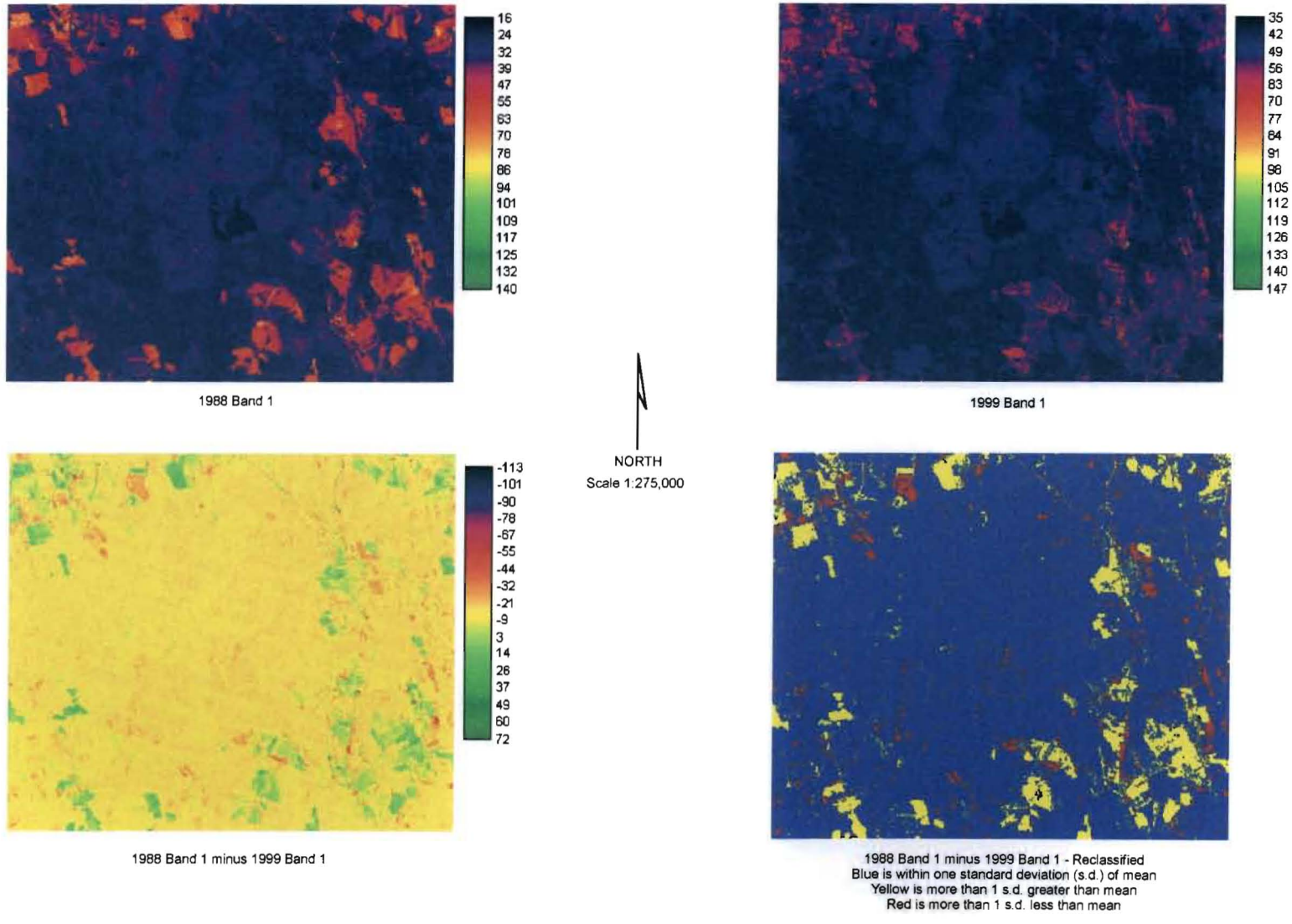

Figure B.1: Image Differencing Band 1 - Endla Nature Reserve

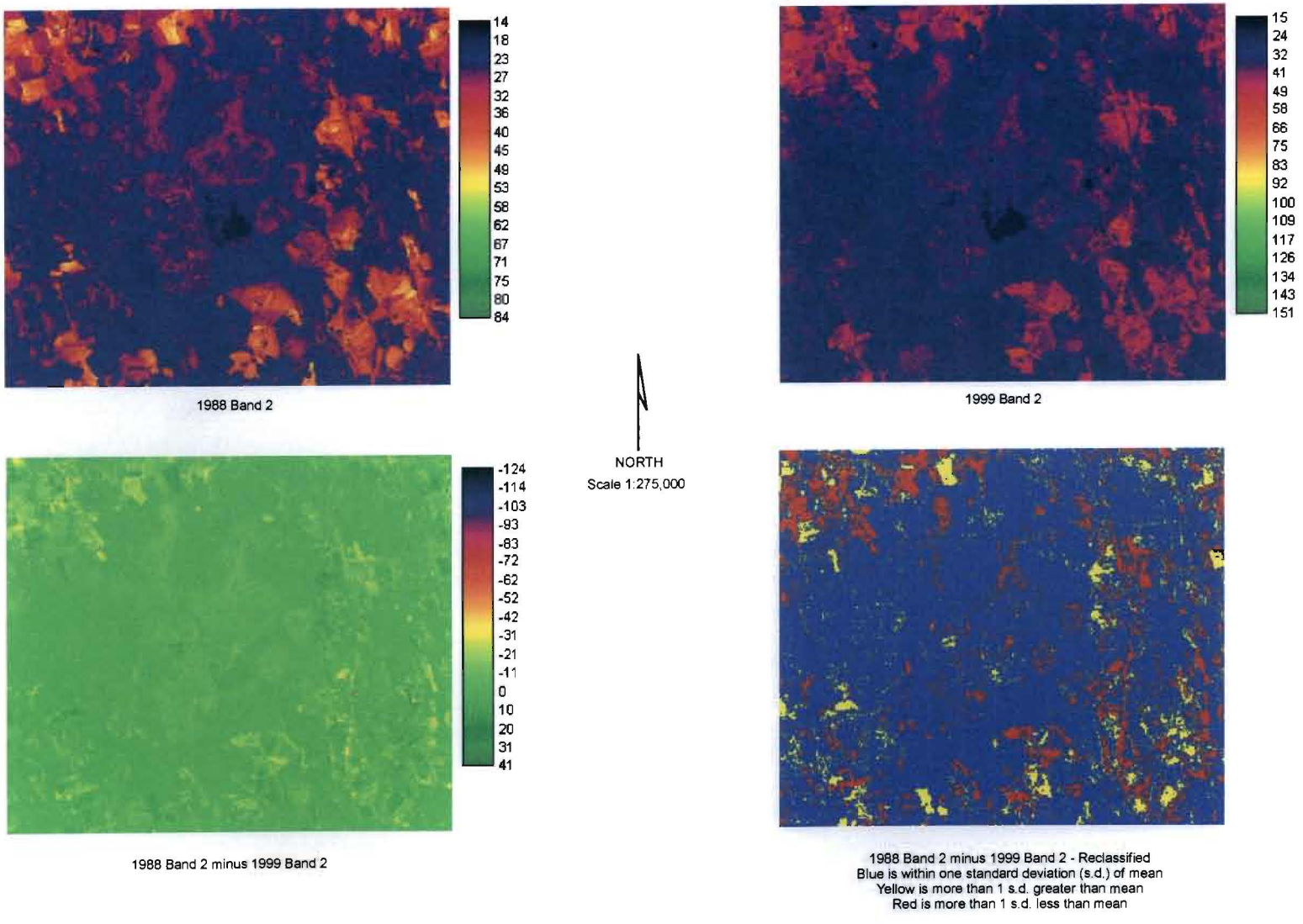

Figure B.2: Image Differencing Band 2 - Endla Nature Reserve

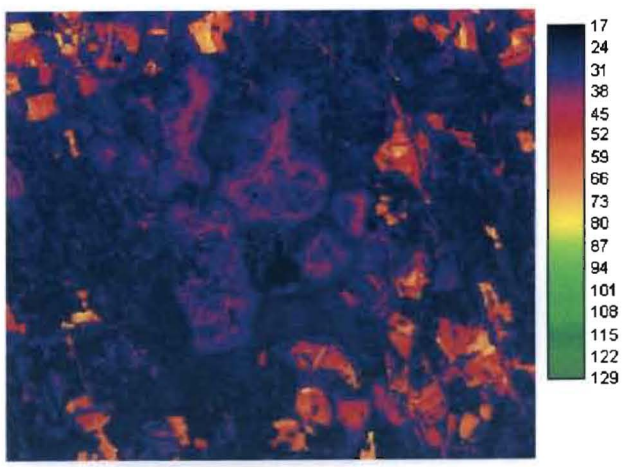

1988 Band 3

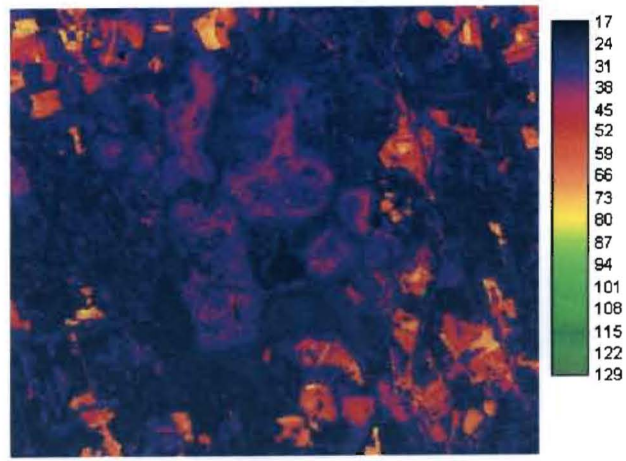

1999 Band 3

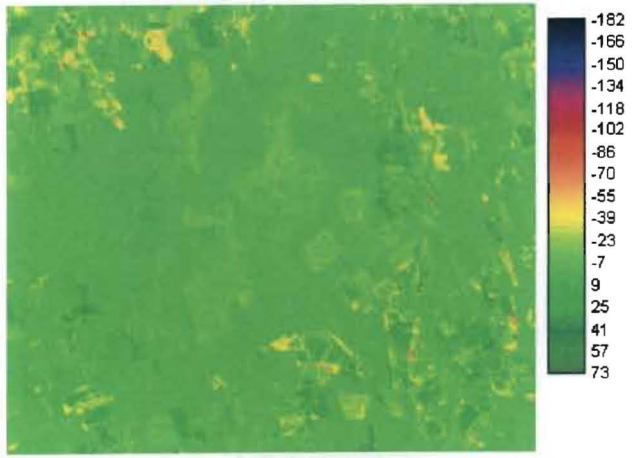

1988 Band 3 minus 1999 Band 3

NORTH
Scale 1:275,000

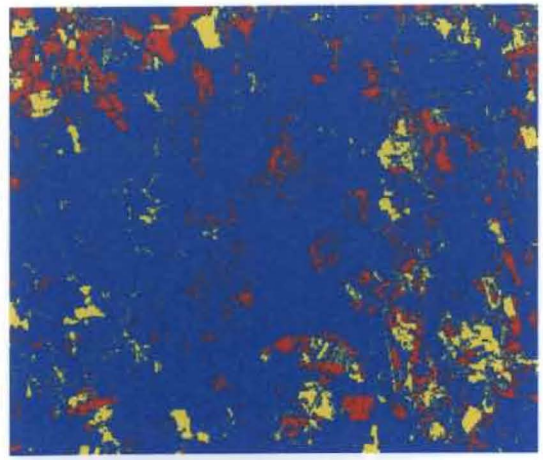

1988 Band 3 minus 1999 Band 3 - Reclassified
Blue is within one standard deviation (s.d.) of mean
Yellow is more than 1 s.d. greater than mean
Red is more than 1 s.d. less than mean

Figure B.3: Image Differencing Band 3 - Endla Nature Reserve

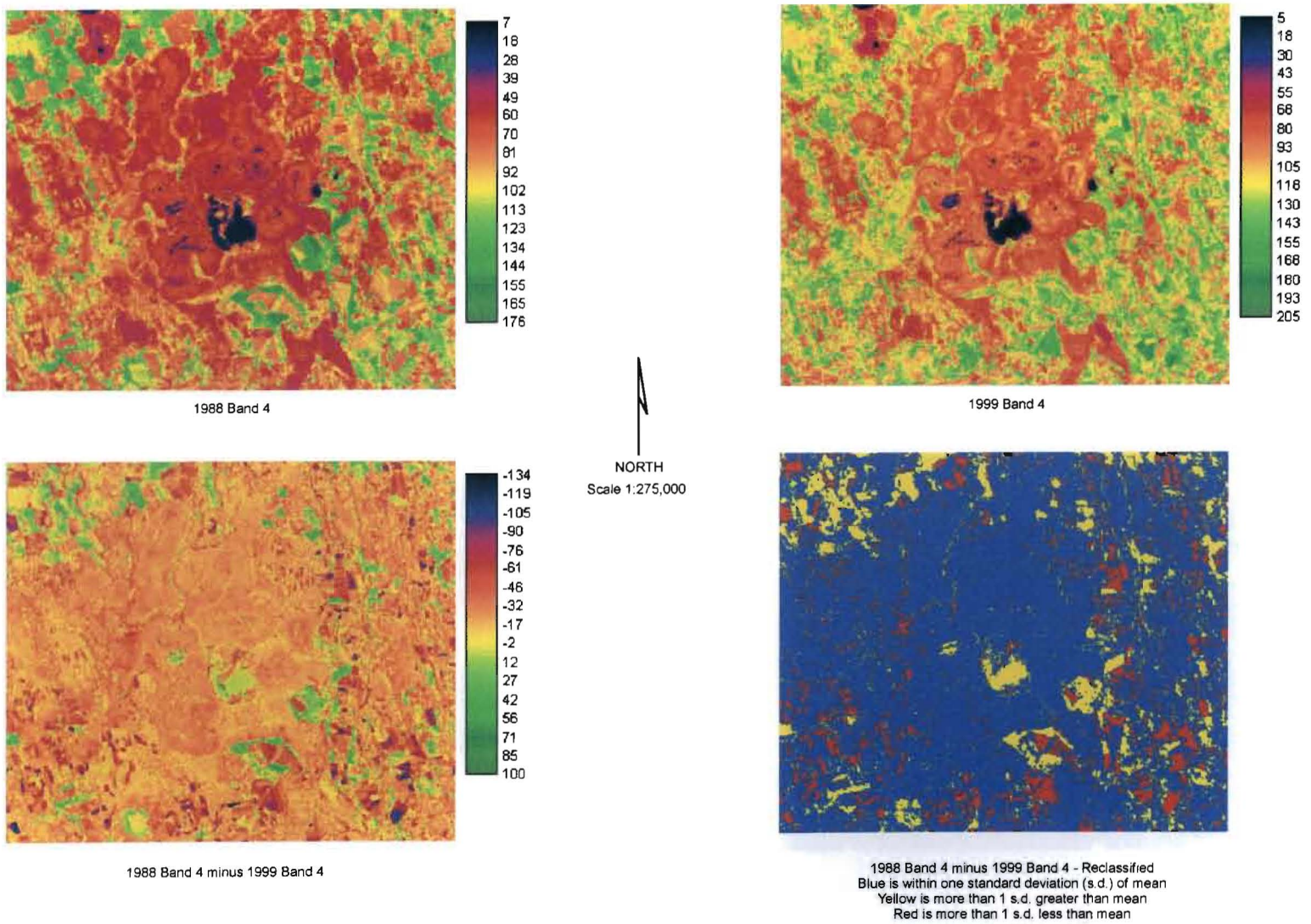

Figure B.4: Image Differencing Band 4 - Endla Nature Reserve

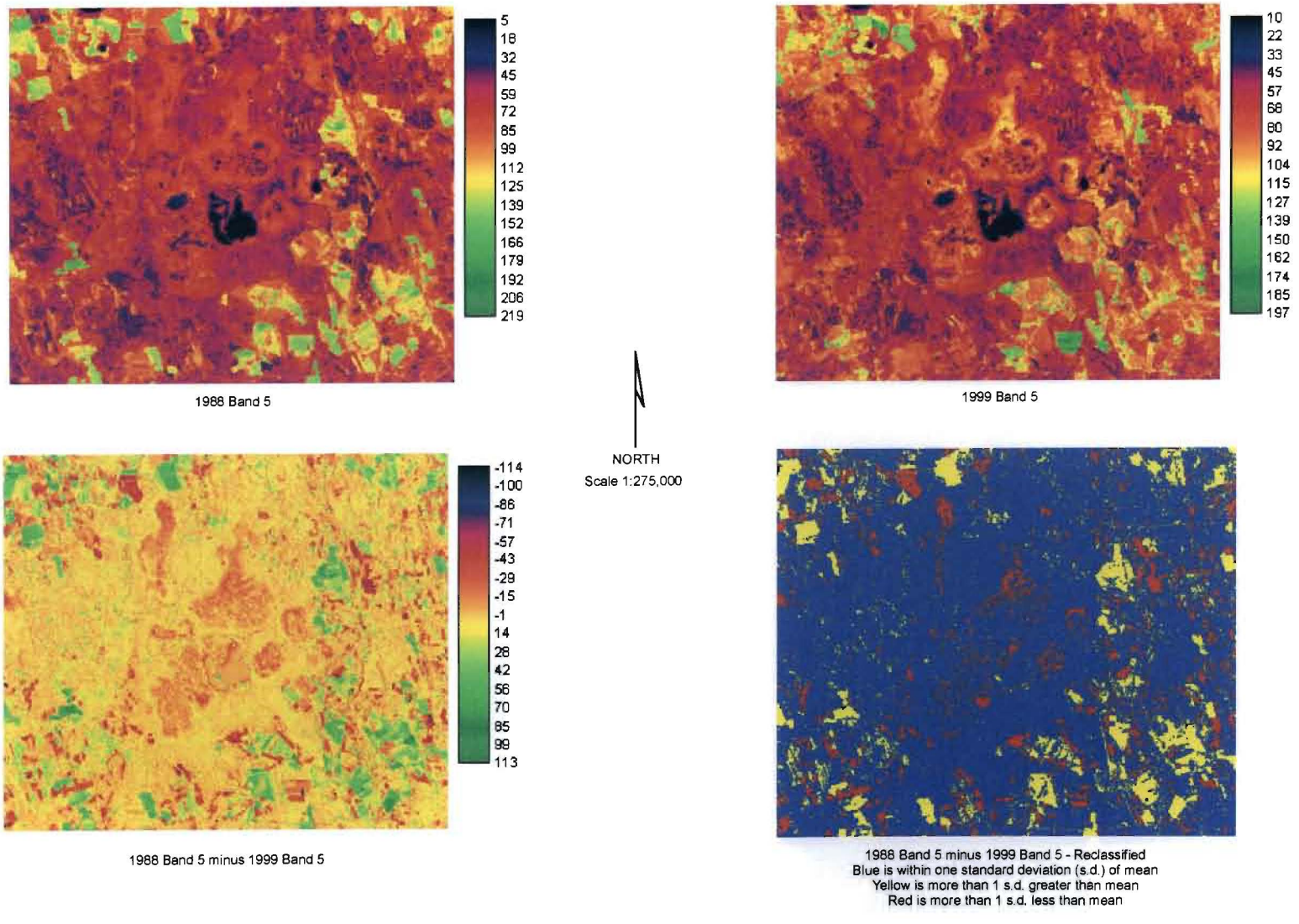

Figure B.5: Image Differencing Band 5 - Endla Nature Reserve

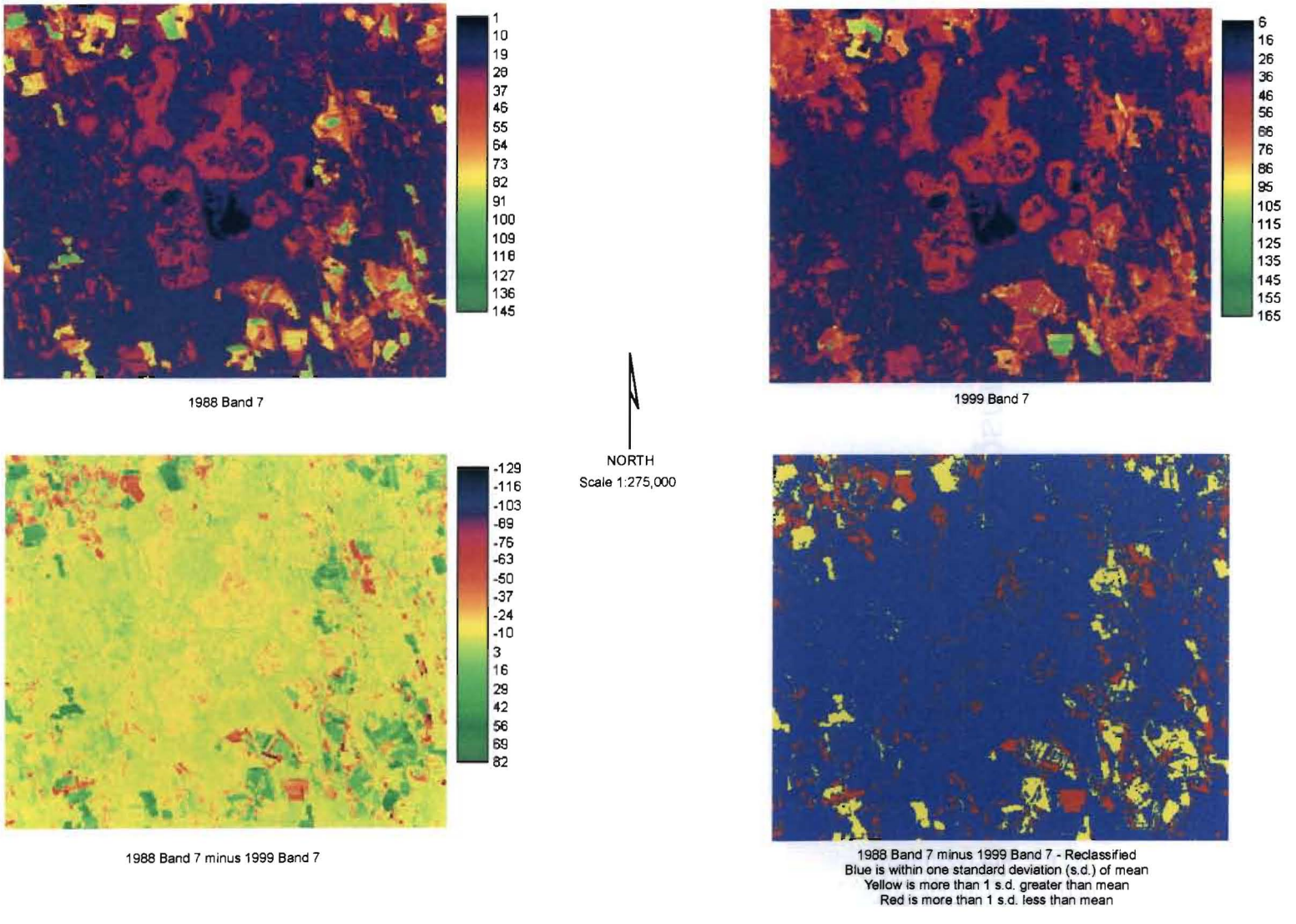

Figure B.6: Image Differencing Band 7 - Endla Nature Reserve

Appendix C:
Image Differencing – Emajõe

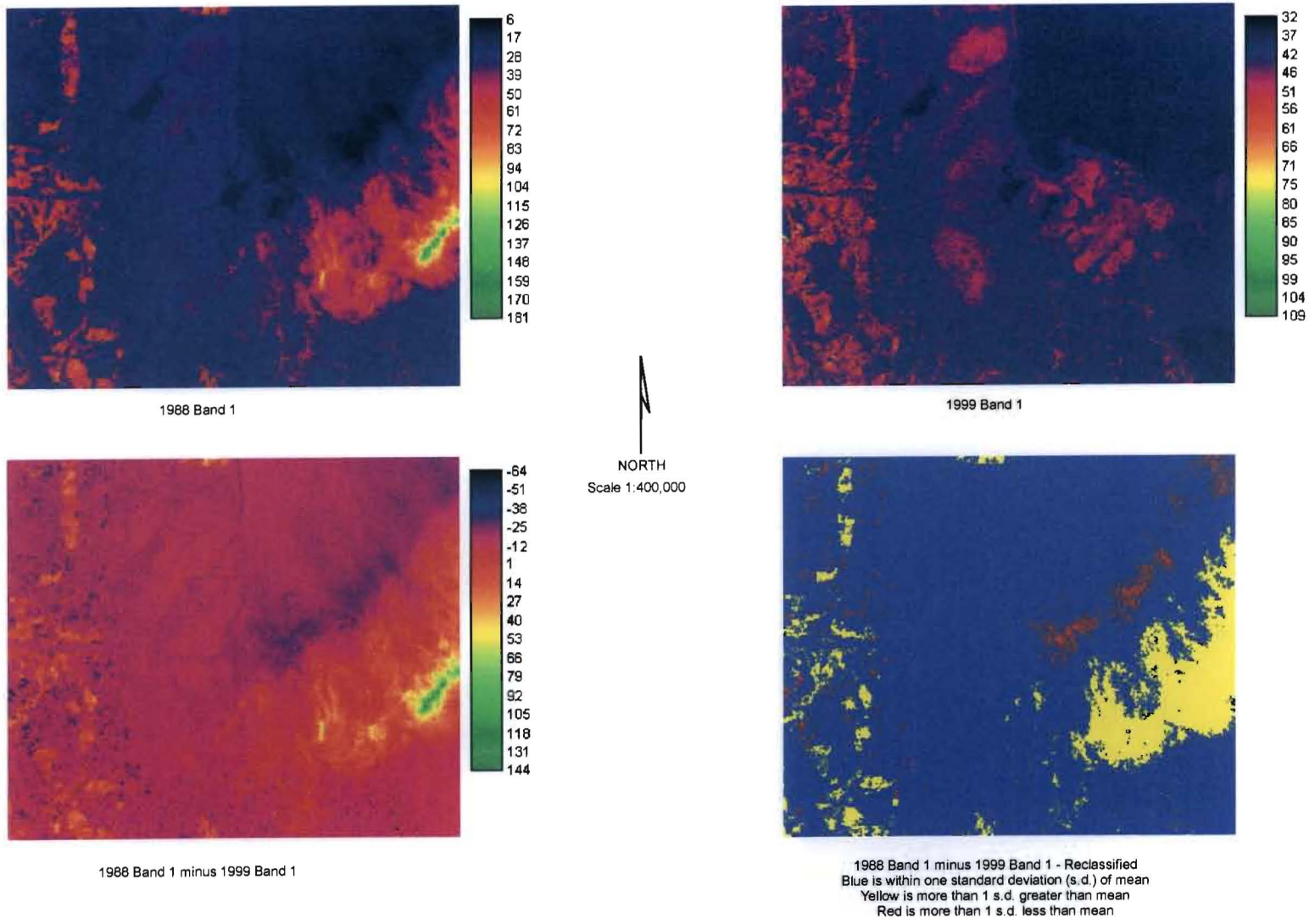

Figure C.1: Image Differencing Band 1 - Emajõe Suursoo Mire Complex

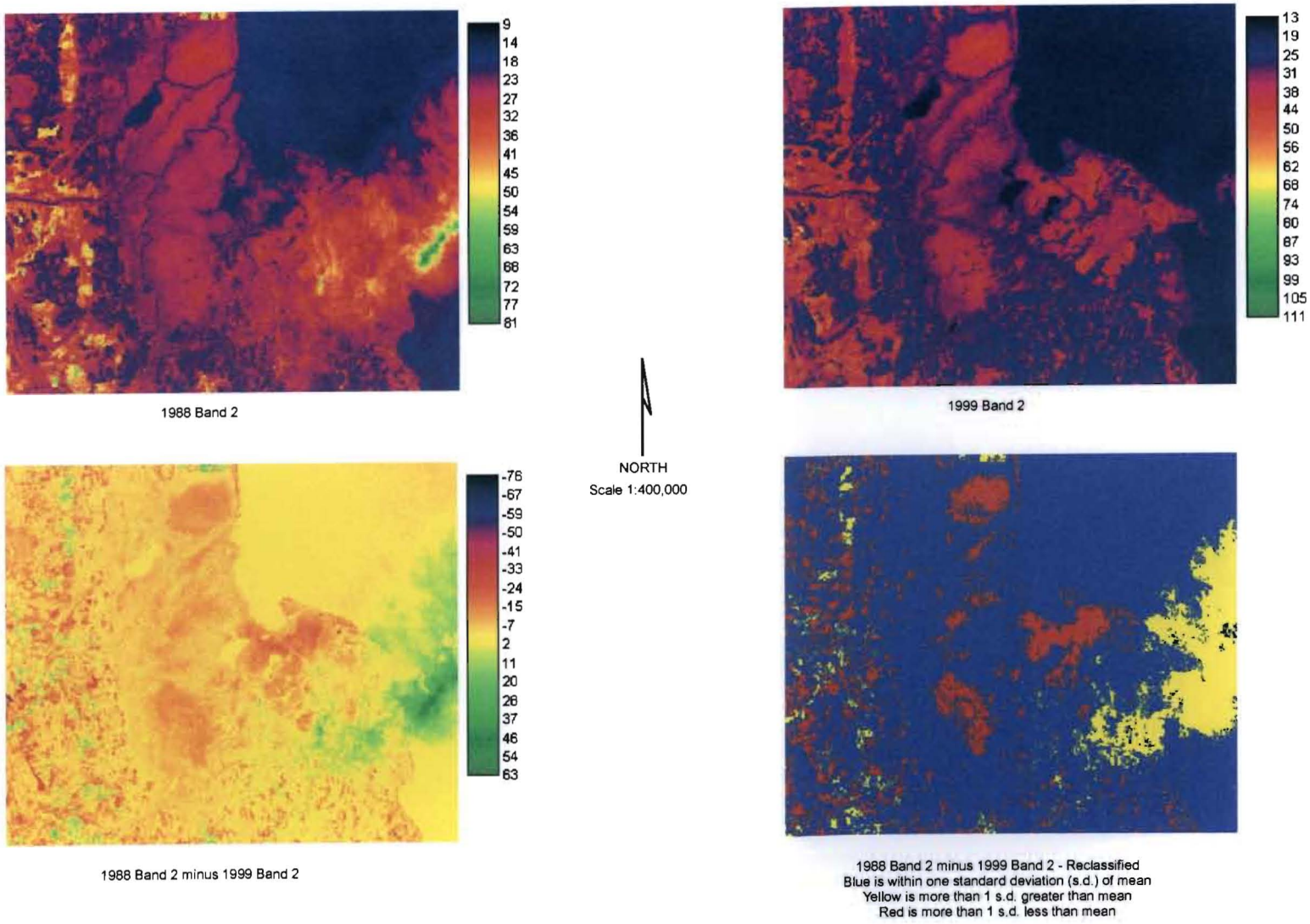

Figure C.2: Image Differencing Band 2 - Emajõe Suursoo Mire Complex

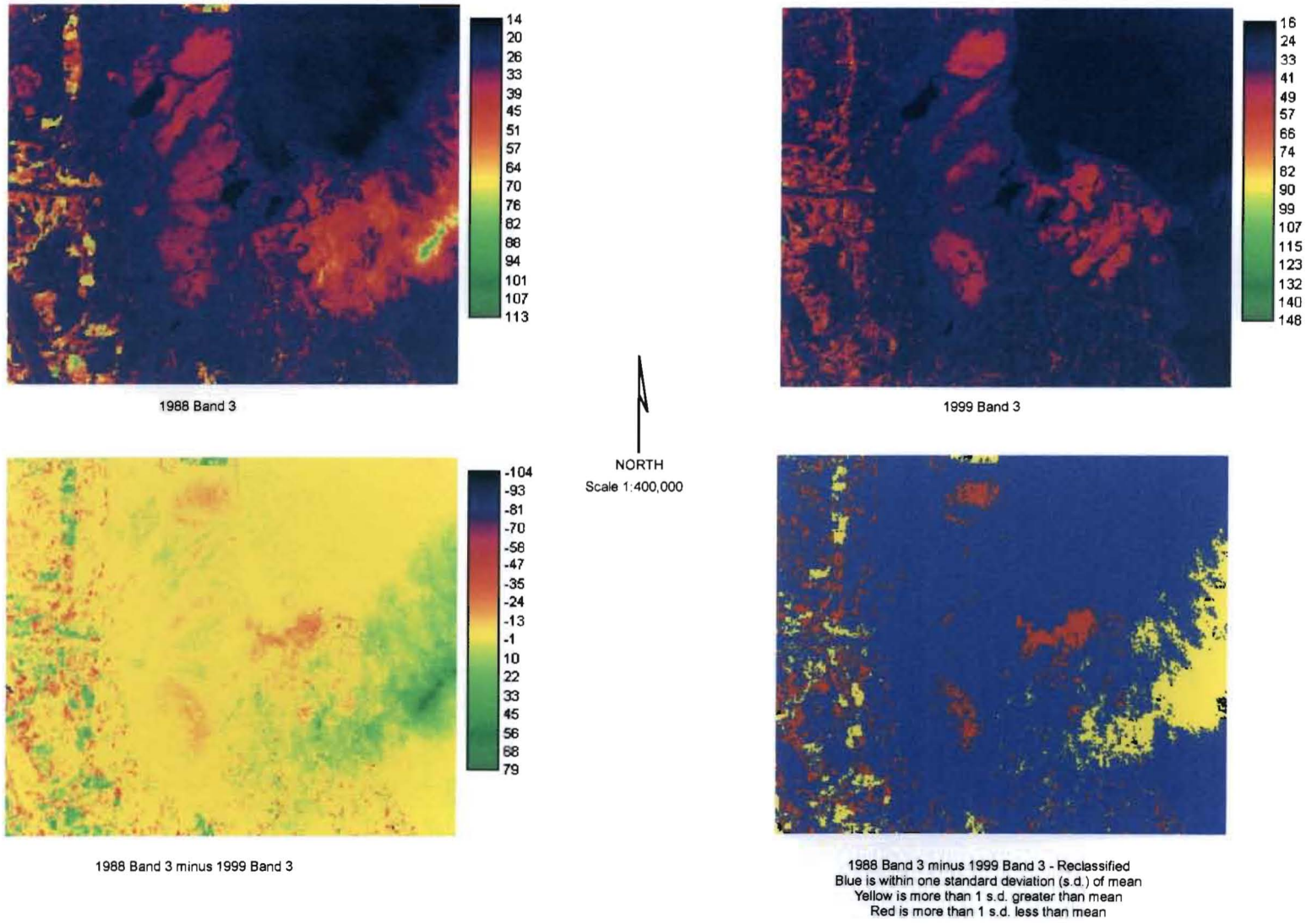

Figure C.3: Image Differencing Band 3 - Emajõe Suursoo Mire Complex

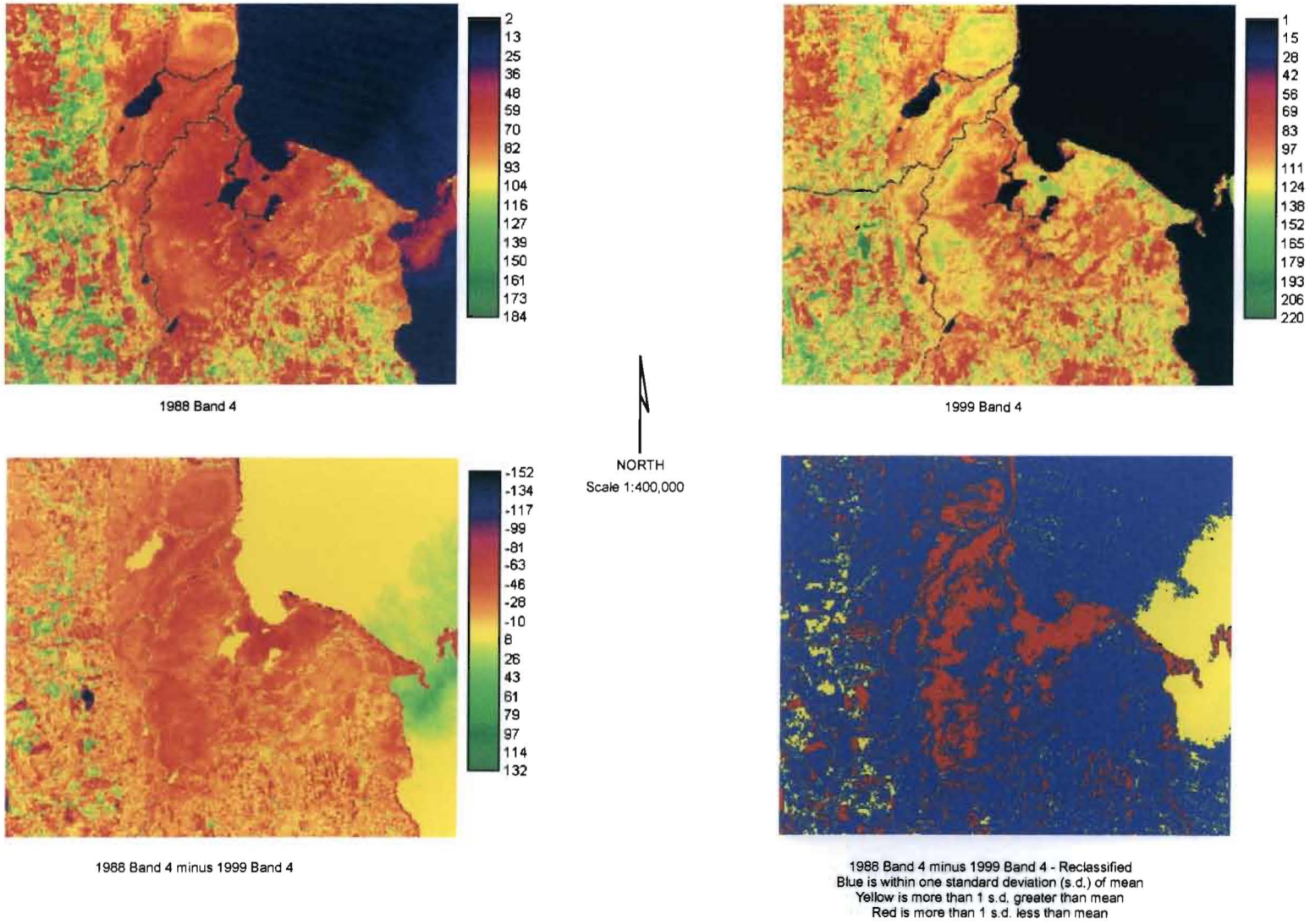

Figure C.4: Image Differencing Band 4 - Emajõe Suursoo Mire Complex

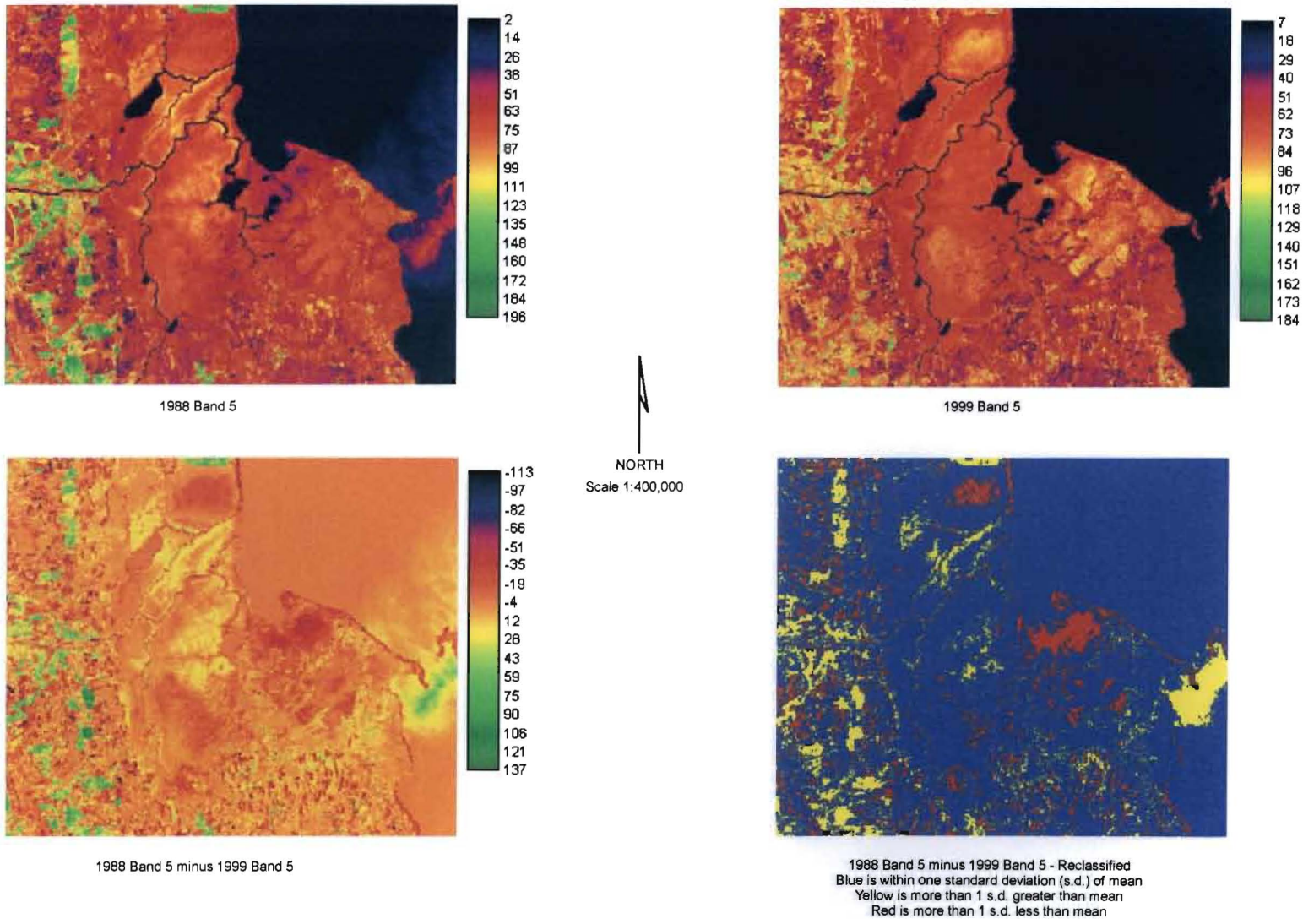

Figure C.5: Image Differencing Band 5 - Emajõe Suursoo Mire Complex

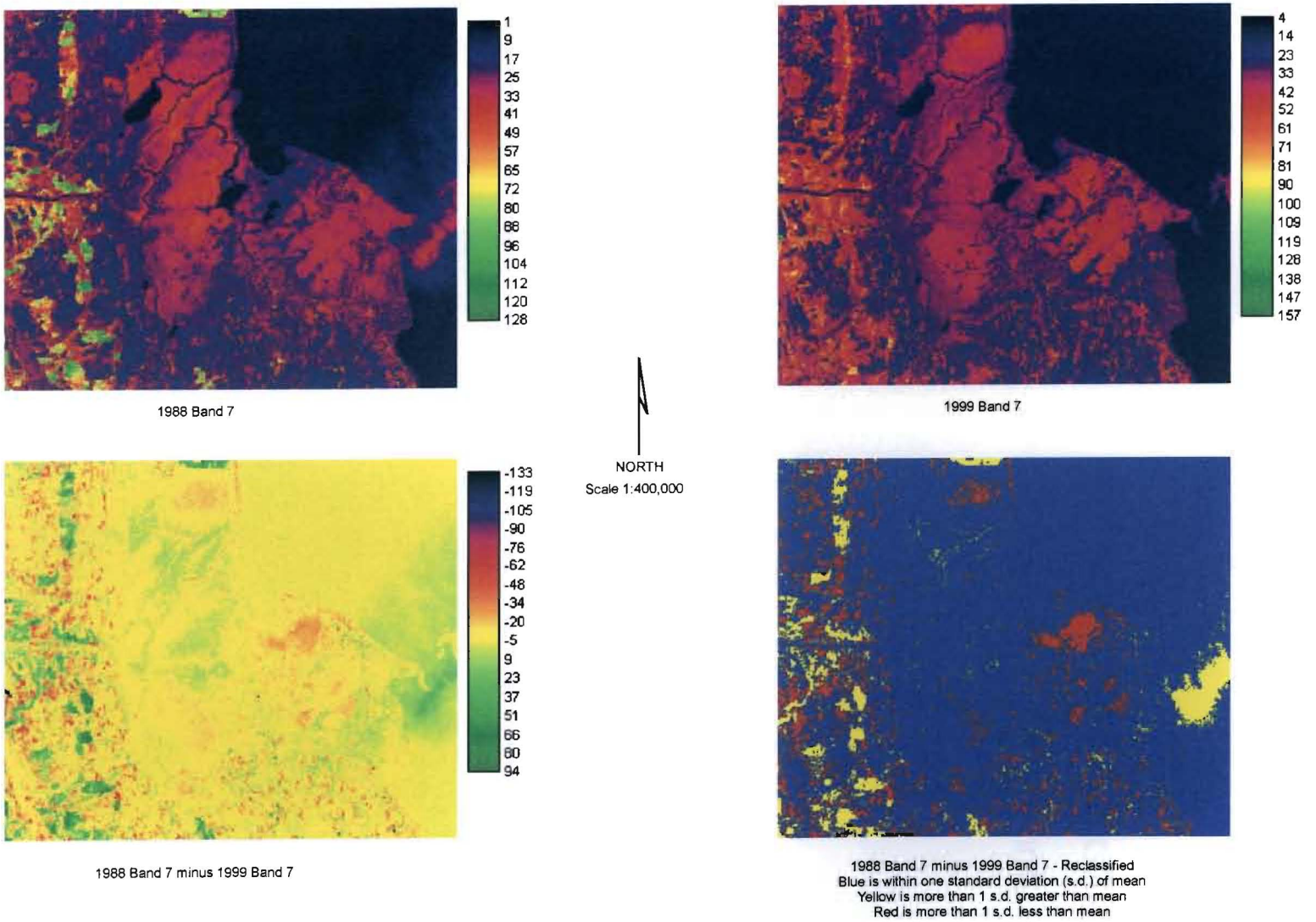

Figure C.6: Image Differencing Band 7 - Emajõe Suursoo Mire Complex

Appendix D:
Image Ratios – Endla

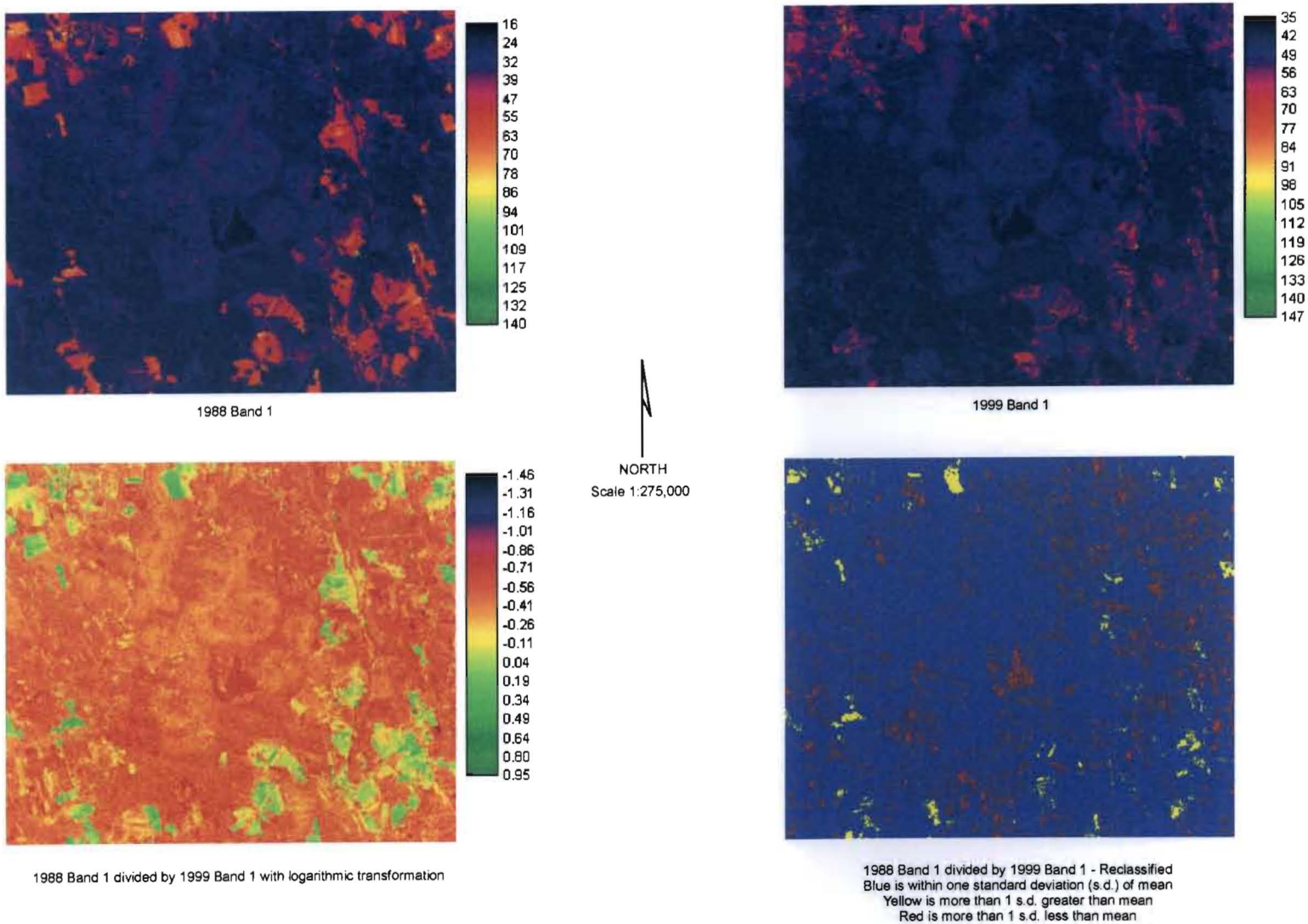

Figure D.1: Image Ratios Band 1 - Endla Nature Reserve

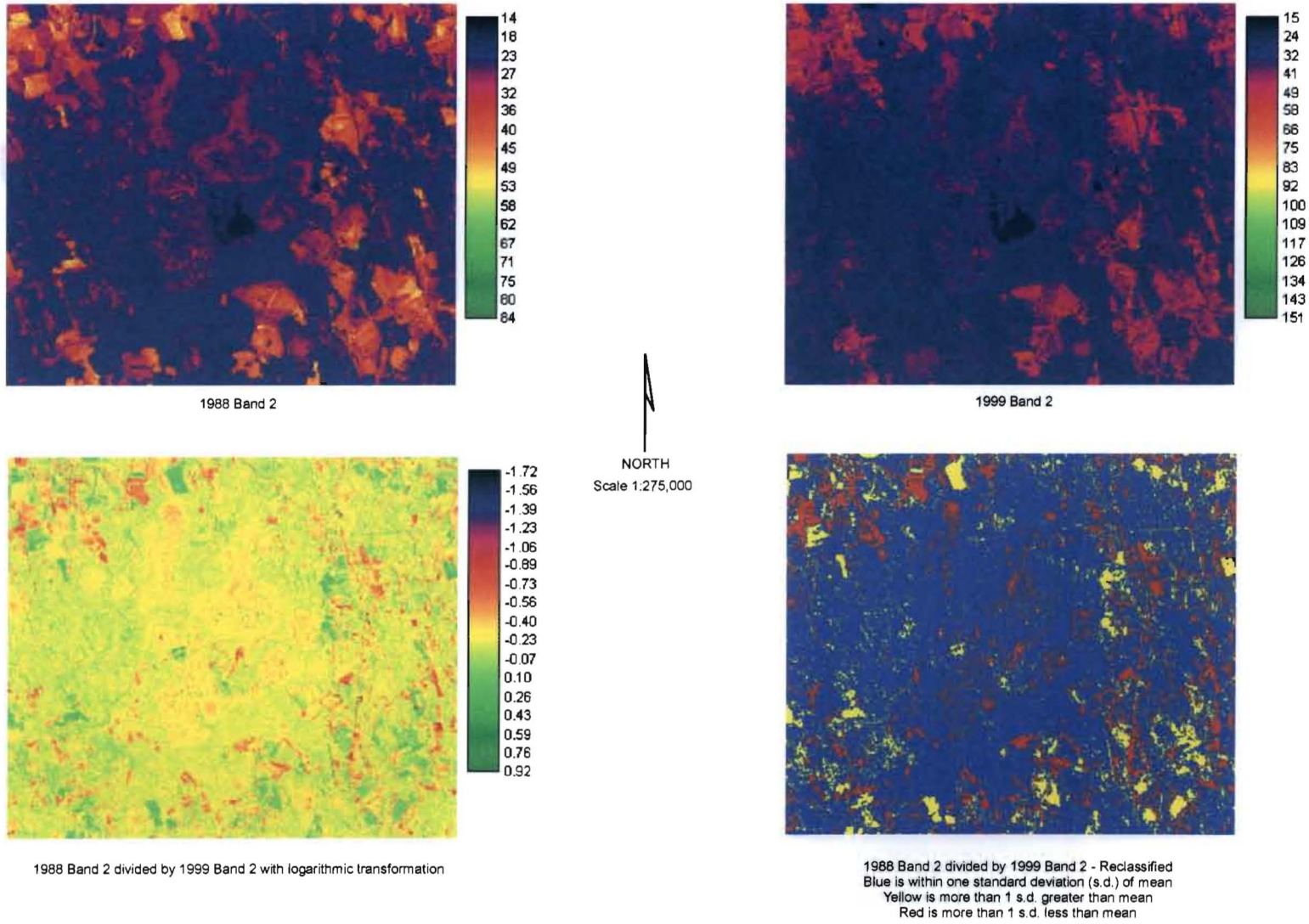

Figure D.2: Image Ratios Band 2 - Endla Nature Reserve

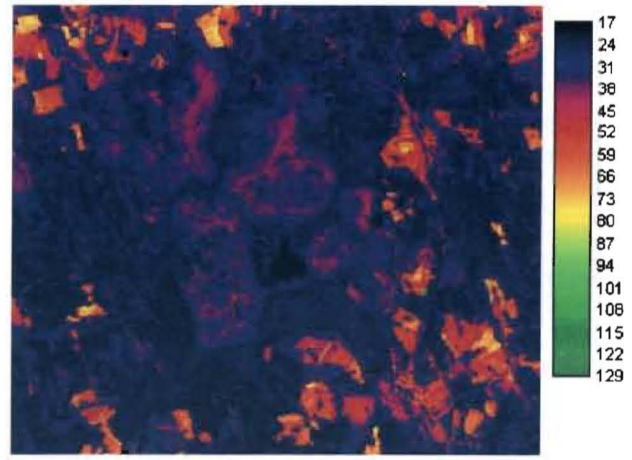

1988 Band 3

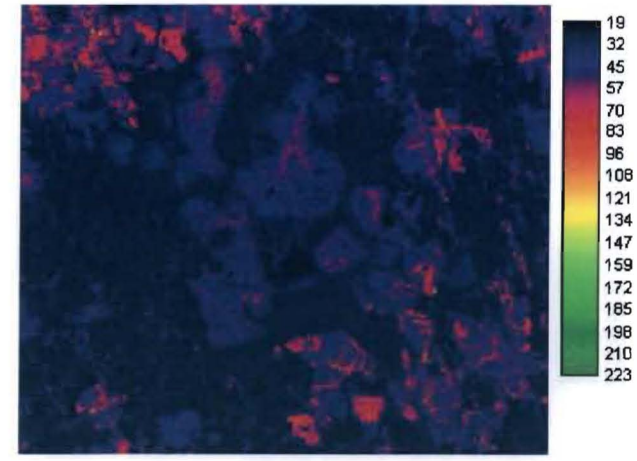

1999 Band 3

NORTH
Scale 1:275,000

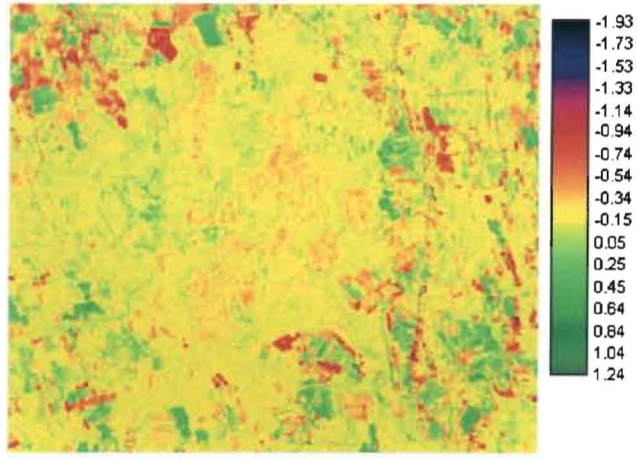

1988 Band 3 divided by 1999 Band 3 with logarithmic transformation

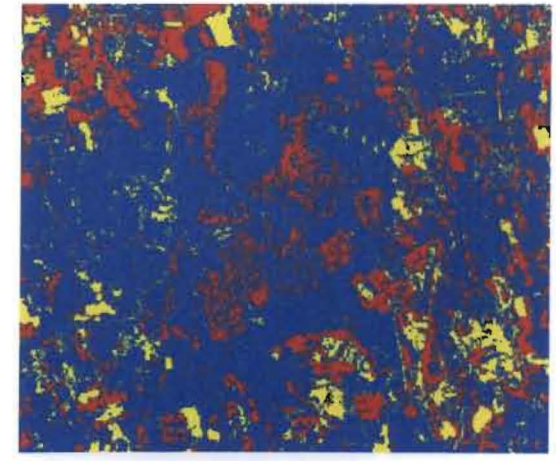

1988 Band 3 divided by 1999 Band 3 - Reclassified
Blue is within one standard deviation (s.d.) of mean
Yellow is more than 1 s.d. greater than mean
Red is more than 1 s.d. less than mean

Figure D.3: Image Ratios Band 3 - Endla Nature Reserve

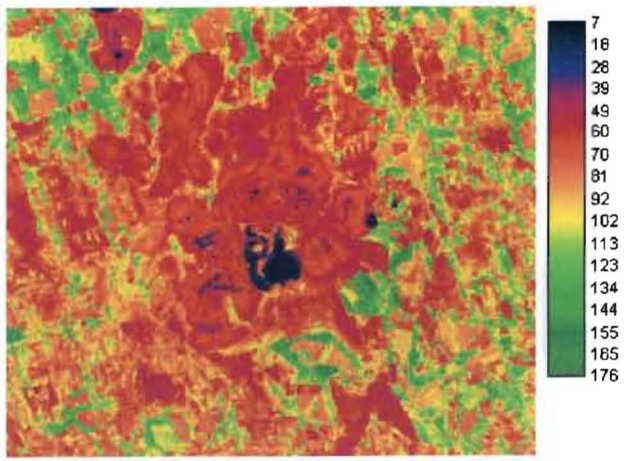

1988 Band 4

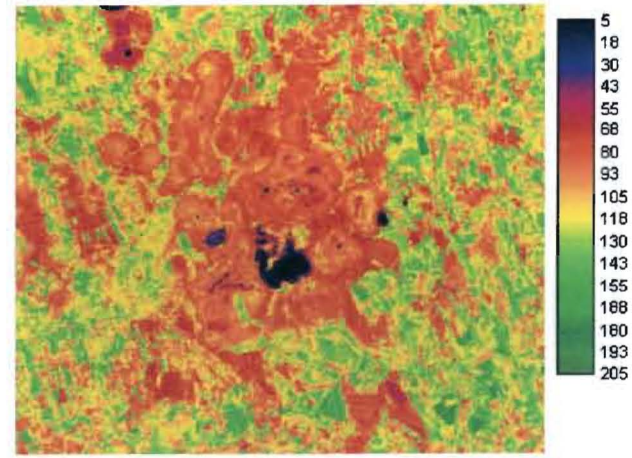

1999 Band 4

NORTH
Scale 1:275,000

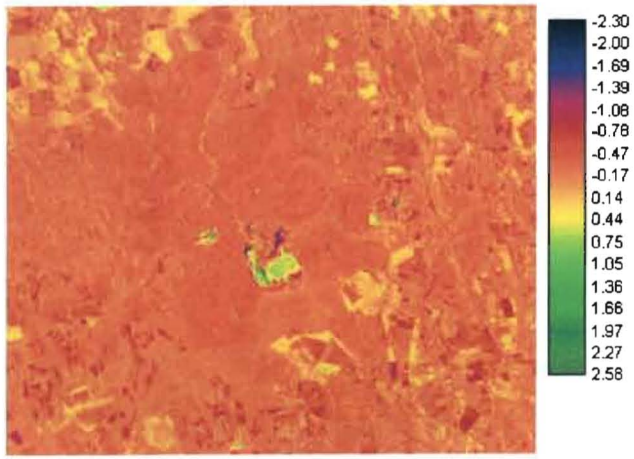

1988 Band 4 divided by 1999 Band 4 with logarithmic transformation

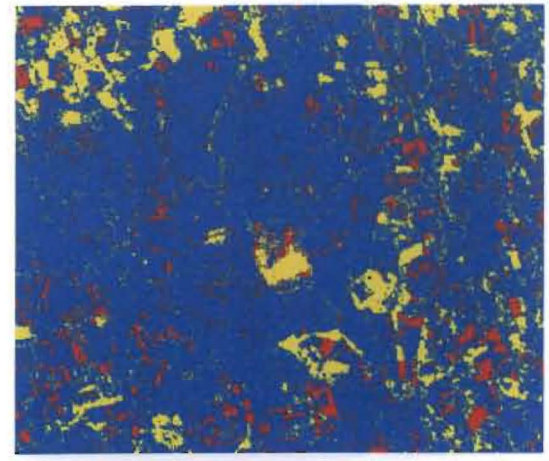

1988 Band 4 divided by 1999 Band 4 - Reclassified
Blue is within one standard deviation (s.d.) of mean
Yellow is more than 1 s.d. greater than mean
Red is more than 1 s.d. less than mean

Figure D.4: Image Ratios Band 4 - Endla Nature Reserve

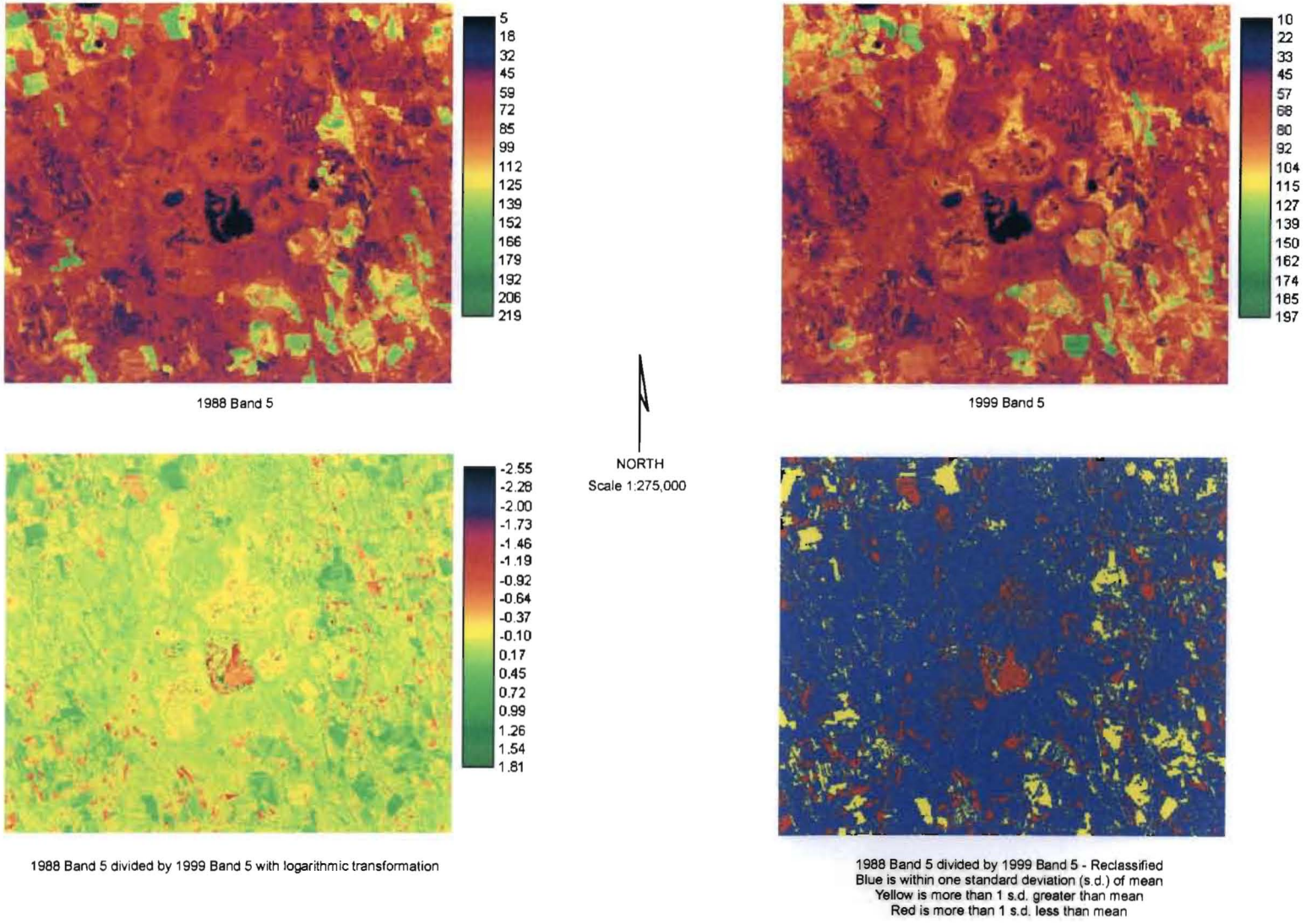

Figure D.5: Image Ratios Band 5 - Endla Nature Reserve

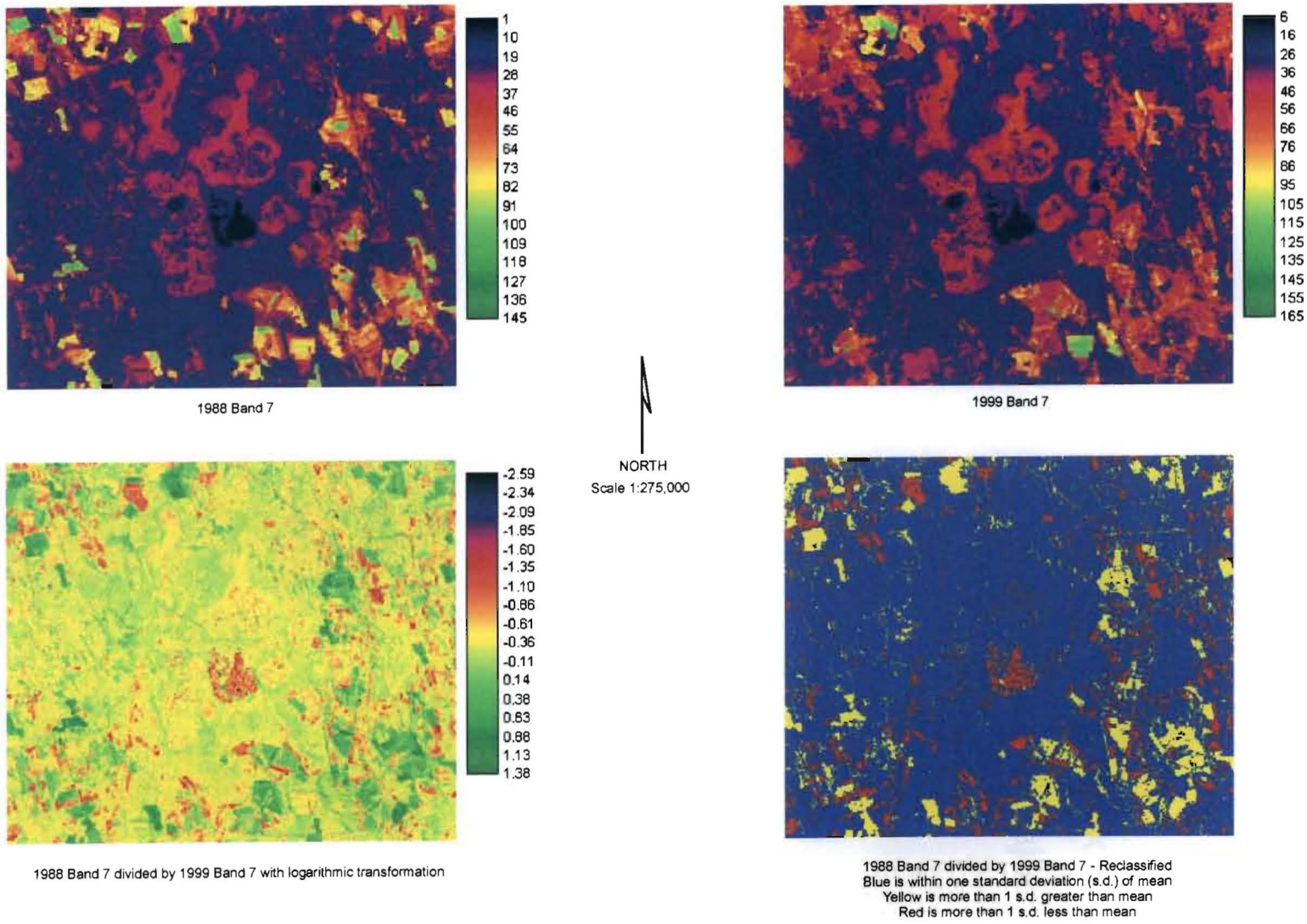

Figure D.6: Image Ratios Band 7 - Endla Nature Reserve

Appendix E:
Image Ratios – Emajõe

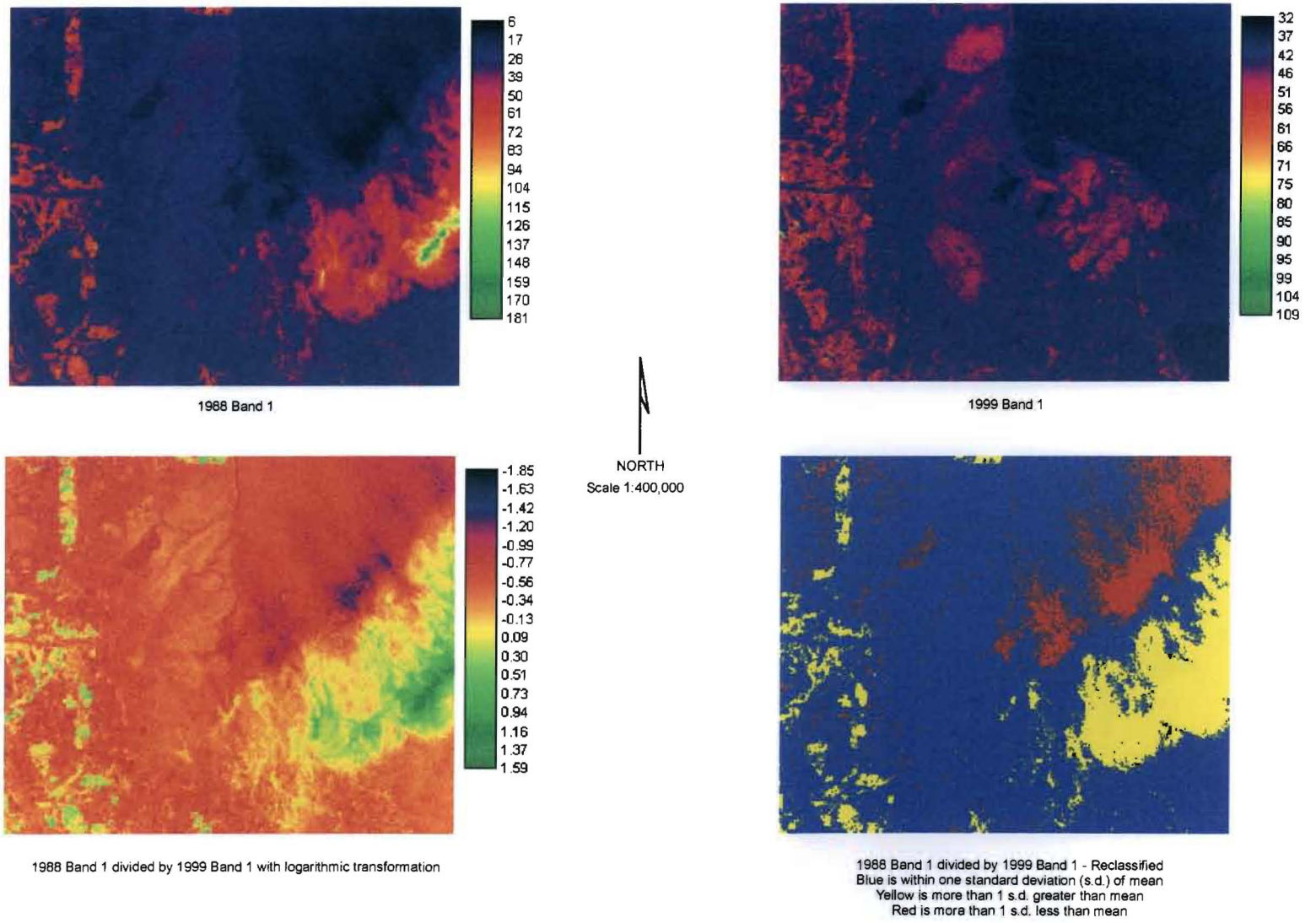

Figure E.1: Image Ratios Band 1 - Emajõe Suursoo Mire Complex

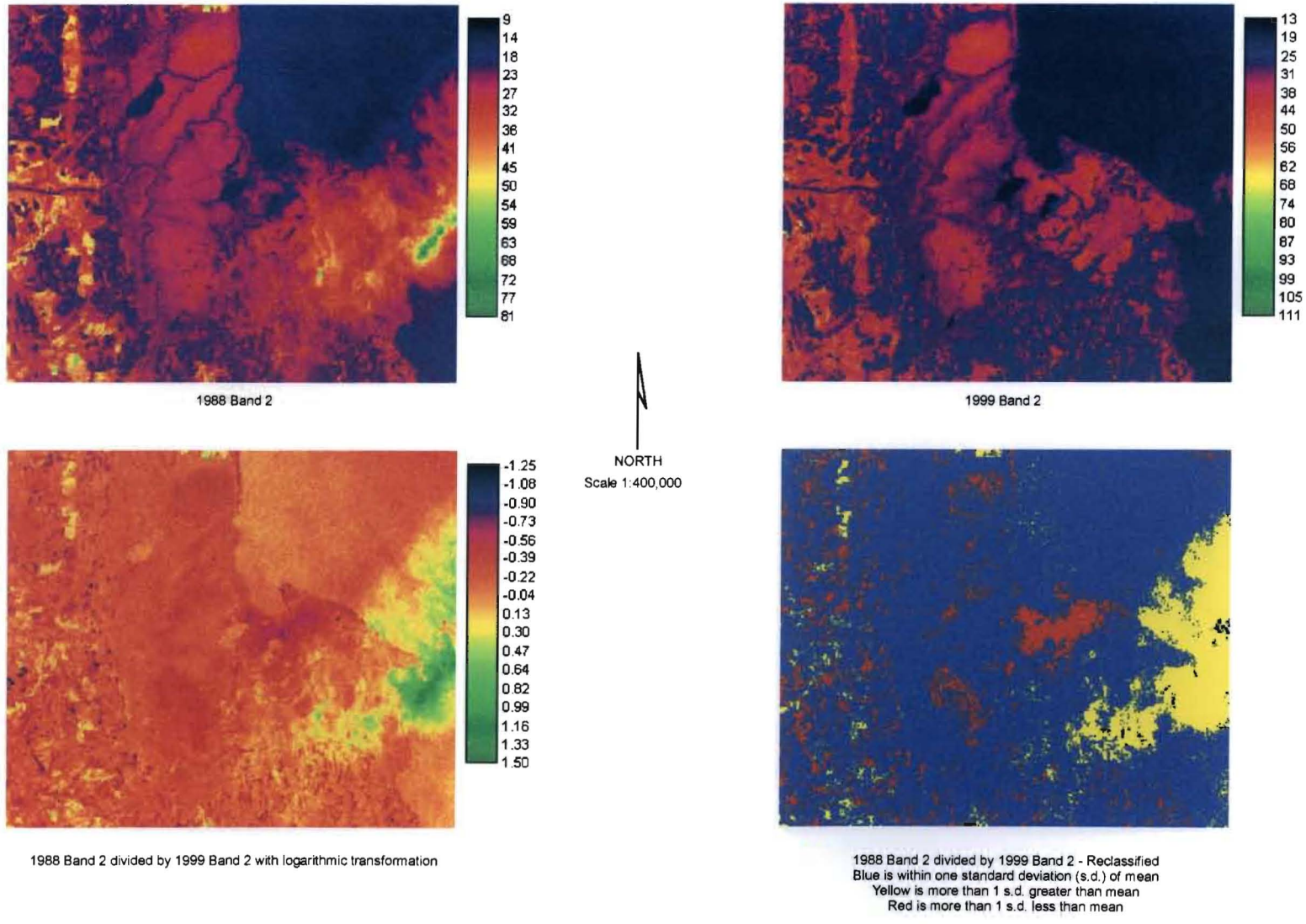

Figure E.2: Image Ratios Band 2 - Emajõe Suursoo Mire Complex

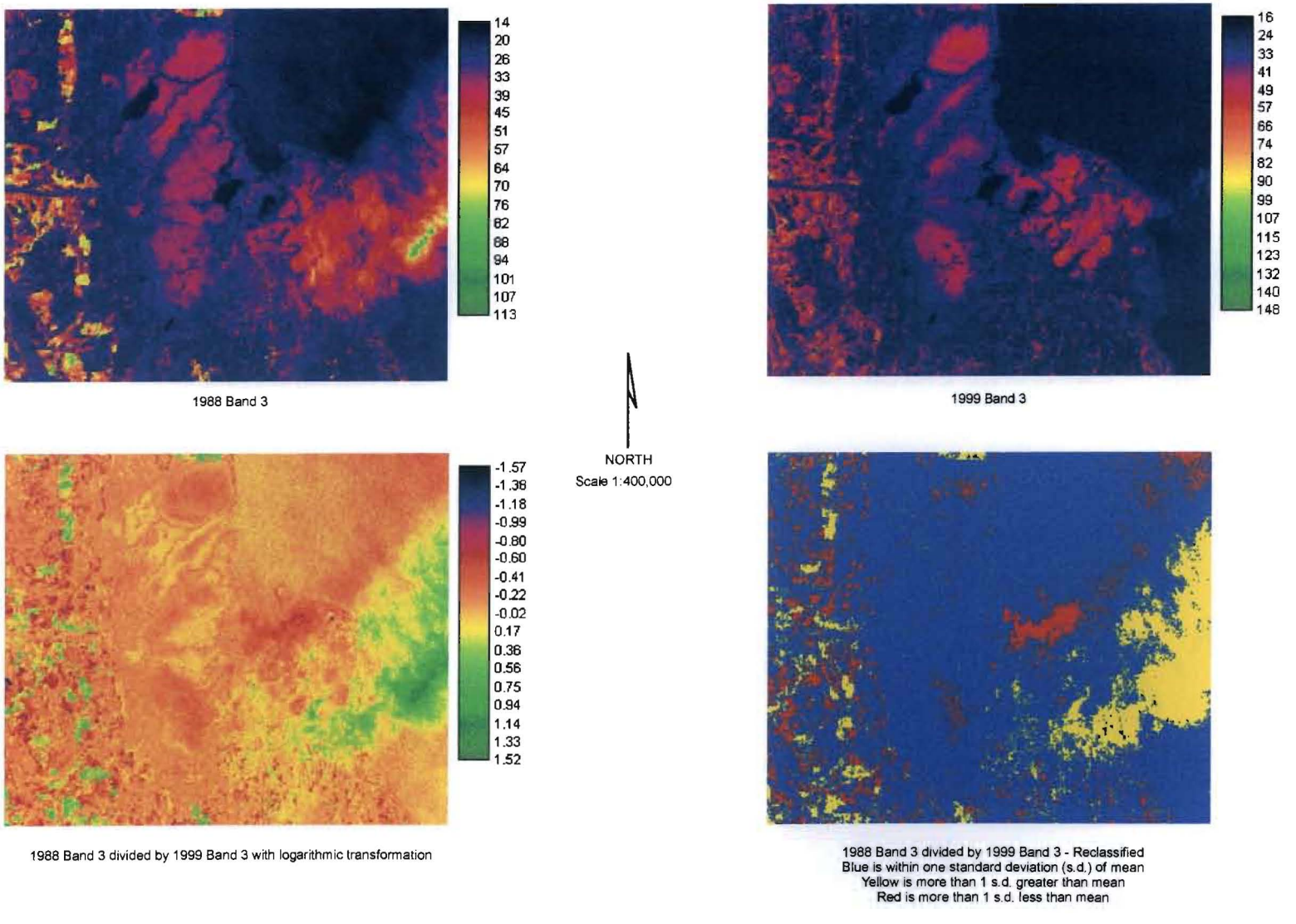

Figure E.3: Image Ratios Band 3 - Emajõe Suursoo Mire Complex

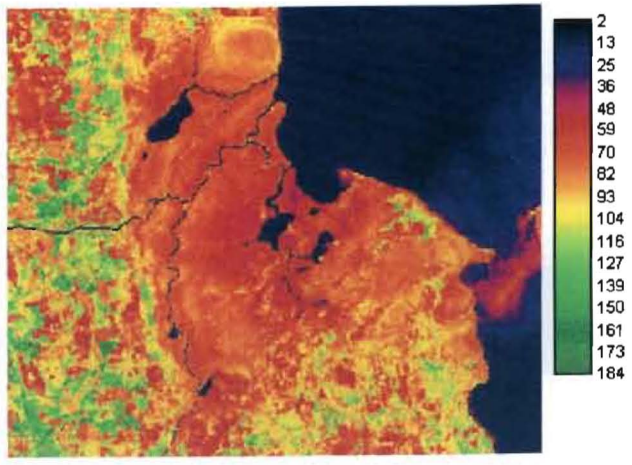

1988 Band 4

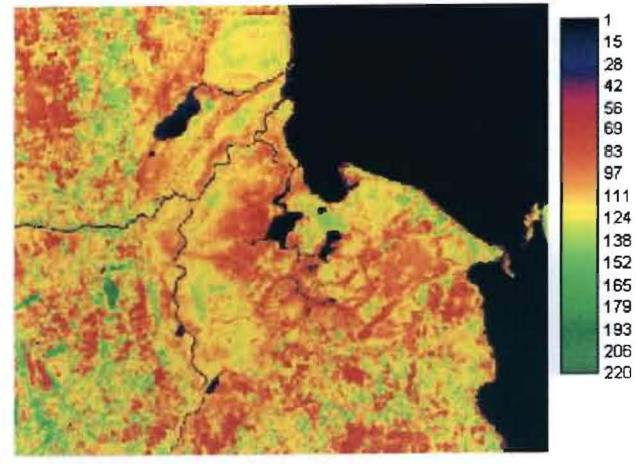

1999 Band 4

NORTH
Scale 1:400,000

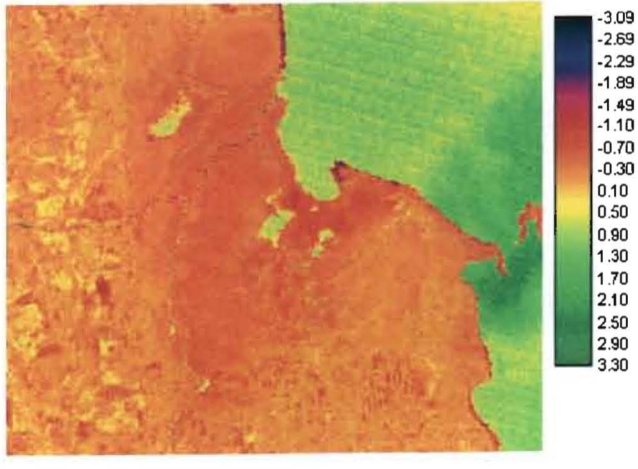

1988 Band 4 divided by 1999 Band 4 with logarithmic transformation

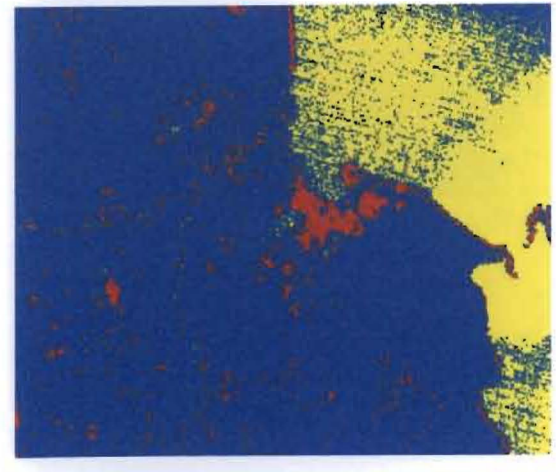

1988 Band 4 divided by 1999 Band 4 - Reclassified
Blue is within one standard deviation (s.d.) of mean
Yellow is more than 1 s.d. greater than mean
Red is more than 1 s.d. less than mean

Figure E.4: Image Ratios Band 4 - Emajõe Suursoo Mire Complex

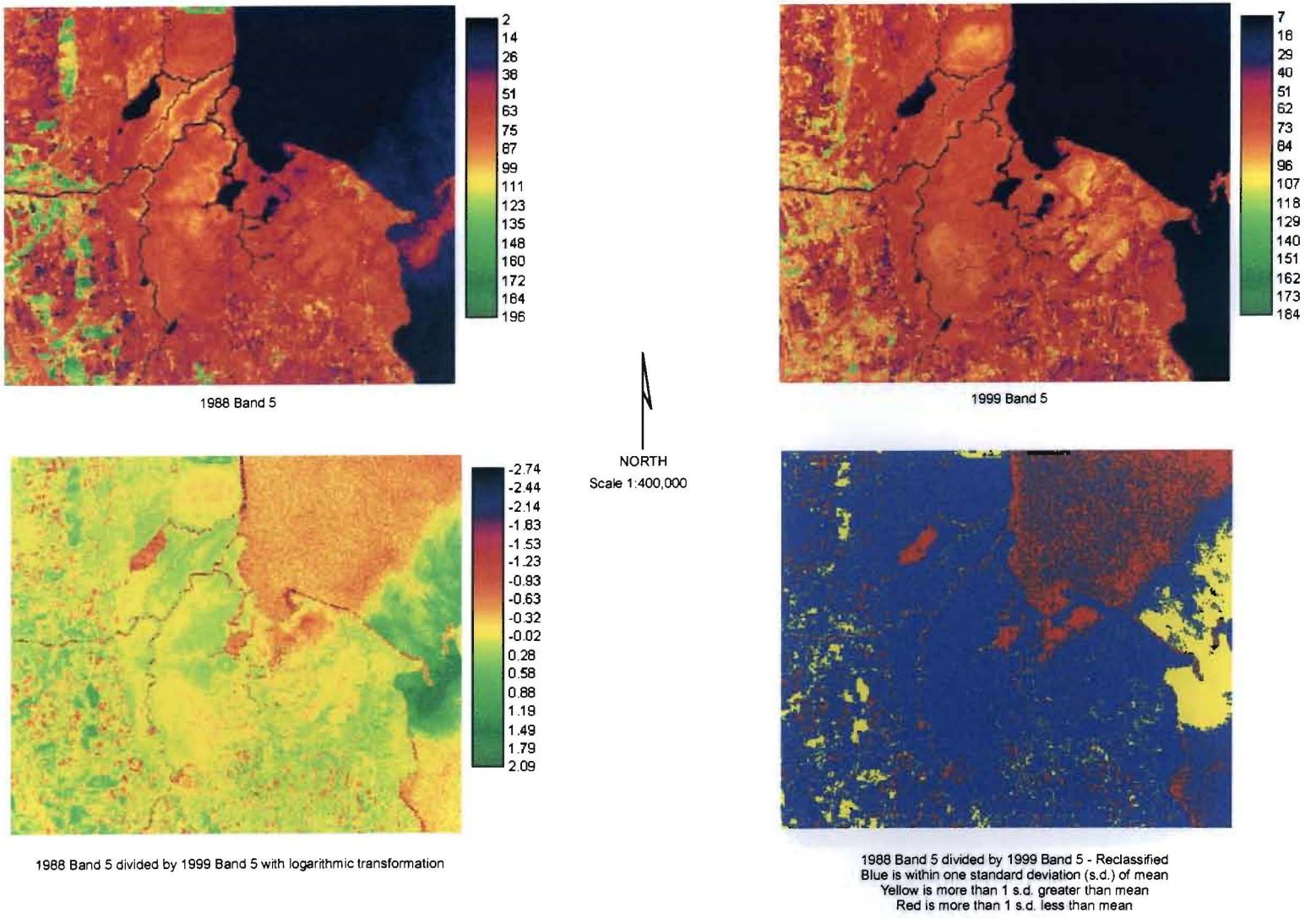

Figure E.5: Image Ratios Band 5 - Emajõe Suursoo Mire Complex

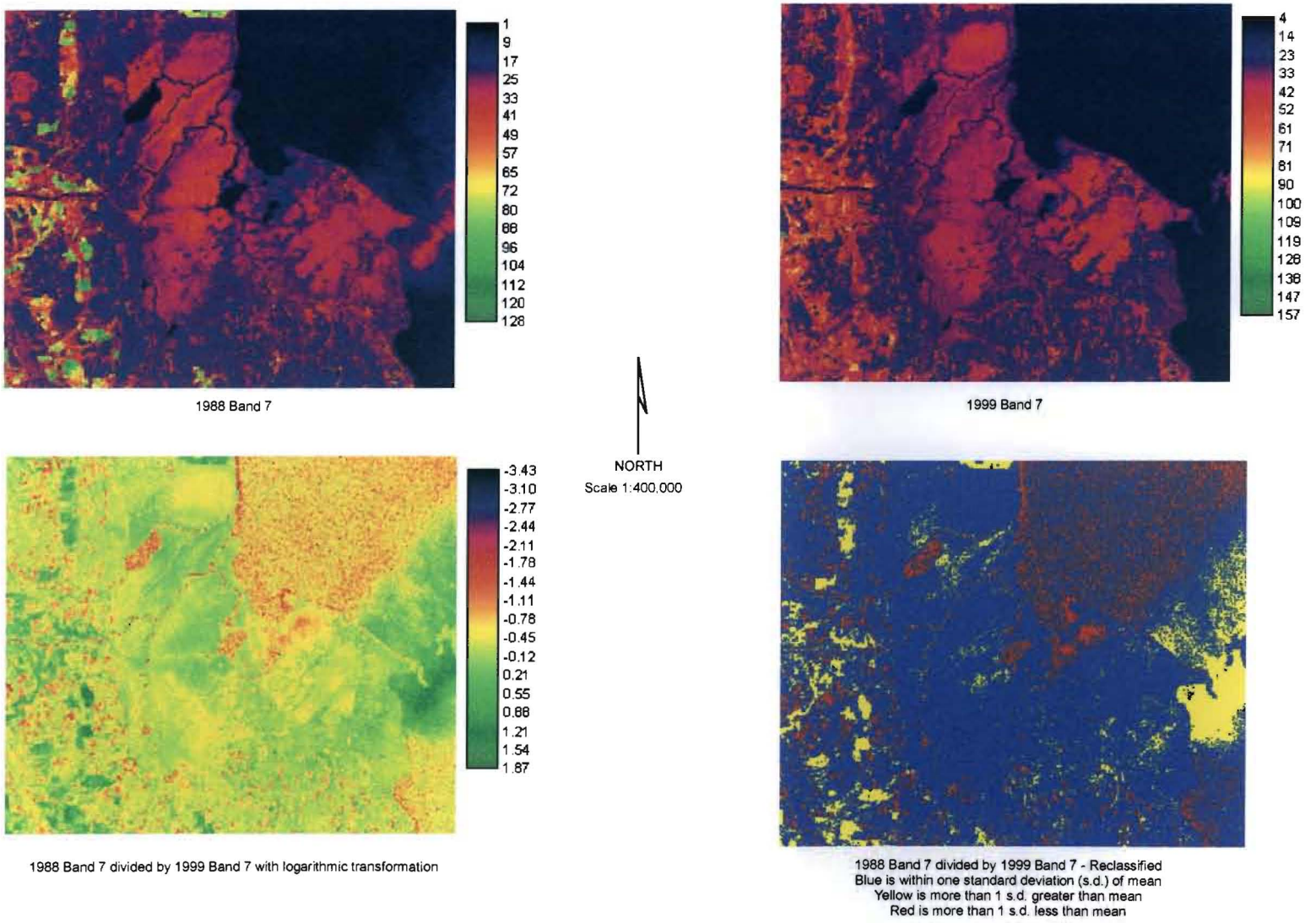

Figure E.6: Image Ratios Band 7 - Emajõe Suursoo Mire Complex

Appendix F:
NDVI Images – Endla

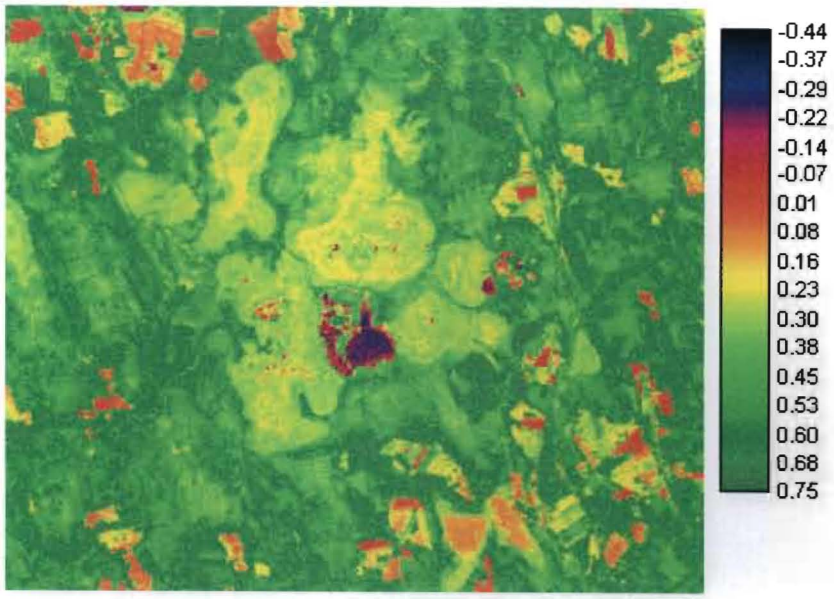

NDVI Image - 1988

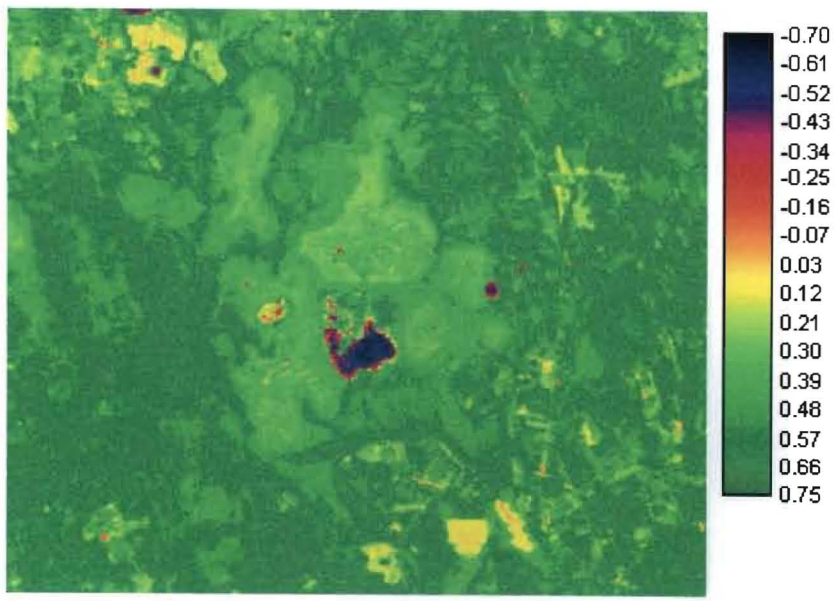

NDVI Image 1999

Scale 1:212,000

Figure F.1: NDVI Images for Endla Nature Reserve - 1988 and 1999

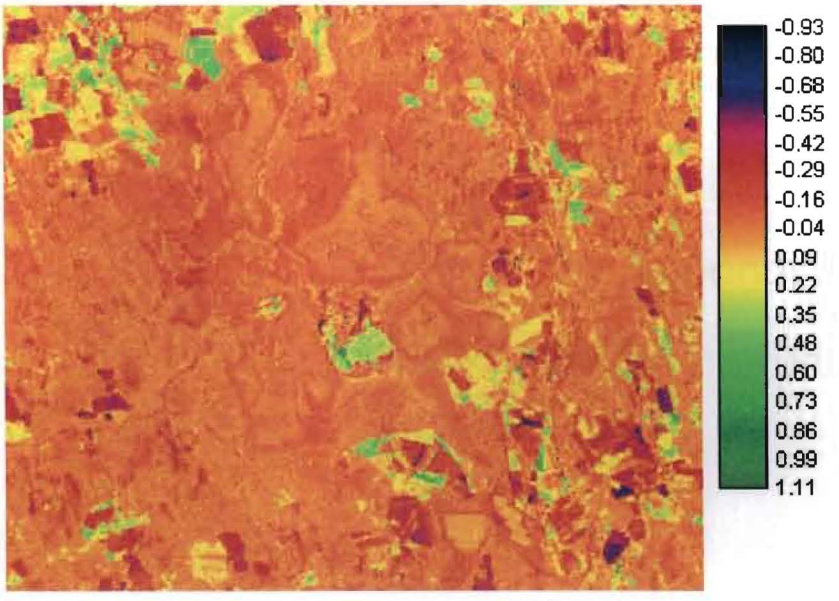

1988 NDVI minus 1999 NDVI

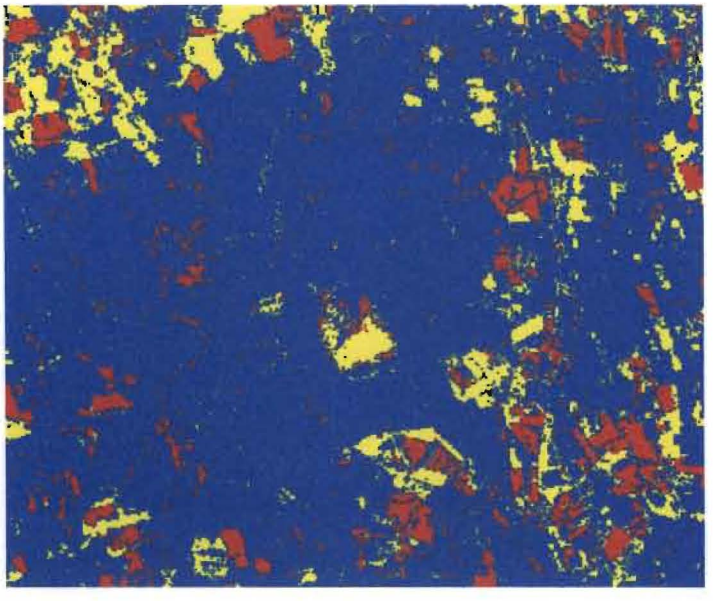

1988 NDVI minus 1999 NDVI - Reclassified
Blue is within one standard deviation (s.d.) of mean
Yellow is more than 1 s.d. greater than mean
Red is more than 1 s.d. less than mean

NORTH

Scale 1:212,000

Figure F.2: NDVI Analytical Images for Endla Nature Reserve - 1988 and 1999

Appendix G:
NDVI Images – Emajõe

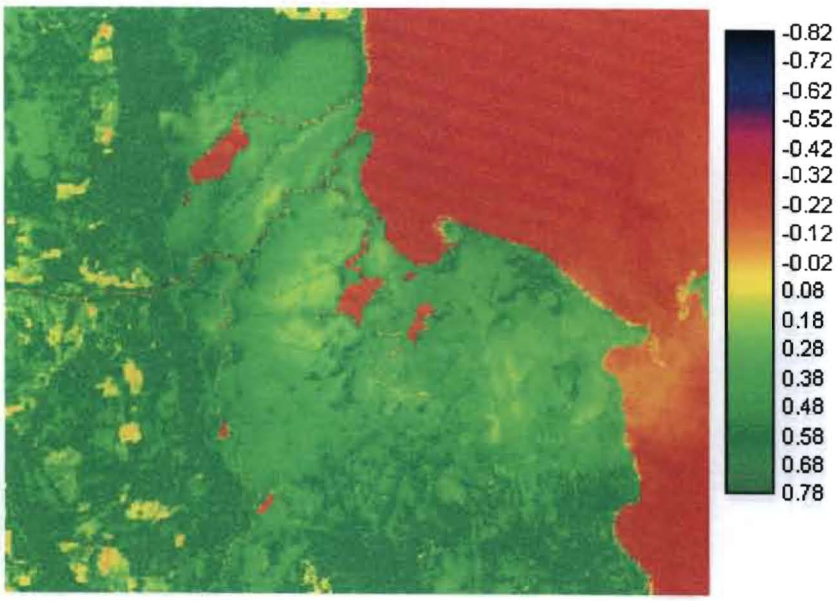

NDVI Image - 1988

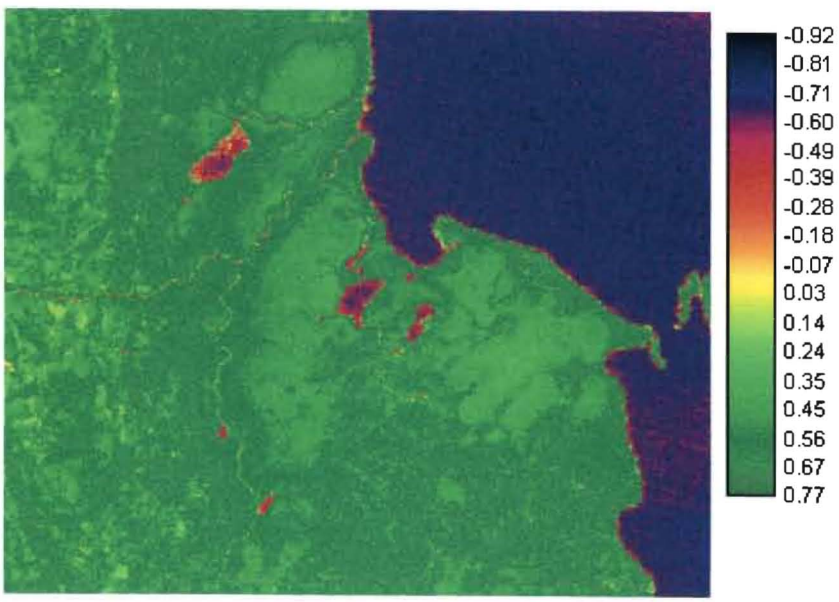

NDVI Image 1999

NORTH

Scale 1:310,000

Figure G.1: NDVI Images for Emajõe Suursoo Mire Complex - 1988 and 1999

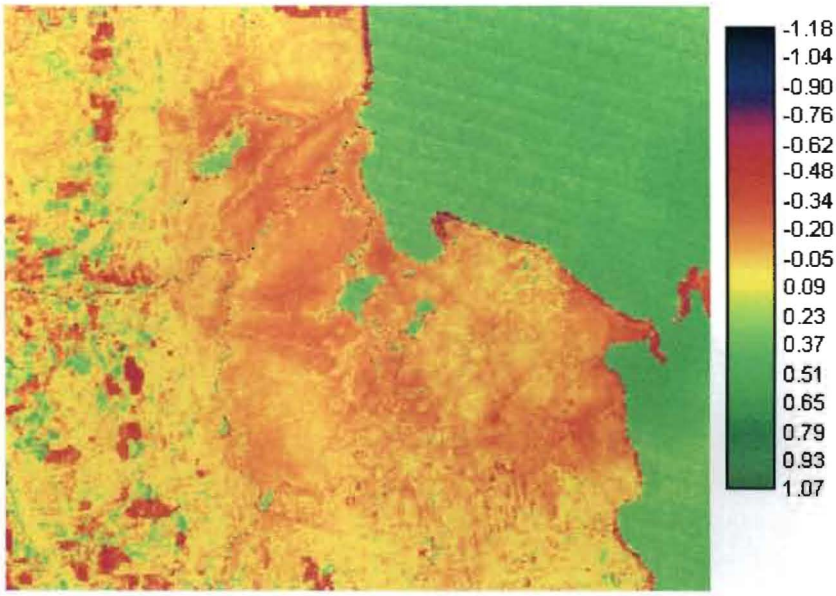

1988 NDVI minus 1999 NDVI

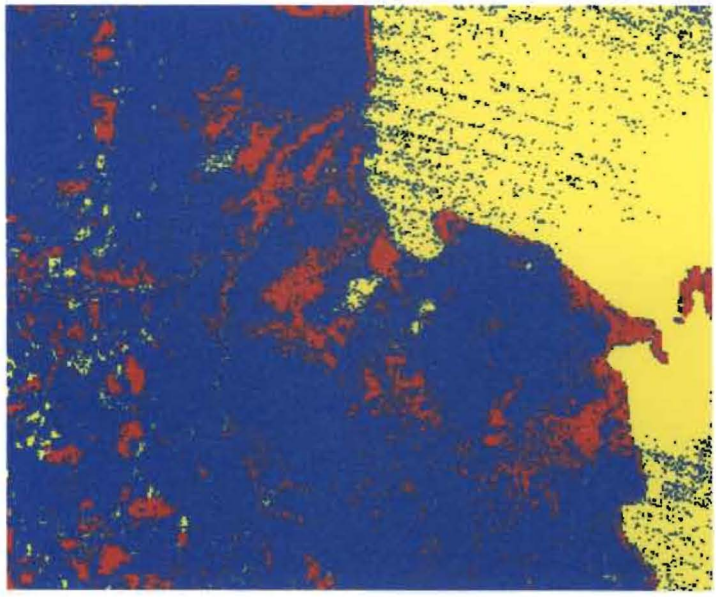

1988 NDVI minus 1999 NDVI - Reclassified
Blue is within one standard deviation (s.d.) of mean
Yellow is more than 1 s.d. greater than mean
Red is more than 1 s.d. less than mean

NORTH

Scale 1:310,000

Figure G.2: NDVI Analytical Images for Emajõe Suursoo Mire Complex - 1988 and 1999

Appendix H:
TCT Images – Endla

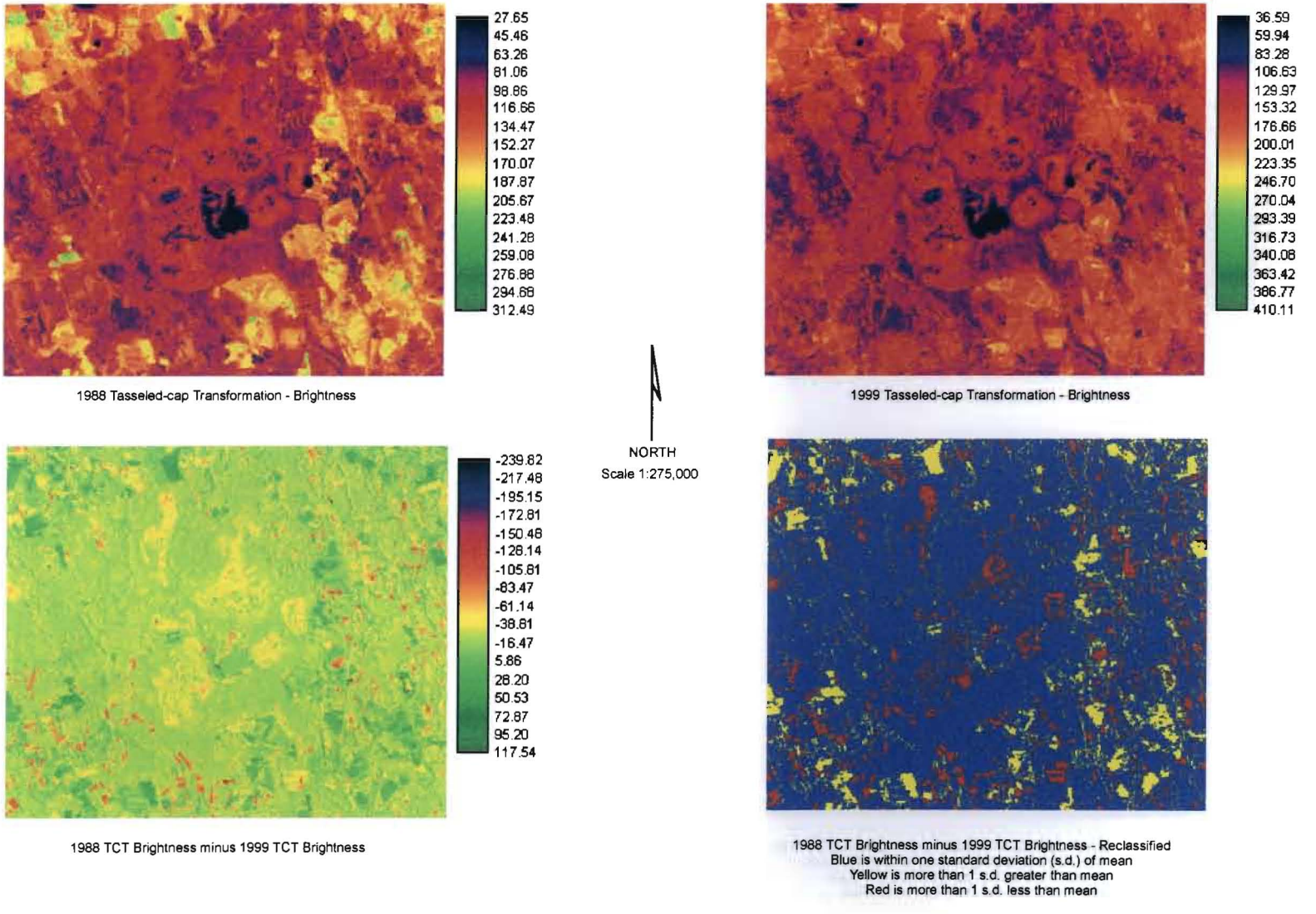

Figure H.1: Tasseled-Cap Transformation Brightness Images - Endla Nature Reserve

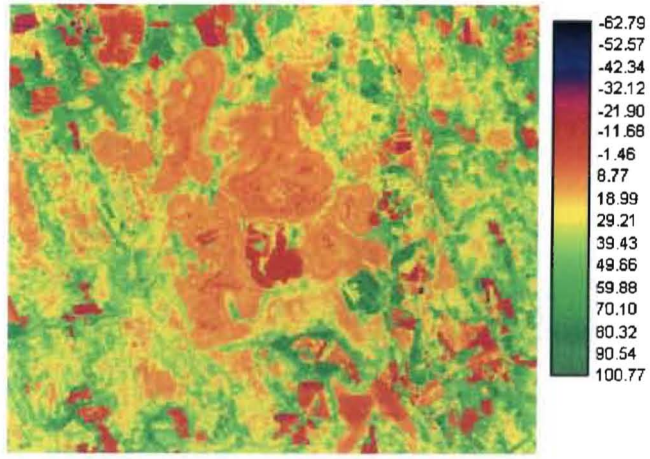

1988 Tasseled-cap Transformation - Greenness

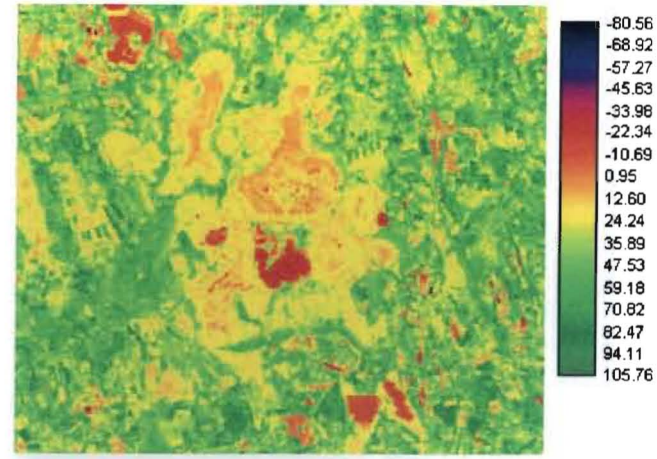

1999 Tasseled-cap Transformation - Greenness

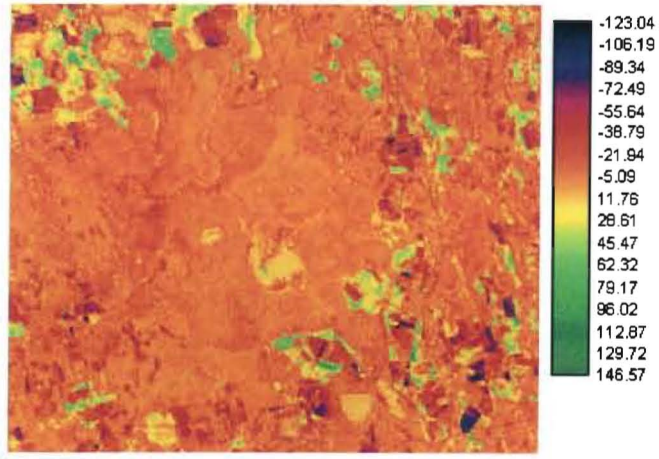

1988 TCT Greenness minus 1999 TCT Greenness

NORTH
Scale 1:275,000

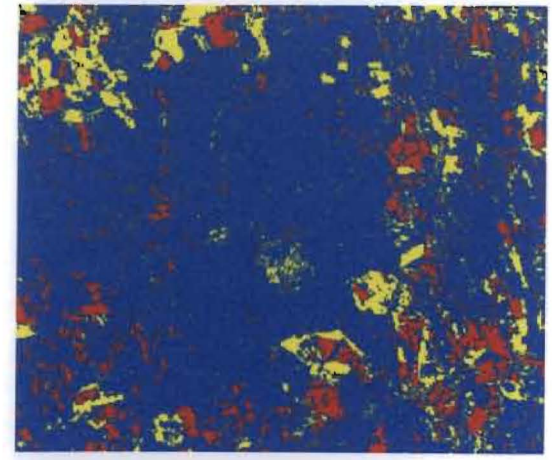

1988 TCT Greenness minus 1999 TCT Greenness - Reclassified
Blue is within one standard deviation (s.d.) of mean
Yellow is more than 1 s.d. greater than mean
Red is more than 1 s.d. less than mean

Figure H.2: Tasseled-Cap Transformation Greenness Images - Endla Nature Reserve

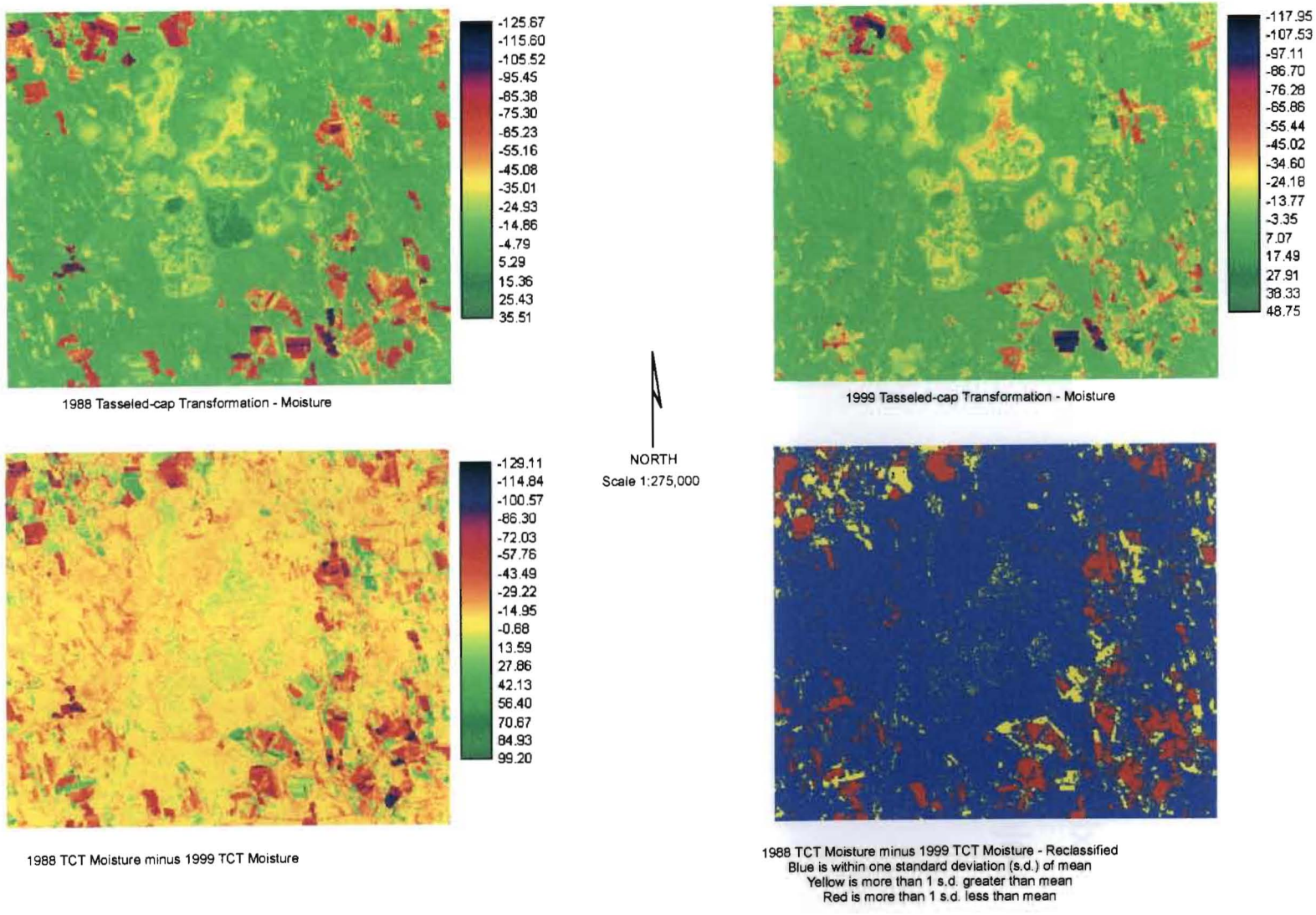

Figure H.3: Tasseled-Cap Transformation Moisture Images - Endla Nature Reserve

Appendix I:
TCT Images – Emajõe

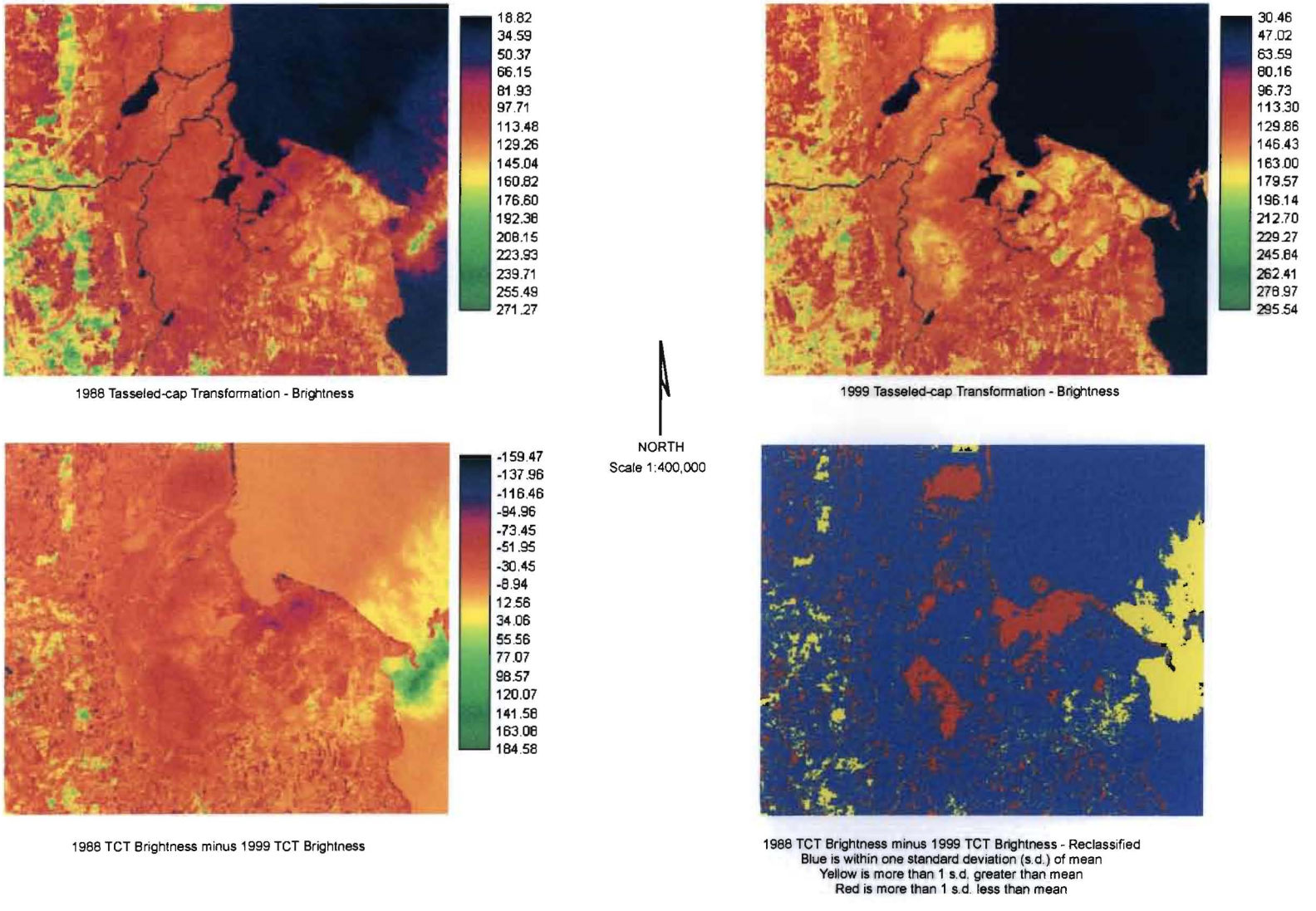

Figure I.1: Tasseled-Cap Transformation Brightness Images - Emajõe Suursoo Mire Complex

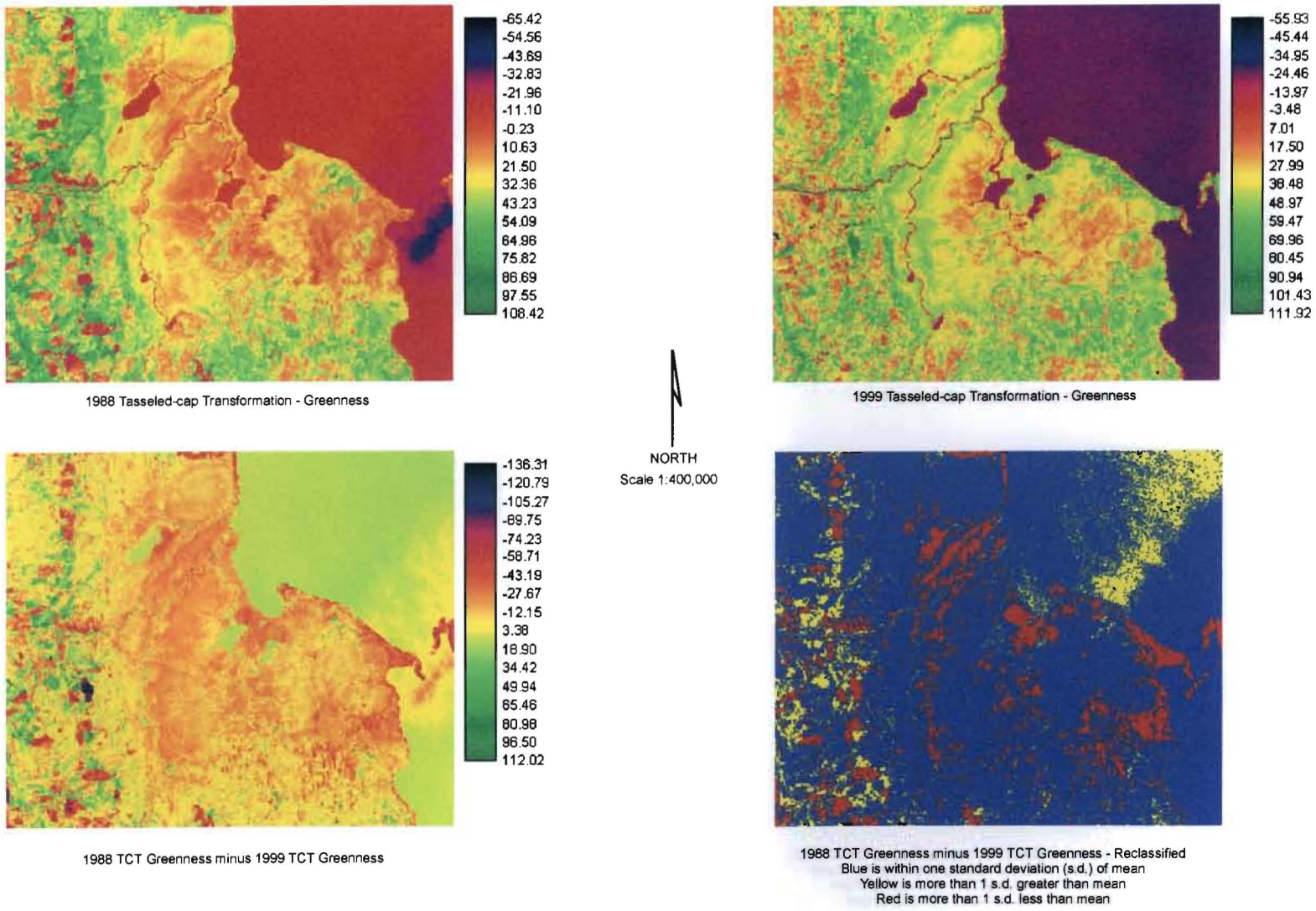

Figure I.2: Tasseled-Cap Transformation Greenness Images - Emajõe Suursoo Mire Complex

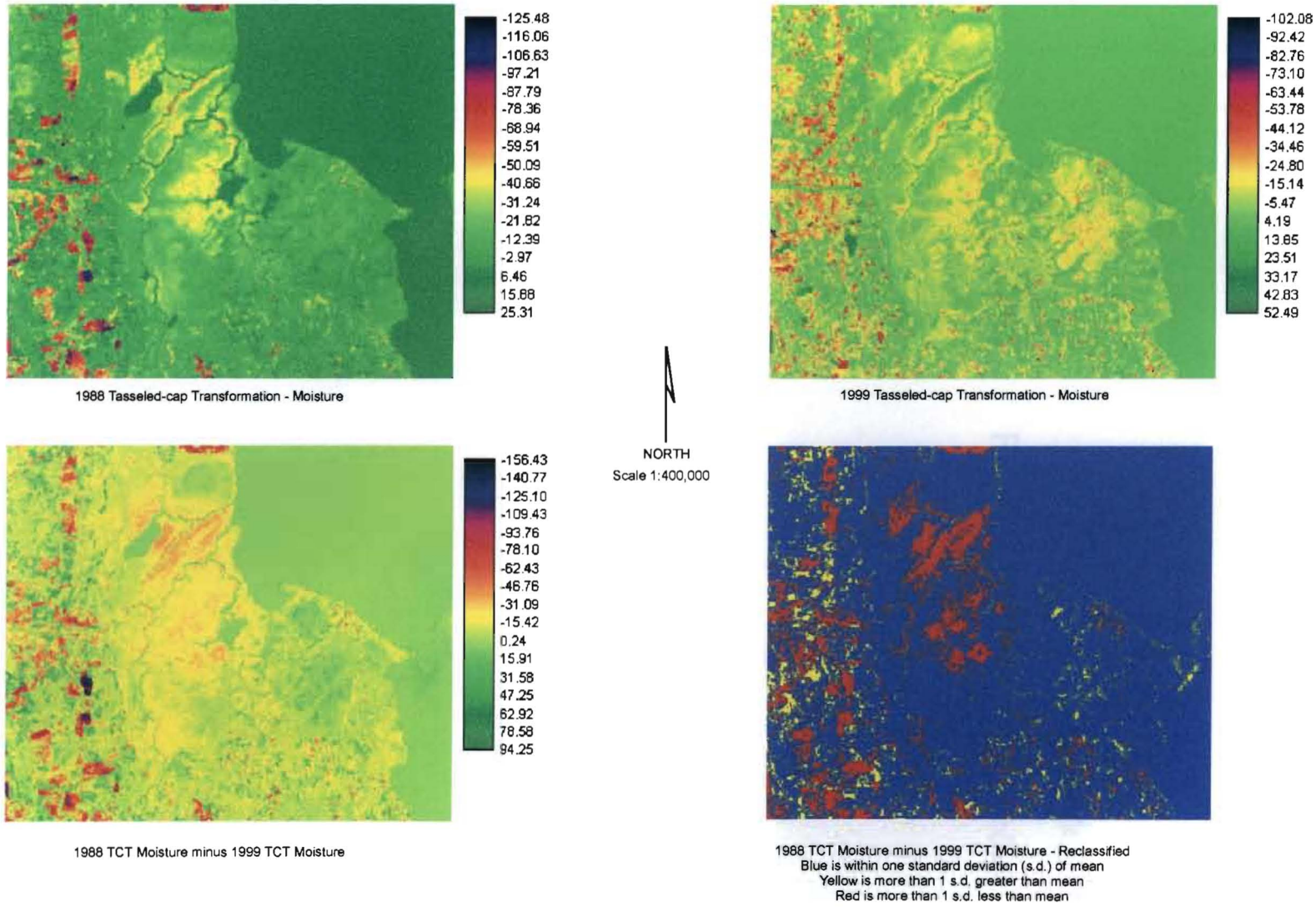

Figure I.3: Tasseled-Cap Transformation Moisture Images - Emajõe Suursoo Mire Complex

Appendix J:
Regression Plots – Endla

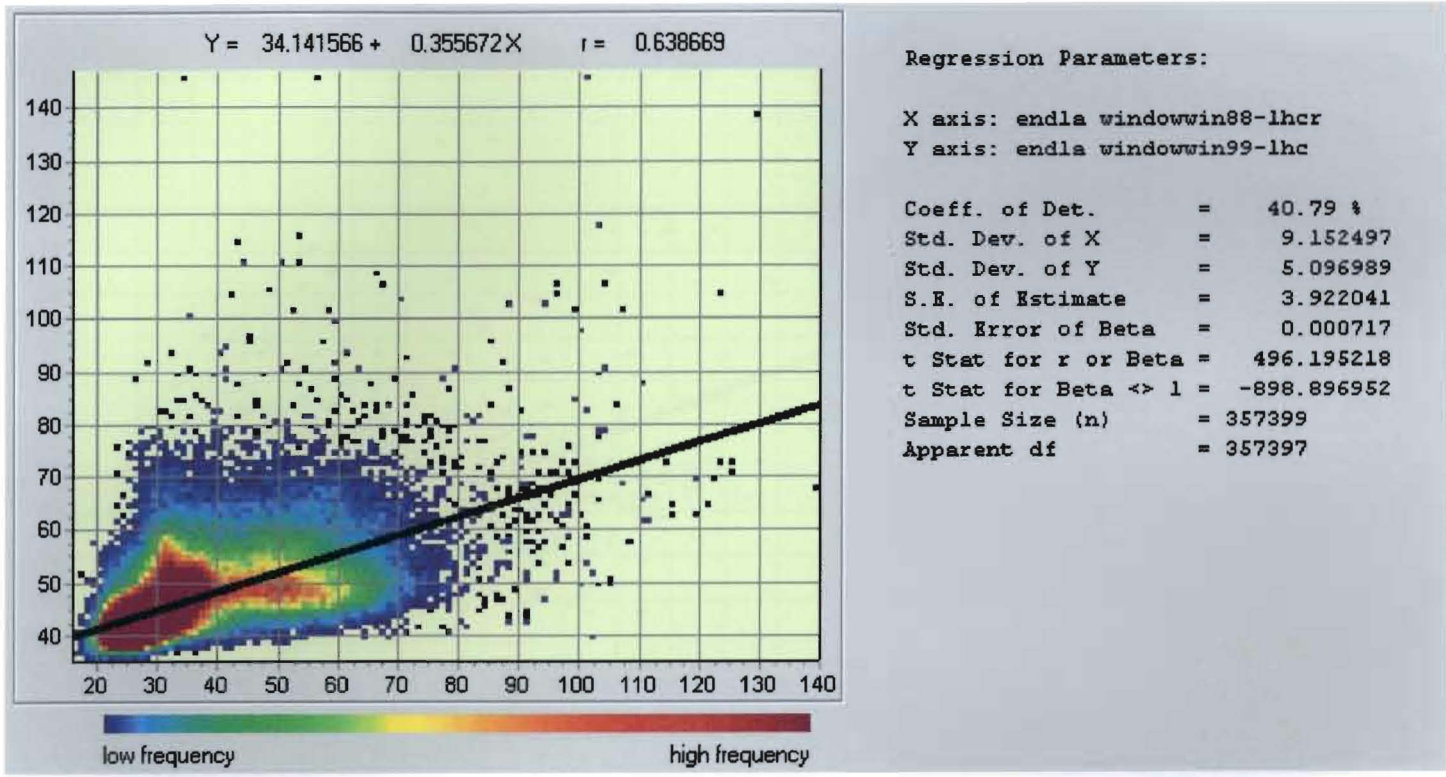

Figure J.1: Regression Plot of Band 1 -- Endla Nature Reserve

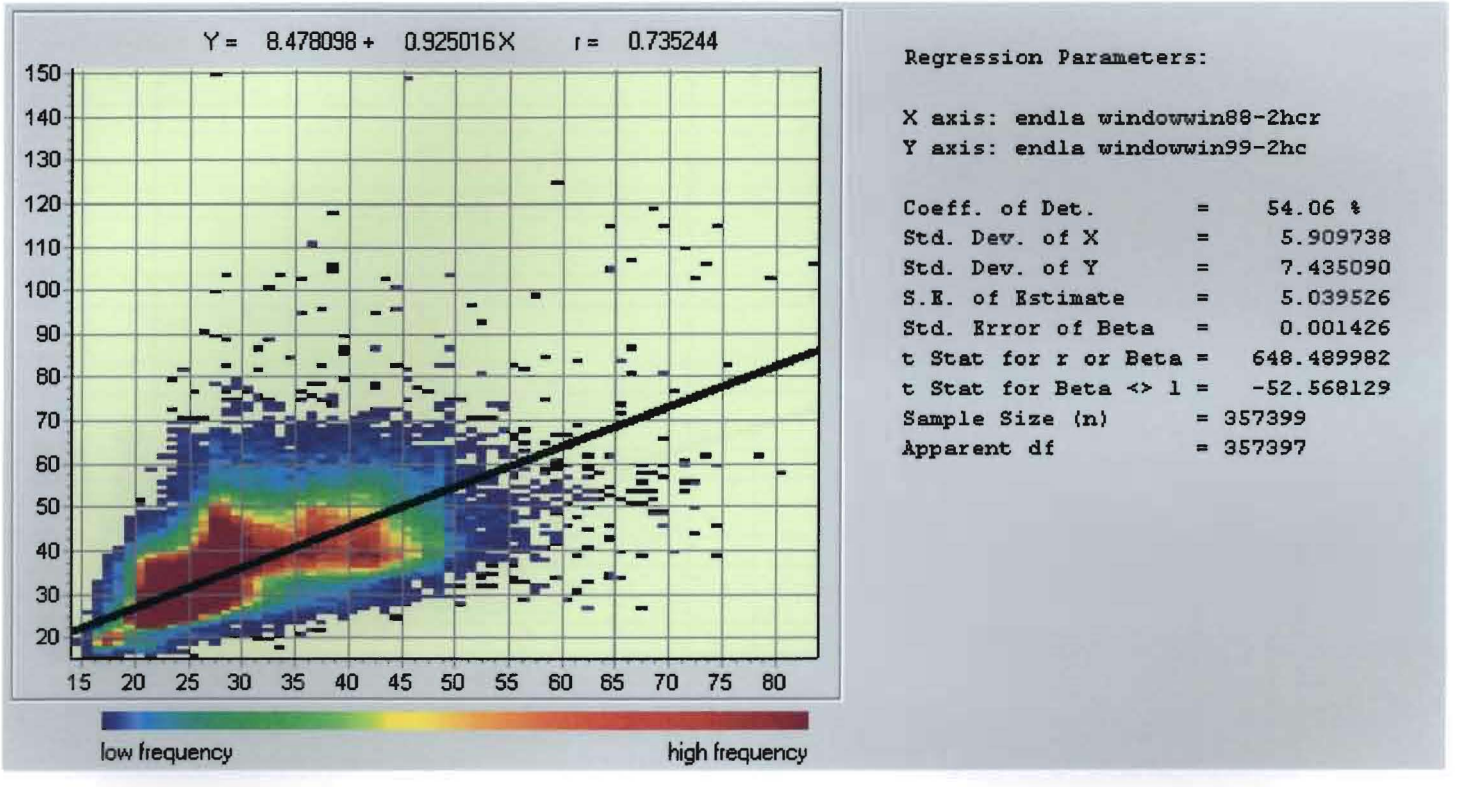

Figure J.2: Regression Plot of Band 2 -- Endla Nature Reserve

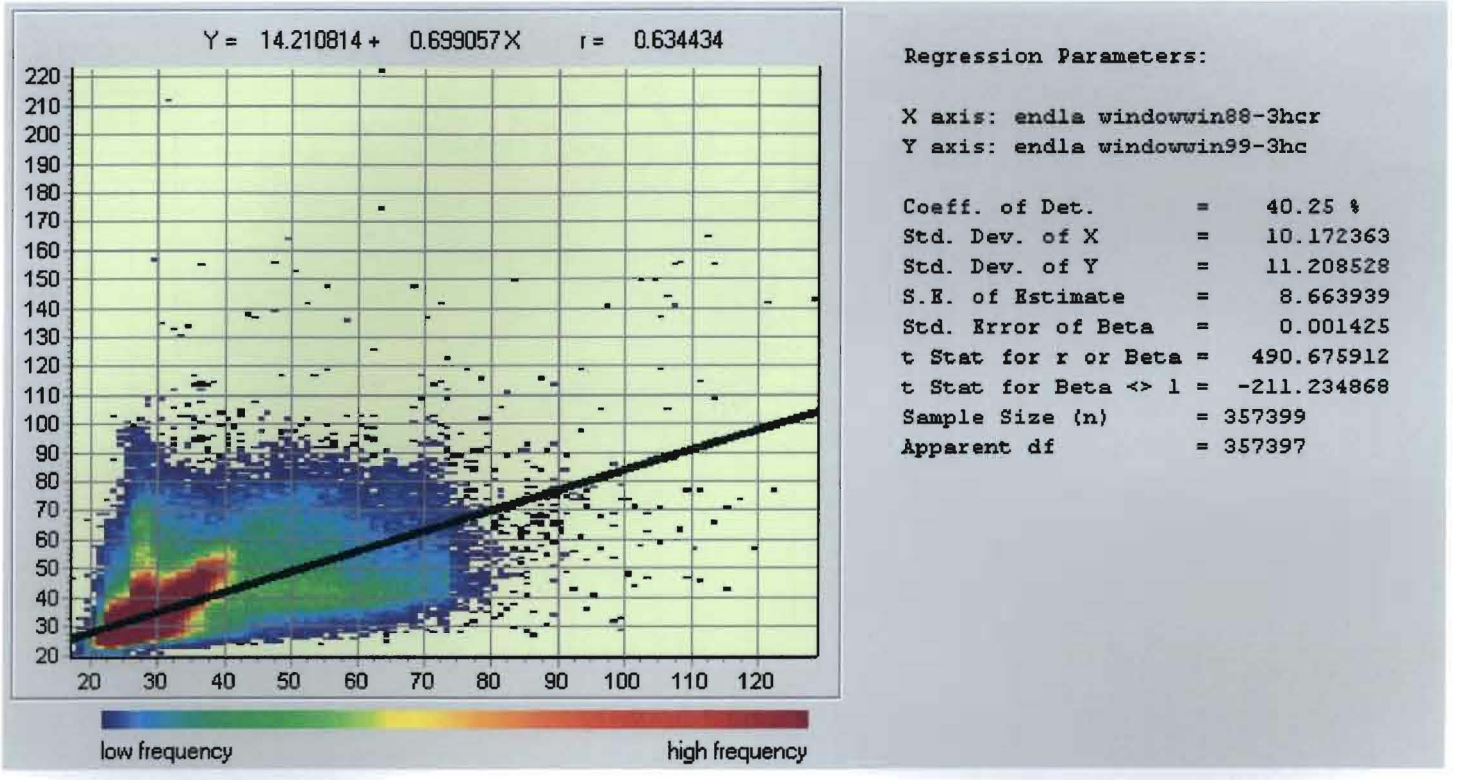

Figure J.3: Regression Plot of Band 3 -- Endla Nature Reserve

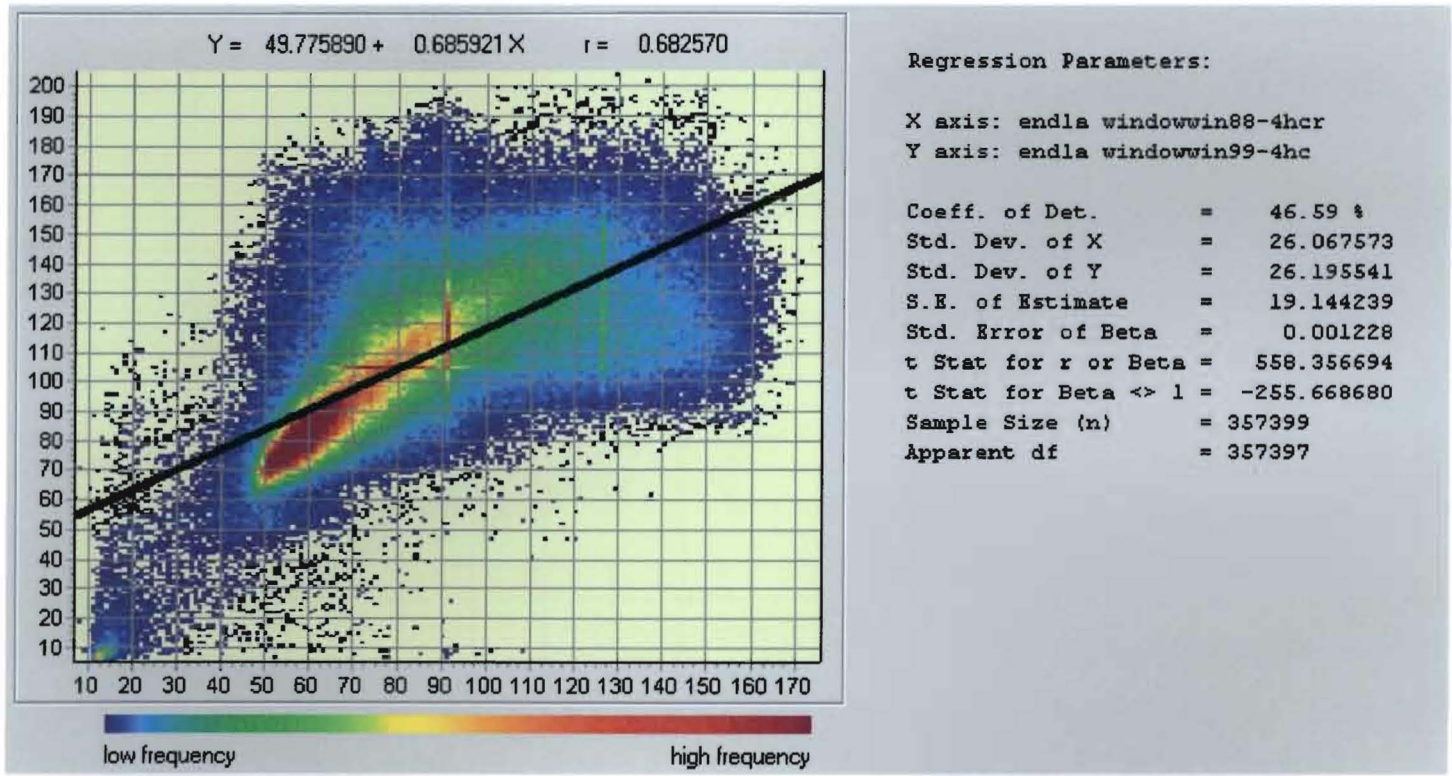

Figure J.4: Regression Plot of Band 4 -- Endla Nature Reserve

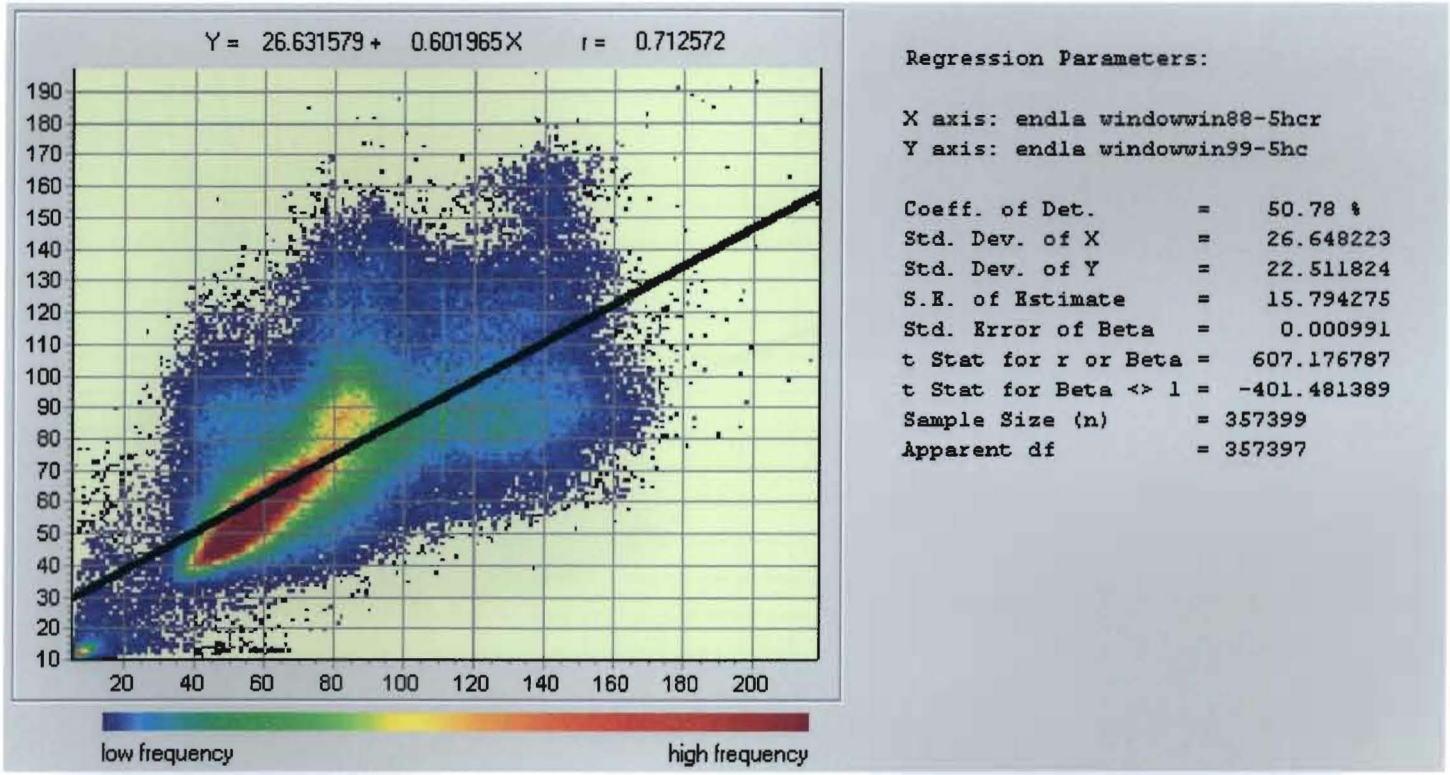

Figure J.5: Regression Plot of Band 5 -- Endla Nature Reserve

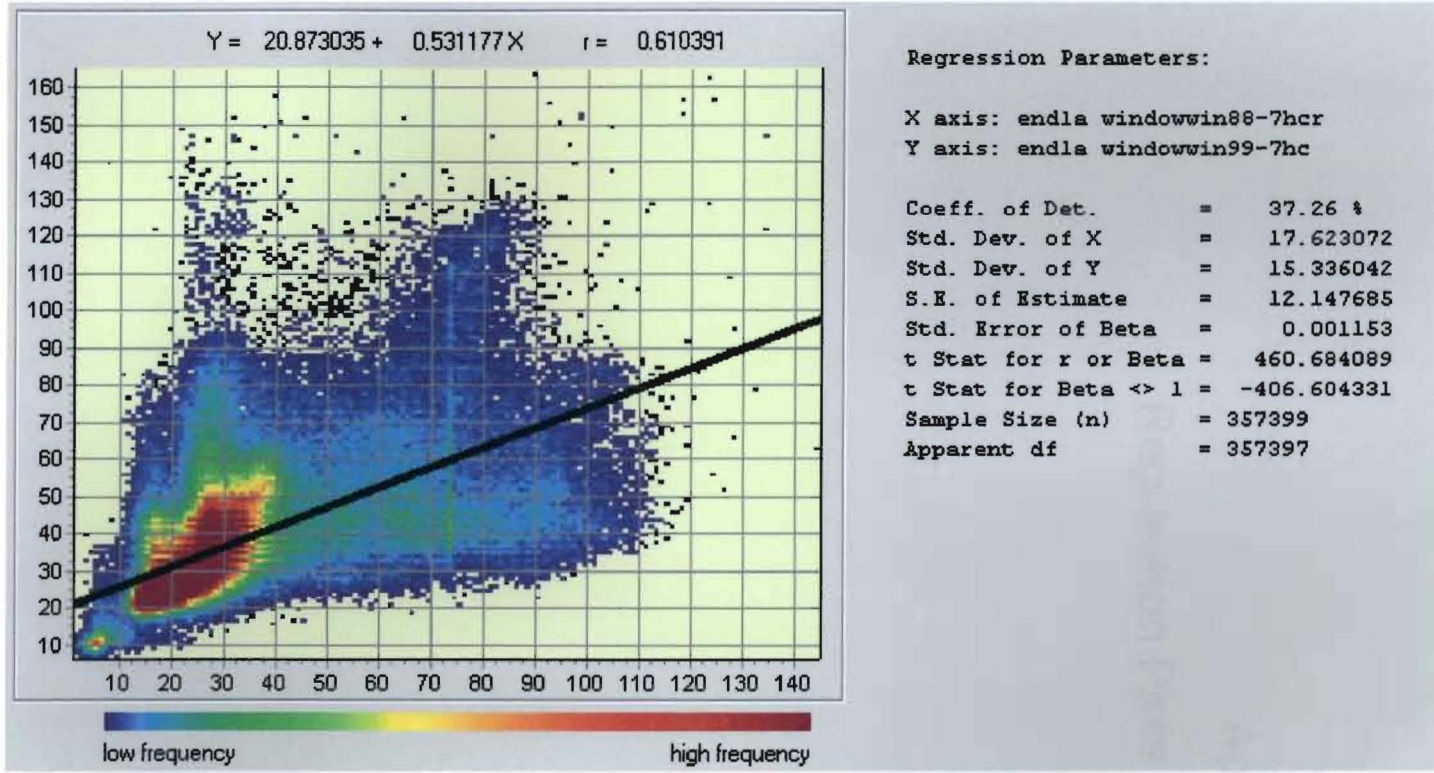

Figure J.6: Regression Plot of Band 7 -- Endla Nature Reserve

Appendix K:
Regression Plots – Emajõe

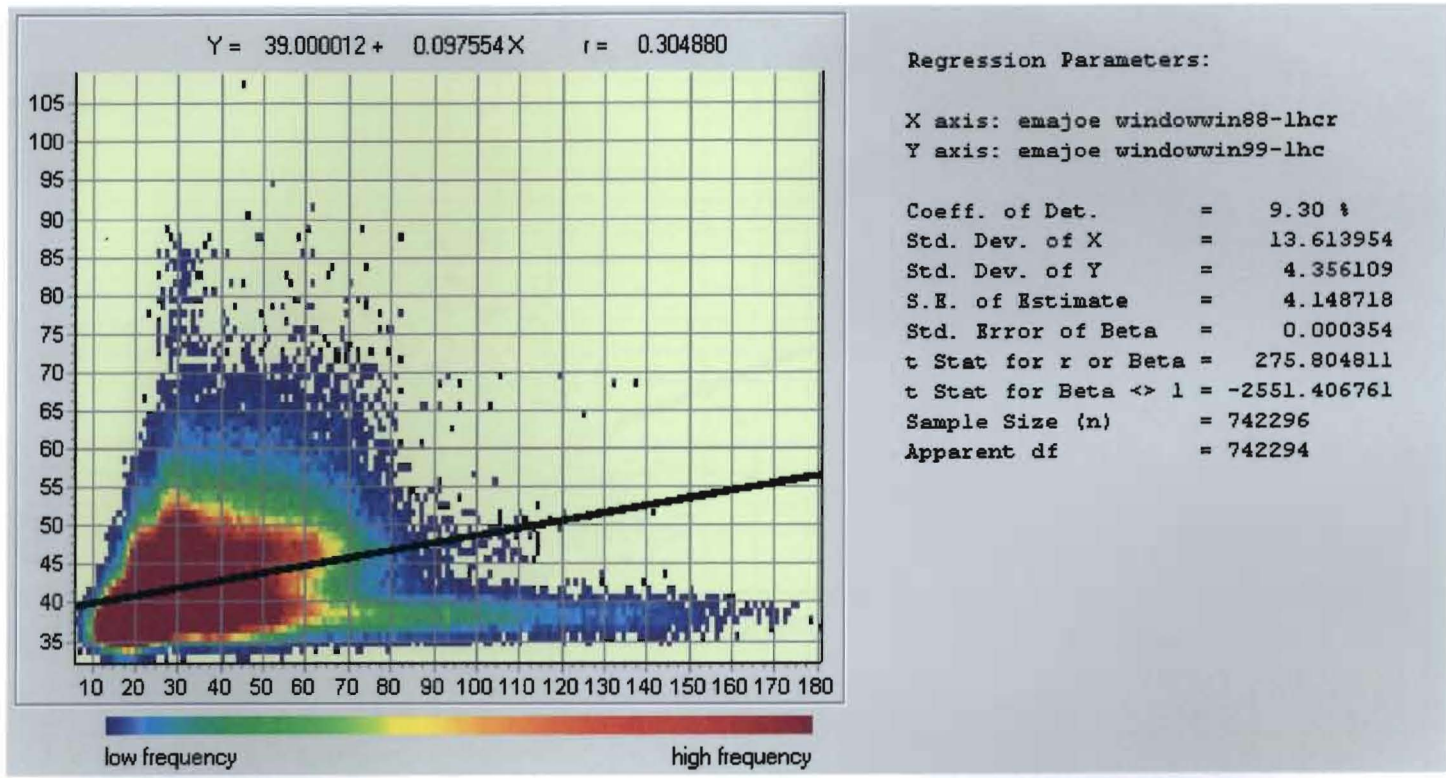

Figure K.1: Regression Plot of Band 1 -- Emajõe Suursoo Mire Complex

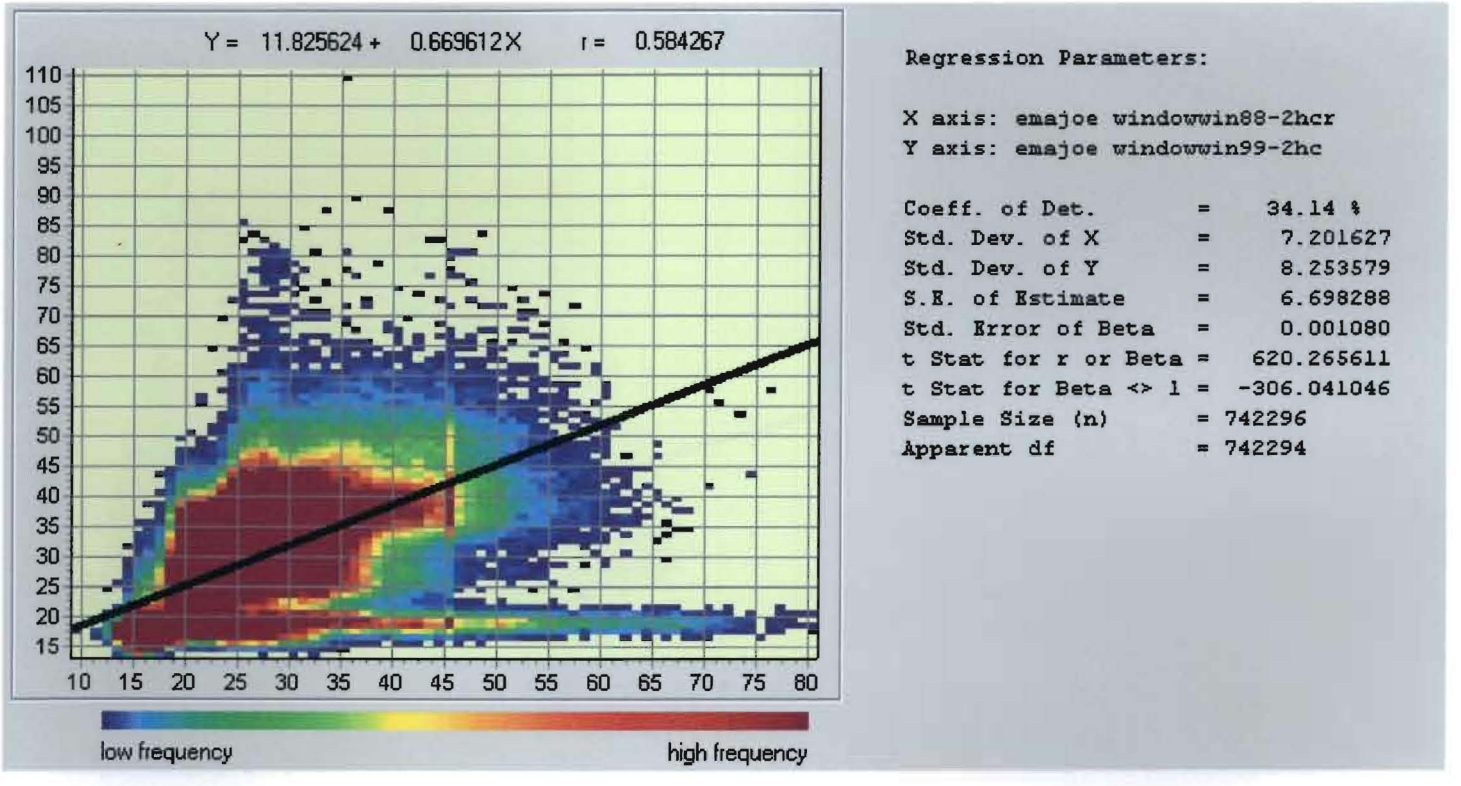

Figure K.2: Regression Plot of Band 2 -- Emajõe Suursoo Mire Complex

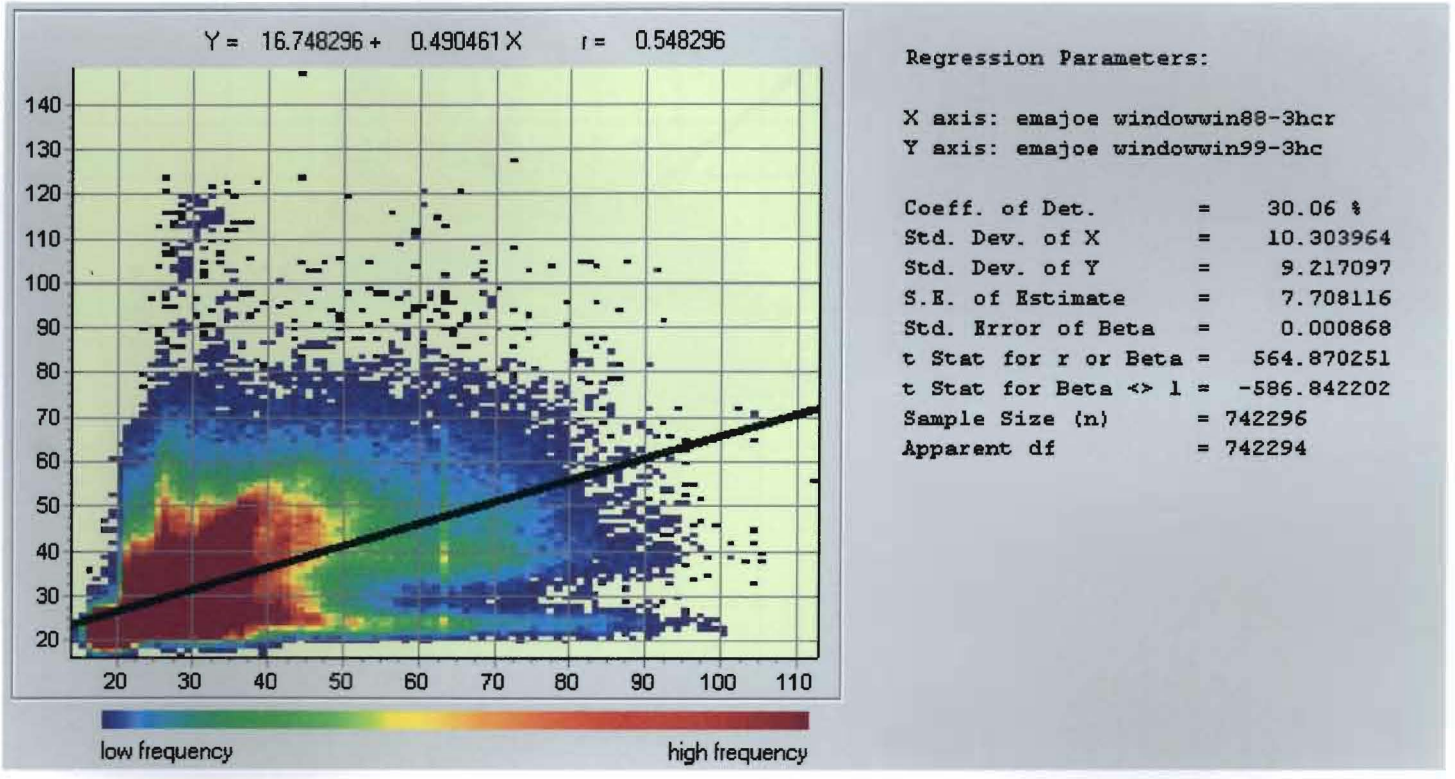

Figure K.3: Regression Plot of Band 3 -- Emajõe Suursoo Mire Complex

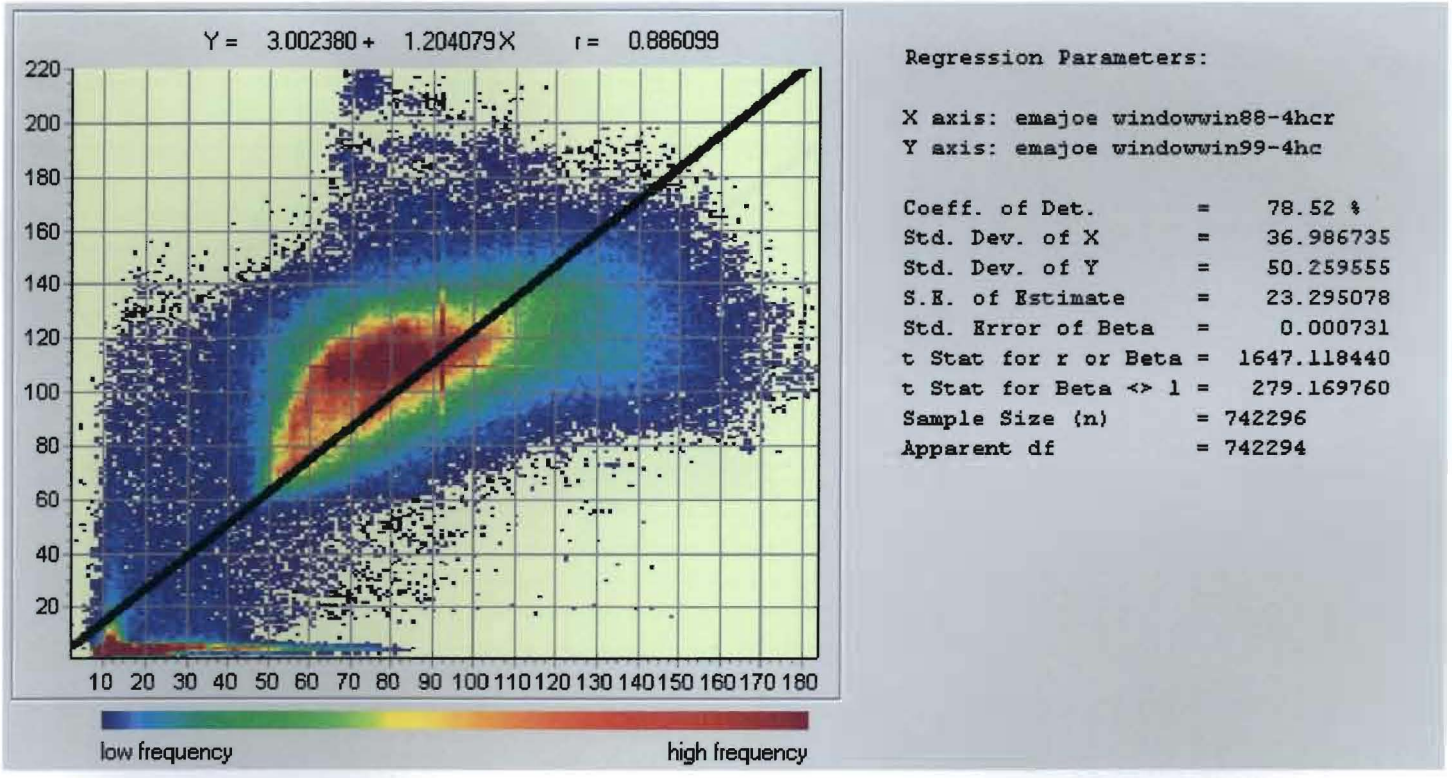

Figure K.4: Regression Plot of Band 4 -- Emajõe Suursoo Mire Complex

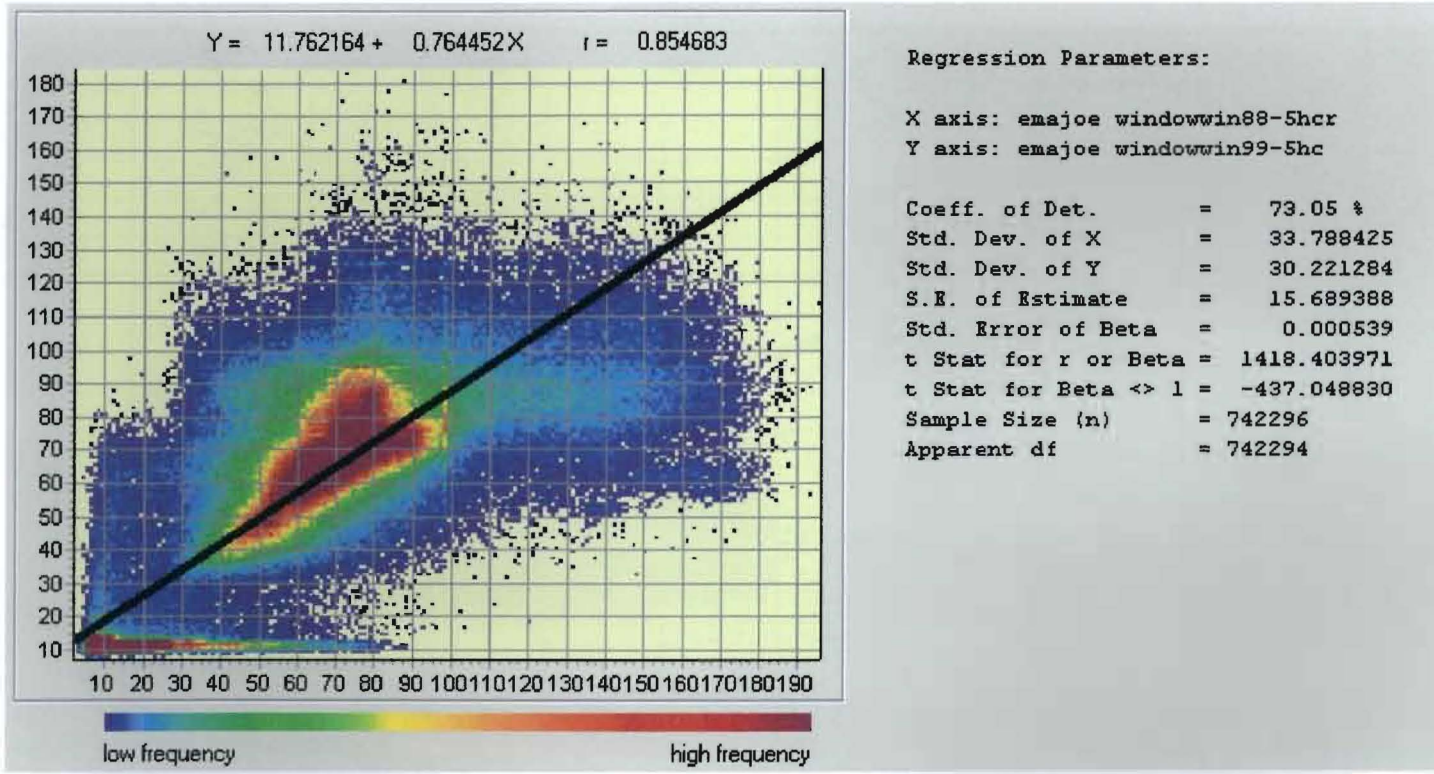

Figure K.5: Regression Plot of Band 5 -- Emajõe Suursoo Mire Complex

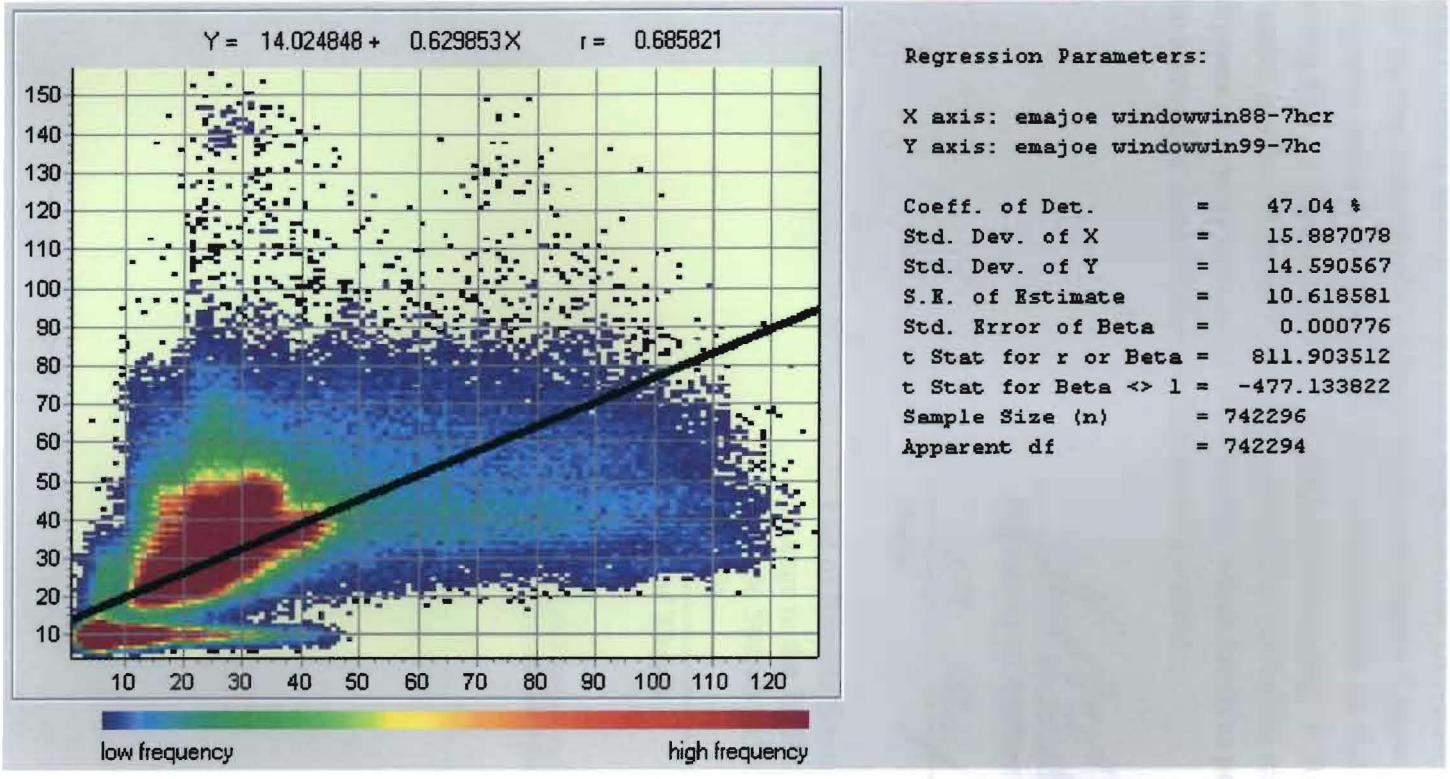

Figure K.6: Regression Plot of Band 7 -- Emajõe Suursoo Mire Complex

Permission to Copy Statement

I, Jack C. Eslick, hereby submit this thesis to Emporia State University as partial fulfillment of the requirements for a Master of Science degree. I agree that the Library of the University may make it available to use in accordance with its regulations governing materials of this type. I further agree that quoting, photocopying, or other reproduction of this document is allowed for private study, scholarship (including teaching) and research purposes of a nonprofit nature. No copying, which involves potential financial gain, will be allowed without written permission of the author.

Jack C. Eslick

Signature of Author

10 May 2002

Date

Use of Remote Sensing Data to Evaluate Change in the Endla Nature Reserve and Emajõe Suursoo Mire Complex in Estonia

Title of Thesis

Mary Cooper

Signature of Graduate Office Staff

5-15-02

Date Received